However, this nuclear translocation was suppressed in the presence of HCV proteins (Fig. 2A) and resulted in the co-localization of the HCV core protein with IRF-3 at perinuclear sites (Fig. 2A, superimposed image of IRF-3 and core protein immunostaining).

To elucidate the mechanism underlying the suppression of IFN-β mRNA in *HCR6-Rz*- and *HCR6-Fse*-expressing cells, we examined the effect of HCV expression on IRF-3 dimerization after NDV infection (Fig. 2B). Interestingly, the levels of IRF-3 dimerization peaked at 12–18 h after NDV infection in the 3 cell lines lacking HCV expression (Day 0; Fig. 2). However, in the *HCR6-Rz*- and *HCR6-Fse*-expressing cell lines, IRF-3 dimerization was found to be significantly reduced, (Fig. 2B and C) when compared to that in the *HCR6-Age*-expressing cells (Fig. 2D).

3.4. Identification of the HCV genome region responsible for the inhibition of IRF-3 dimerization and IFN-β induction

To identify the HCV genome region responsible for suppression of IRF-3 dimerization, HepG2 cells were transfected to express the HCV core regions derived from HCR6, E1, or E2 (genotype 1b; Fig. 3A). Protein expression was confirmed by western blotting (data not shown). The HCV core protein suppressed IRF-3 dimerization, but E1 and E2 expressions had no effect on the dimerization (Fig. 3B). Expression of E1, E2, or the vector alone did not alter the levels of IFN-β mRNA induced by NDV infection in HepG2 cells (Fig. 3C), but significantly reduced IFN-β mRNA levels at both 12 and 18 h after infection (Fig. 3C).

3.5. Effect of HCV core protein expression on IRF-3 dimerization through TLR3

Among the synthetic dsRNAs, poly(I:C) is a potent inducer of IFN-β through TLR3. Accordingly, HepG2 cells transfected with poly(I:C) and the vector control (pEF1-vector) showed IRF-3 dimerization (Fig. 3D). In contrast, IRF-3 dimerization was suppressed in HepG2 cells expressing the HCV core protein albeit the induction of IFN-β mRNA following poly(I:C) expression (data not shown).

3.6. Effect of the HCV core protein NS3 and core proteins derived from genotype 2a on IRF-3 dimerization, compared to proteins derived from genotype 1b

Further, we investigated whether the HCV core protein NS3 and core proteins derived from other genotypes exerted the same effects on IRF-3 after 18 h of NDV infection. The core proteins derived from genotypes 1b (R6) and 2a (R24-12Q and R24-12K) suppressed IRF-3 dimerization in cells infected with NDV (Fig. 3E(a)). In contrast, IRF-3 dimerization remained unaltered in the presence of R6 clone NS3 protein, but was suppressed by the N clone NS3 protein. Thus, NS3-4A protein of R6 clone suppressed IRF-3 dimerization to a relatively lesser extent compared to that of the N1 strain. Similar results were obtained for the phosphorylation at Ser386 in IRF-3 (Fig. 3E(b)). The IFN-β mRNA transcription was quantified in HepG2 cells by RT-PCR after transfection with these expression vectors (Fig. 3F).

3.7. Identification of the HCV core region responsible for suppressing IRF-3 dimerization

We sought to identify the region of the HCV core protein responsible for suppressing IRF-3 dimerization. Expression vectors encoding the entire HCV core or the core region lacking 1 of the 3 basic amino acid regions (BR) that influenced nuclear translocation [17] were transfected into HepG2 cells, and the effects on IRF-3 dimerization were examined (Fig. 4A). Protein

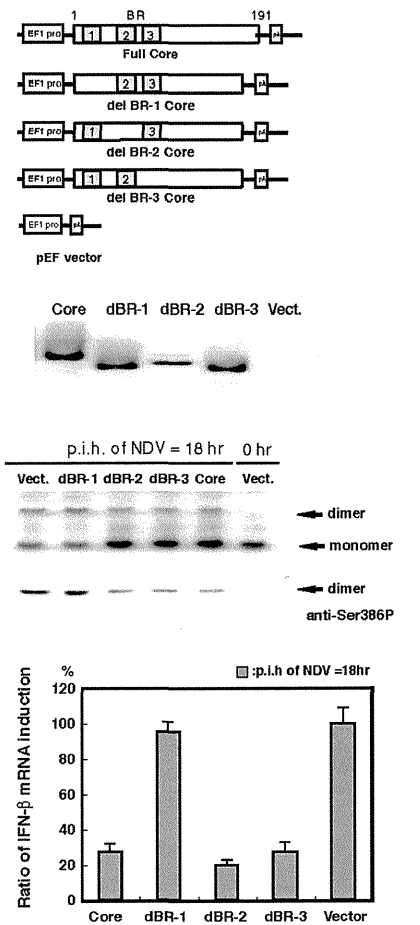

Fig. 4. (A) Structures of the HCR6 core, E1, and E2 expression vectors carrying the complete core, BR1 deletion (aa 4–14), BR2 deletion (aa 37–44), and BR3 deletion (aa 57–72). (B) Western blotting to confirmed the expression of the mutated core proteins. (C) Effects of the expression of various mutated core proteins on IRF-3 dimerization and IRF-3 phosphorylation at Ser386, 18 h after NDV inoculation. (D) Effects of the expression of each type of core protein region on IFN-β mRNA synthesis, 18 h after NDV inoculation. The results are expressed relative to the induction levels of IFN-β in HepG2 cells transfected with the vector alone (100%). IFN-β mRNA levels were assayed by RT-PCR.

expression of the core and the deletion mutants (BR1, BR2, and BR3) was confirmed by western blotting (Fig. 4B). IRF-3 dimerization, phosphorylation at Ser386 of IRF-3, and induction of IFN-β mRNA were suppressed in HepG2 cells expressing the entire core, a deletion of BR2, or a deletion of BR3 (Fig. 4C), but not in cells expressing the BR1-deleted HCV core regions (Fig. 4C and D).

4. Discussion

The present study indicates that the HCV core protein inhibits IRF-3 dimerization, IRF-3 phosphorylation at Ser386, and IFN-β induction. In addition, our study showed that the effect of the core protein derived from genotype 1b was similar to that of the core protein derived from genotype 2a, indicating that the inhibitory effect of the core protein might be effective in several genotypes of HCV. These findings are corroborated by a previous study by Foy et al. [12] who showed that HCV NS3/4 disrupts virus-associated-kinase-mediated IRF-3 activation, which further results in the suppression of IRF-3 phosphorylation, nuclear translocation, and IRF-3-dependent ISRE/PRDI activation. These findings indicate that attenuation of the IFN system was achieved through NS3/4A proteins via the interference of IRF-3 activation, thus strengthening our results, which show the potential of HCV core protein to interfere with IRF-3 activation in promoting persistent infection.

Furthermore, the present study showed that the N-terminal region of the core protein and BR-1 domain in particular are responsible for inactivating IRF-3. The N-terminal region (amino acids 1–59) of the HCV core protein has been identified as the binding region for a DEAD box protein (DDX3) [22]. Human DDX3, a putative RNA helicase, is a member of the highly conserved DEAD box subclass that includes the expression of murine PL10, *Xenopus* An3, and yeast Ded 1 proteins. Recently, expression of DDX3 was found to enhance IFN-β promoter induction by TBK1/IKKε, whereas silencing of DDX3 inhibited IFN-β promoter and virus- or dsRNA-induced IRF-3 activation [23]. It was shown that Vaccinia virus K7 protein also binds to DDX3 and inhibits pattern recognition receptor-induced IFN-β induction by preventing TBK1/IKKε-mediated IFN-β induction via impaired TBK1/IKKε-induced activation of IRF-3 [23]. A previous study by Oshiumi et al. showed that DDX3 C-terminal region (amino acids 622–662) directly binds to the IFN-beta promoter stimulator-1 (IPS-1) CARD-like domain [24] as well as the N-terminal HCV core protein [36]. The present study demonstrated that the expression of the core protein decreased the levels of DDX3 expression (data not shown). This is in agreement with the result of a previous study, which showed that DDX3 is downregulated in HCV-associated hepatocellular carcinoma (HCC) and silencing of DDX3 accelerates cell growth [25]. Collectively, these findings suggest that DDX3 may be the target of the core protein for inhibiting IRF-3 activation.

In conclusion, our study revealed a crucial region of the HCV core protein, basic amino acid region 1, to interfere with IRF-3 activation and thereby inhibit the IFN signaling cascades. Therefore, the inhibitory effects that result in the IRF-3 pathway impairment could be rescued by deleting the basic region 1 of core protein, thus suggesting that it might be an effective treatment for HCV infection. Future studies involving DDX3 modification by the HCV core protein may be interesting to explore the cell growth-dysregulation mechanisms.

Acknowledgments

This study was supported in part by a grant from the Ministry of Education, Culture, Sports, Science and Technology of Japan; a grant from the Ministry of Health, Labour and Welfare of Japan; and the Program for Promotion of Fundamental Studies in Health Sciences of the National Institute of Biomedical Innovation of Japan; and the Cooperative Research Project on Clinical and Epidemiological Studies of Emerging and Re-emerging Infectious Diseases.

Appendix A. Supplementary data

Supplementary data associated with this article can be found, in the online version, at http://dx.doi.org/10.1016/j.bbrc.2012.10.079.

References

[1] N. Kato, M. Hijikata, Y. Ootsuyama, et al., Molecular cloning of the human hepatitis C virus genome from Japanese patients with non-A, non-B hepatitis, Proc. Natl. Acad. Sci. USA 87 (1990) 9524–9528.
[2] L.B. Seeff, F.B. Hollinger, H.J. Alter, et al., Long-term mortality and morbidity of transfusion-associated non-A, non-B, and type C hepatitis: a National Heart, Lung, and Blood Institute collaborative study, Hepatology 33 (2001) 455–463.
[3] H.B. El-Serag, Hepatocellular carcinoma and hepatitis C in the United States, Hepatology 36 (2002) S74–S83.
[4] D. Thomas, The hepatitis C viruses, in: C. Hagedorn, C. Rice (Eds.), Hepatitis C Epidemiology, Springer-Verlag, Berlin, 1999, pp. 25–42.
[5] G.R. Foster, Interferons in host defense, Semin. Liver Dis. 17 (1997) 287–295.
[6] R. Kaufman, Translation control of genome expression, in: N Sonenberg, J Hershey, M Matthews (Eds.), The double strand RNA-activated protein kinase PKR, Cold Spring Harbor, New York, 2000, pp. 503–527.
[7] M.J. *Gale Jr., M.J. Korth, N.M. Tang, et al., Evidence that hepatitis C virus* resistance to interferon is mediated through repression of the PKR protein kinase by the nonstructural 5A protein, Virology 230 (1997) 217–227.
[8] D.R. Taylor, S.T. Shi, P.R. Romano, et al., Inhibition of the interferon-inducible protein kinase PKR by HCV E2 protein, Science 285 (1999) 107–110.
[9] M. Yoneyama, W. Suhara, Y. Fukuhara, et al., Direct triggering of the type I interferon system by virus infection: activation of a transcription factor complex containing IRF-3 and CBP/p300, Embo. J. 17 (1998) 1087–1095.
[10] J. Hiscott, Triggering the innate antiviral response through IRF-3 activation, J. Biol. Chem. 282 (2007) 15325–15329.
[11] E.F. Meurs, A. Breiman, The interferon inducing pathways and the hepatitis C virus, World J. Gastroenterol. 13 (2007) 2446–2454.
[12] E. Foy, K. Li, C. Wang, et al., Regulation of interferon regulatory factor-3 by the hepatitis C virus serine protease, Science 300 (2003) 1145–1148.
[13] E. Meylan, J. Curran, K. Hofmann, et al., Cardif is an adaptor protein in the RIG-I antiviral pathway and is targeted by hepatitis C virus, Nature 437 (2005) 1167–1172.
[14] X.D. Li, L. Sun, R.B. Seth, et al., Hepatitis C virus protease NS3/4A cleaves mitochondrial antiviral signaling protein off the mitochondria to evade innate immunity, Proc. Natl. Acad. Sci. USA 102 (2005) 17717–17722.
[15] R. Lin, J. Lacoste, P. Nakhaei, et al., Dissociation of a MAVS/IPS-1/VISA/Cardif-IKKepsilon molecular complex from the mitochondrial outer membrane by hepatitis C virus NS3-4A proteolytic cleavage, J. Virol. 80 (2006) 6072–6083.
[16] K. Li, E. Foy, J.C. Ferreon, et al., Immune evasion by hepatitis C virus NS3/4A protease-mediated cleavage of the Toll-like receptor 3 adaptor protein TRIF, Proc. Natl. Acad. Sci. USA 102 (2005) 2992–2997.
[17] R. Suzuki, Y. Matsuura, T. Suzuki, et al., Nuclear localization of the truncated hepatitis C virus core protein with its hydrophobic C terminus deleted, J. Gen. Virol. 76 (Pt 1) (1995) 53–61.
[18] W. Suhara, M. Yoneyama, I. Kitabayashi, et al., Direct involvement of CREB-binding protein/p300 in sequence-specific DNA binding of virus-activated interferon regulatory factor-3 holocomplex, J. Biol. Chem. 277 (2002) 22304–22313.
[19] M. Mori, M. Yoneyama, T. Ito, et al., Identification of Ser-386 of interferon regulatory factor 3 as critical target for inducible phosphorylation that determines activation, J. Biol. Chem. 279 (2004) 9698–9702.
[20] K. Tsukiyama-Kohara, S. Tone, I. Maruyama, et al., Activation of the CKI-CDK-Rb-E2F pathway in full genome hepatitis C virus-expressing cells, J. Biol. Chem. 279 (2004) 14531–14541.
[21] T. Nishimura, M. Kohara, K. Izumi, et al., Hepatitis C virus impairs p53 via persistent overexpression of 3beta-hydroxysterol Delta24-reductase, J. Biol. Chem. 284 (2009) 36442–36452.
[22] A.M. Owsianka, A.H. Patel, Hepatitis C virus core protein interacts with a human DEAD box protein DDX3, Virology 257 (1999) 330–340.
[23] M. Schroder, M. Baran, A.G. Bowie, Viral targeting of DEAD box protein 3 reveals its role in TBK1/IKKepsilon-mediated IRF activation, EMBO J. 27 (2008) 2147–2157.
[24] H. Oshiumi, K. Sakai, M. Matsumoto, T. Seya, DEAD/H BOX 3 (DDX3) helicase binds the RIG-I adaptor IPS-1 to up-regulate IFN-beta-inducing potential, Eur. J. Immunol. 40 (4) (2010) 940–948.
[25] P.C. Chang, C.W. Chi, G.Y. Chau, et al., DDX3, a DEAD box RNA helicase, is deregulated in hepatitis virus-associated hepatocellular carcinoma and is involved in cell growth control, Oncogene 25 (2006) 1991–2003.

Journal of Medical Virology 84:733–746 (2012)

Hepatitis C Virus Promotes Expression of the 3β-Hydroxysterol Δ24-Reductase Through Sp1

Makoto Saito,[1] Michinori Kohara,[2] and Kyoko Tsukiyama-Kohara[1]*

[1]*Department of Experimental Phylaxiology, Faculty of Life Sciences, Kumamoto University, Kumamoto, Japan*
[2]*Department of Microbiology and Cell Biology, Tokyo Metropolitan Institute of Medical Science, Tokyo, Japan*

Hepatitis C virus (HCV) establishes chronic infection, which often causes hepatocellular carcinoma. Overexpression of 3β-hydroxysterol Δ24-reductase (DHCR24) by HCV has been shown to impair the p53-mediated cellular response, resulting in tumorigenesis. In the present study, the molecular mechanism by which HCV promotes the expression of *DHCR24* was investigated. A significant increase in *DHCR24* mRNA transcription was observed in a cell line expressing complete HCV genome, whereas no significant difference in the expression of *DHCR24* was seen in cell lines expressing individual viral proteins. The 5′-flanking genomic region of *DHCR24* was characterized to explore the genomic region and host factor(s) involved in the transcriptional regulation of *DHCR24*. As a result, the HCV response element (−167/−140) was identified, which contains AP-2α, MZF-1, and Sp1 binding motifs. The binding affinity of the host factor to this response element was increased in nuclear extracts from cells infected with HCV and corresponded with augmented affinity of Sp1. Both mithramycin A (Sp1 inhibitor) and small interfering RNA targeting Sp1 prevented the binding of host factors to the response element. Silencing of Sp1 also downregulated the increased expression of *DHCR24*. The binding affinity of Sp1 to the response element was augmented by oxidative stress, whereas upregulation of *DHCR24* in cells expressing HCV was blocked significantly by a reactive oxygen species scavenger. Elevated phosphorylation of Sp1 in response to oxidative stress was mediated by the ATM kinase. Thus, activation of Sp1 by oxidative stress is involved in the promotion of expression of *DHCR24* by HCV. ***J. Med. Virol. 84:733–746, 2012.*** © 2012 Wiley Periodicals, Inc.

KEY WORDS: HCV; DHCR24; Sp1; oxidative stress

INTRODUCTION

Hepatitis C virus (HCV) causes chronic hepatitis and hepatocellular carcinoma [Koike, 2007]. The estimated worldwide prevalence of HCV infection is 2.2–3.0% (130–170 million people) [Lavanchy, 2009], and chronic HCV infection is a major global public health concern. The most effective current treatment for HCV infection comprises combination therapy with PEGylated interferon-α and ribavirin [Bruchfeld et al., 2001; Lu et al., 2008]. However, this therapy has limited clinical efficacy, as sustained virological responses develop in only about half of patients infected with HCV genotype 1 [Kohara et al., 1995; Nakamura et al., 2002]. Efforts to develop therapies to treat HCV are also hindered by the high level of viral variation and the capacity of HCV to cause chronic infection. Therefore, there is an urgent need to develop effective treatments against chronic HCV infection.

Additional supporting information may be found in the online version of this article.

Grant sponsor: Ministry of Health and Welfare of Japan; Grant sponsor: Ministry of Education, Culture, Sports, Science and Technology of Japan; Grant sponsor: Program for Promotion of Fundamental Studies in Health Sciences of the National Institute of Biomedical Innovation; Grant sponsor: Cooperative Research Project on Clinical and Epidemiological Studies of Emerging and Re-emerging Infectious Diseases.

Kyoko Tsukiyama-Kohara present address is Transboundary Animal Diseases Center, Faculty of Agriculture, Kagoshima University, 1-21-24 Korimoto, Kagoshima-city 890-0065, Japan.

*Correspondence to: Kyoko Tsukiyama-Kohara, PhD, Department of Experimental Phylaxiology, Faculty of Life Sciences, Kumamoto University, 1-1-1 Honjo, Kumamoto City, Kumamoto 860-8556, Japan. E-mail: kkohara@kumamoto-u.ac.jp, kkohara@agri.kagoshima-u.ac.jp

Accepted 16 January 2012

DOI 10.1002/jmv.23250
Published online in Wiley Online Library (wileyonlinelibrary.com).

A cell line that expresses complete HCV genome (RzM6-LC) was established to investigate the effects of persistent expression of HCV on cell growth [Tsukiyama-Kohara et al., 2004]. A monoclonal antibody (2-152a mAb) against the RzM6-LC cell line was also developed to produce clones that recognize both cell surface and intracellular molecules. As a result, 3β-hydroxysterol Δ24-reductase (DHCR24) was identified as the target of 2-152a mAb [Nishimura et al., 2009].

DHCR24 is an oxidoreductase with a broad expression pattern and shares homology with a family of flavin-adenine dinucleotide-dependent reductases [Waterham et al., 2001]. In mammals, DHCR24 functions as an enzyme to catalyze the conversion of desmosterol to cholesterol in the post-squalene cholesterol biosynthetic pathway, and it is essential for normal tissue development and maintenance [Waterham et al., 2001; Crameri et al., 2006]. DHCR24 regulates cholesterol synthesis and promotes recruitment of domain components into detergent-resistant membrane fractions [Crameri et al., 2006]. An absence of DHCR24 leads to desmosterolosis—a rare disorder of cholesterol biosynthesis [Waterham et al., 2001]. Expression of DHCR24 is downregulated in areas of the brain affected by Alzheimer's disease [Greeve et al., 2000], suggesting that DHCR24 has alternative functions. Indeed, DHCR24 is also known as seladin-1 (the selective Alzheimer's disease indicator 1), reflecting the association between DHCR24/seladin-1 and the selective vulnerability of the neurons in the affected areas of the brain. High levels of DHCR24/seladin-1 exert protective effects, conferring resistance against oxidative stress and preventing apoptotic cell death [Greeve et al., 2000; Benvenuti et al., 2005; Di Stasi et al., 2005; Luciani et al., 2005; Lu et al., 2008]. Endogenous DHCR24/seladin-1 levels are upregulated in response to acute oxidative stress [Wu et al., 2004; Benvenuti et al., 2006; Kuehnle et al., 2008], whereas the expression declines to low levels upon chronic exposure [Benvenuti et al., 2006; Kuehnle et al., 2008]. Therefore, DHCR24/seladin-1 may be involved in integrating cellular responses to oxidative stress. DHCR24 also functions as a hydrogen peroxide scavenger [Lu et al., 2008]. Based on these findings, DHCR24 may play a crucial role in maintaining cellular physiology by regulating both cholesterol synthesis and cellular defense against oxidative stress.

HCV infection impairs apoptosis induced by oxidative stress and inhibits p53 function via overexpression of DHCR24 [Nishimura et al., 2009]. Augmented expression of DHCR24 also facilitates efficient replication of HCV [Takano et al., 2011b]. Since DHCR24 may play a significant role in viral replication and in the tumorigenicity of the hepatocellular carcinoma related to HCV, the molecular mechanism of overexpression of DHCR24 in response to HCV was examined in the present study.

MATERIALS AND METHODS

Cell Lines

The HepG2 hepatoblastoma cell line, the HepG2-derived RzM6 cell line, which is capable of conditional control of expression of HCV genome (genotype 1b) based on the Cre/*loxP* system (RzM6-0d, no switching; RzM6-LC, switching of full genome HCV induced by tamoxifen), and HepG2-derived CN5 cell line, in which all HCV proteins were expressed conditionally by cre adenovirus (CN5-Cre) [Tsukiyama-Kohara et al., 2004] were propagated in Dulbecco's modified Eagle's medium (DMEM) supplemented with 10% fetal bovine serum (FBS). Using a stable expression system based on lentiviral vectors, HepG2/Lenti cell lines (core, E1, E2, NS2, NS3/4A, NS4B, NS5A, and NS5B) were established [Takano et al., 2011a]. An additional cell line—HepG2-emp—was infected with an empty lentiviral vector. Cells from the human hepatoma HuH-7 cell line were maintained in DMEM supplemented with 10% FBS and 0.4% glucose. The cell lines harboring HCV replicon, namely, R6FLR-N (genotype 1b) and FLR3-1 (genotype 1b), which are derived from HuH-7 [Takano et al., 2011b], were maintained under selective pressure with G418 (500 μg/ml for R6FLR-N and FLR3-1) in DMEM GlutaMAX (Invitrogen, Carlsbad, CA) containing 10% FBS. Cured/HuH-7 K4 cells—cured of HCV by interferon-α treatment—were maintained in DMEM GlutaMAX containing 10% FBS without G418. The JFH/K4 cell line, which shows persistent infection with the HCV JFH-1 strain, was maintained in DMEM containing 10% FBS. The human fetal hepatic cell line WRL68 was obtained from the American Type Culture Collection and maintained in DMEM supplemented with 10% FBS, 1 mM sodium pyruvate, and 0.1 mM nonessential amino acids. The human hepatoma cell line PLC/PRF/5 was obtained from the Cell Resource Center for Biomedical Research Institute of Development, Aging and Cancer, Tohoku University, and cultured in Eagle's minimum essential medium supplemented with 10% FBS.

Construction of DHCR24 Promoter Reporter Plasmids

Genomic DNA was extracted from HepG2 cells, and the 5′-flanking sequence of the predicted transcription start site of *DHCR24* (~5 kb) was isolated. The genomic region was inserted upstream of the firefly luciferase gene in pGL3-Basic (Promega, Madison, WI). Deletion constructs of the *DHCR24* promoter region were constructed using restriction enzymes and PCR (sense primer for −4956, 5′-GATCCTCGAGCACTCCTGCTCACCACTGAT-3′; sense primer for −2982, 5′-GATCCTCGAGGAGGCTCACATTGTAGAAAG-3′; antisense primer, 5′-GTAGTAGATATCGAAGATAAGCGAGAGCGG-3′) and cloned into pGL3-Basic at the *Xho*I and *Nco*I sites.

Dual Luciferase Reporter Assay

HepG2 cells (1×10^4 cells/well in a 96-well plate) were transfected with each of the 3 *DHCR24* promoter reporter plasmids and their deletion constructs (0.25 μg/well) using cationic lipid (Lipofectamine LTX, Invitrogen). Samples were analyzed with the Dual-Glo Luciferase Assay System (Promega) at 48 h post-transfection, and luminescence was measured using a TriStar LB941 microplate reader (Berthold, Bad Wildbad, Germany). To account for differences in transfection efficiency, the luminescence produced by firefly luciferase (FL) was normalized to that produced by Renilla luciferase (RL), which was expressed by co-transfection with phRL-TK (Promega; 0.025 μg/well).

Electrophoresis Mobility Shift Assay

Nuclear extracts were prepared from 5×10^6 to 1×10^7 cells as described previously [Dignam et al., 1983]. Electrophoresis mobility shift assays (EMSAs) were performed by a nonradioactive method using the DIG Gel Shift Kit (Roche, Indianapolis, IN). Briefly, binding reactions were performed by mixing the following components: 1 μg of poly[d(I-C)], 0.1 μg of poly L-lysine, 40 fmol DIG-labeled double-stranded oligonucleotide probe (HCV response element −167/−140 [28-mer], 5′-CCCCCGCCTCGCGCGGCGGCGGGGAGAA-3′; Sp1 consensus sequence [22-mer], 5′-ATTCGATCGGGGCGGGGCGAGC-3′; MZF1.1-4 consensus sequence [21-mer], 5′-GATCTAAAAGTGGGGAGAAAA-3′; AP-2α consensus sequence [26-mer], 5′-GATCGAACTGACCGCCCGCGGCCCGT-3′), and 10 μg of the nuclear extract in binding buffer (10 mM Tris–HCl, pH 7.5; 50 mM NaCl; 5 mM $MgCl_2$; 0.5 mM EDTA). Where indicated, reactions were supplemented with unlabeled/competitive oligonucleotide at a 50-fold molar excess concentration before addition of the probe. Mithramycin A (MMA; Sigma, St. Louis, MO), which blocks the binding of Sp1 to target sequences, was added at different final concentrations (2.5, 5, and 10 μM) and incubated at 4°C for 1 h. For supershift assays, 1 μg of monoclonal anti-Myc Tag antibody (Upstate Biotechnology, Lake Placid, NY) was added 30 min prior to addition of the probe. Binding reactions were carried out at 25°C for 30 min and electrophoresed on 6% acrylamide–0.5× TBE gels, transferred to positively charged nylon membranes, and detected by a chemiluminescence method (Roche) and a LAS1000 scanner (Fujifilm Co., Tokyo, Japan).

Silencing of Sp1, HCV, and DHCR24 by siRNA

SP1 Validated Stealth RNAi™ siRNA (VHS40867, Invitrogen) was designed with the BLOCK-iT RNAi designer to target the human Sp1 mRNA sequence. RzM6-0d and RzM6-LC cells (1.5×10^6 cells in a 100-mm dish) were transfected with Sp1 siRNA (final concentration, 30 nM) using Lipofectamine RNAiMAX (Invitrogen) in Opti-MEM (Invitrogen) and incubated for 48 h at 37°C. The siRNAs specific for DHCR24 and HCV were designed and utilized as described previously [Nishimura et al., 2009].

Kinase Inhibitors

ATM kinase inhibitor KU55933 (Wako Pure Chemical Industry, Osaka, Japan; final concentration, 10 μM), PI3K inhibitor LY294002 (Cell Signaling Technology, Beverly, MA; 50 μM), and MEK1 inhibitor PD98059 (Cell Signaling Technology; 50 μM) were added to cell cultures, which were incubated for 8 h at 37°C.

Western Blotting

Western blotting was performed as described previously [Tsukiyama-Kohara et al., 2004] with the following primary antibodies: rabbit monoclonal anti-DHCR24/Seladin-1 (C59D8; Cell Signaling Technology); rabbit polyclonal anti-Sp1, anti-phospho-Akt (Ser473), and mouse monoclonal anti-phospho-ERK (Santa Cruz Biotechnology, Inc., Santa Cruz, CA); mouse monoclonal anti-HCV core (clone 31-2), E1 (clone 384), E2 (clone 544), NS4A (c14II-2-1), NS5A (32-2), NS5B (14-5), rabbit polyclonal anti-NS2, NS3 (R212), and NS4B (RR10) [Tsukiyama-Kohara et al., 2004]. Phosphorylation of Sp1 was investigated by 5% SDS–PAGE and immunoblotting with a polyclonal antibody against Sp1 phosphorylated at Ser101 (Active Motif, Carlsbad, CA) or Thr453 (Abcam, Cambridge, MA). Detection of γH2AX was performed by 15% SDS–PAGE and immunoblotting with mouse monoclonal anti-phospho-histone H2AX (Ser139) (JBW301; Upstate Biotechnology). Phosphorylated ATM (Ser1981) and ATR (Ser428) were detected by specific antibodies (Cell Signaling Technology). Monoclonal anti-actin (Sigma), anti-histone H1 (Santa Cruz Biotechnology, Inc.), anti-HAUSP (Calbiochem, San Diego, CA), and anti-heat shock protein 90 (Stressgen, Victoria, BC, Canada) primary antibodies were used for normalization of Western blotting. Bound antibody was detected with a horseradish peroxidase-conjugated secondary antibody and visualization using ECL reagents (GE Healthcare, Piscataway, NJ) and an LAS1000 scanner (Fujifilm). Densitometric analysis of protein bands was performed with Image Quant software (Molecular Dynamics, Sunnyvale, CA).

Quantitative PCR and HCV Infection

Total RNA was extracted from cell lines using ISOGEN, and reverse transcription of total RNA (125 ng) was performed with SuperScript III Reverse Transcriptase and Random Primers (Invitrogen). Synthesized cDNA samples were subjected to a TaqMan gene expression assay (Applied Biosystems, Foster City, CA), and the level of expression of *DHCR24* mRNA in each sample was normalized to the level of expression of *GAPDH* mRNA and represented as a ratio of the control (Hep-emp, CN5-Hep, or RzM6-0d). Infection of the human hepatocytes from human liver-uPA/SCID chimeric mice with HCV was performed,

and HCV RNA, *DHCR24* mRNA, and 18S rRNA were measured by quantitative PCR (qPCR), as described previously [Takano et al., 2011a].

Statistical Analysis

The Student's *t*-test was used to analyze the statistical significance of the results; P values < 0.05 were considered statistically significant.

RESULTS

DHCR24 Expression Is Upregulated by the Complete HCV Genome But Not by Individual Viral Proteins

Overexpression of *DHCR24* in human hepatocytes from human liver-uPA/SCID chimeric mice has been observed after HCV infection (Fig. 1A). The overexpression of *DHCR24* in cells expressing HCV decreased to a similar extent as that observed in control cells following treatment with HCV siRNA (Fig. 1B). Since these findings suggest that overexpression of *DHCR24* is associated with the expression or infection by HCV, the identity of the viral factor involved in the augmentation of expression of *DHCR24* was examined. The level of expression of *DHCR24* mRNA was measured by quantitative RT-PCR (Fig. 1C) in HepG2-derived cell lines that stably express individual HCV proteins (core, E1, E2, NS2, NS3/4A, NS4B, NS5A, or NS5B; Supplementary Fig. 1). The level of expression of *DHCR24* mRNA was slightly higher in the cells expressing NS4B and NS5A than in control cells; however, there was no significant difference in the expression of *DHCR24* mRNA among these cell

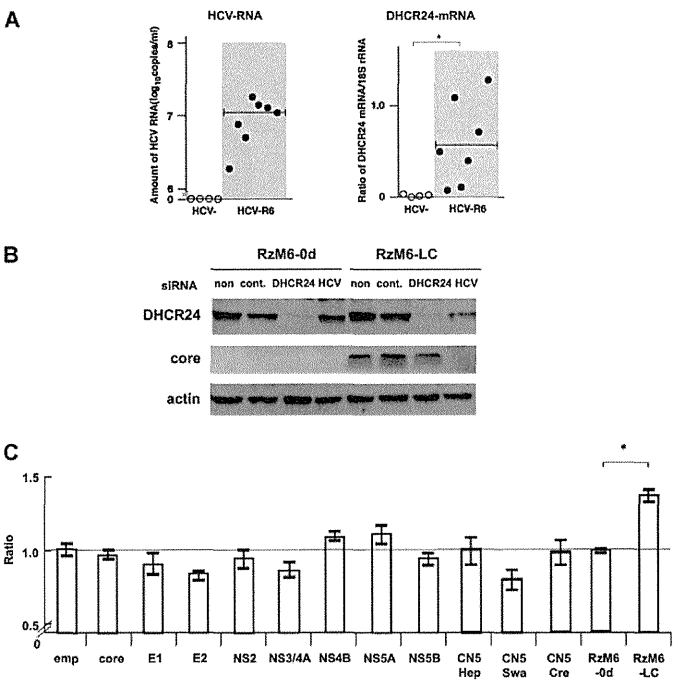

Fig. 1. *DHCR24* expression is induced in the presence of the complete HCV genome. **A**: The amount of HCV RNA in chimeric mice infected with HCV-R6 (genotype 1b) was quantified by qPCR (left panel). The amount of DHCR24 mRNA was measured, and the ratio to the amount of 18S rRNA was calculated in the tissues (right panel). **B**: Western blotting of DHCR24, HCV core, and actin protein in RzM6-0d and LC cells following treatment with the indicated siRNA. **C**: Level of *DHCR24* mRNA expression in cell lines with stable expression of individual HCV proteins, the HCV open reading frame, or the complete HCV genome. Total RNA from HepG2/Lenti cell lines (emp, core, E1, E2, NS2, NS3/4A, NS4B, NS5A, and NS5B), CN5 cell lines (CN5-Hep, CN5-Swa, and CN5-Cre), or RzM6 cell lines (RzM6-0d and RzM6-LC) were prepared, and reverse transcription was performed. Synthesized cDNA was subjected to quantitative PCR. The level of expression of *DHCR24* mRNA for each sample was normalized to that of *GAPDH* mRNA and represented as a ratio of HepG2-emp ($^*P < 0.05$).

lines. No significant upregulation of *DHCR24* mRNA was observed in the CN5-Cre cell line, which expresses all HCV proteins and is negative for viral replication [Tsukiyama-Kohara et al., 2004]. In contrast, significant upregulation of *DHCR24* was observed in a cell line that expresses the complete HCV genome (RzM6-LC) compared with the expression in HCV-negative control cells (RzM6-0d). Thus, expression of viral proteins alone is insufficient to reproduce the augmentation of expression of *DHCR24* induced by HCV.

DHCR24 Promoter Activity Is Potentiated by the Expression of HCV

The 5′-flanking region contains a number of possible transcriptional regulatory elements, including three candidate-binding motifs for the endoplasmic reticulum (ER) stress-responsive transcription factor, XBP1. Cellular ER stress is induced in response to the expression of the HCV gene and infection by HCV [Tardif et al., 2005]. Thus, to explore host factors involved in the transcriptional regulation of *DHCR24*, the 5′-flanking genomic region (~5 kb) of *DHCR24* was isolated. Subsequently, *DHCR24* promoter reporter plasmids that contain the 5′-flanking region of *DHCR24* and the firefly luciferase gene were constructed (Fig. 2A). Relevant regions of the promoter were defined by constructing deletion mutants of the 5′-flanking regions, which were analyzed by a dual luciferase reporter assay in the presence or absence of full-length HCV genome expression—resulting from transfection with pCA-Rz [Tsukiyama-Kohara et al., 2004] or the control pCAGGS vector, respectively (Fig. 2B). Progressive shortening of the 5′-flanking regions did not result in significant differences in the basal promoter activity (Fig. 2B). The −515/+113 construct also produced a significant response in the presence of full-length HCV genome expression.

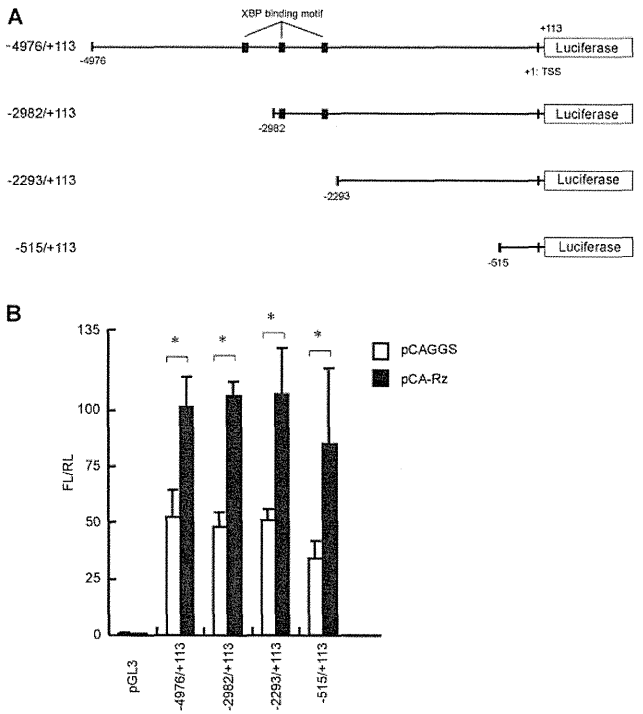

Fig. 2. *DHCR24* promoter activity is augmented by the expression of HCV. **A:** The 5′-flanking region of *DHCR24* was cloned from HepG2 and inserted upstream of the firefly luciferase gene in pGL3 (−4976/+113). A deletion series of the 5′-flanking regions was also constructed (−2982/+113, −2293/+113, and −515/+113). The black boxes indicate potential binding sites for the ER stress-responsive transcription factor, XBP-1. TSS, transcription start site (+1). **B:** HepG2 cells (1×10^4 cells/well in a 96-well plate) were co-transfected with each *DHCR24* promoter reporter plasmid (0.25 μg/well), a Renilla luciferase expression vector (phRL-TK; 0.025 μg/well), and either an expression vector containing the HCV full-length genome (pCA-Rz; 0.5 μg/well) or an empty expression vector (pCAGGS). Luciferase activity at 48 h post-transfection is shown as the ratio of firefly luciferase (FL) to Renilla luciferase (RL). Data are shown as the mean ± SD from 2 representative experiments performed in triplicate ($^*P < 0.05$).

Additional reporter deletion mutants were constructed to define the region in the *DHCR24* promoter that is responsive to HCV expression. To this aim, potential binding motifs for transcription factors were predicted in the minimized *DHCR24* promoter sequence (nucleotides −515/+113; Fig. 3A), and a series of promoter mutants containing sequential 100-bp deletions was constructed. As shown in Fig. 3A, while the promoter activity of −515/+113, −400/+113, −300/+113, and −200/+113 constructs was increased significantly by expression of HCV ($^*P < 0.05$), the promoter activity of the −100/+113 construct was unchanged. Therefore, an HCV-responsive sequence appears to be located in the upstream region (−200 to −100 bp) from the transcriptional start site of *DHCR24*, which includes sequences with similarity to the consensus-binding motifs for AP-2α, Sp1, MZF-1, Pax-4, and NF-Y.

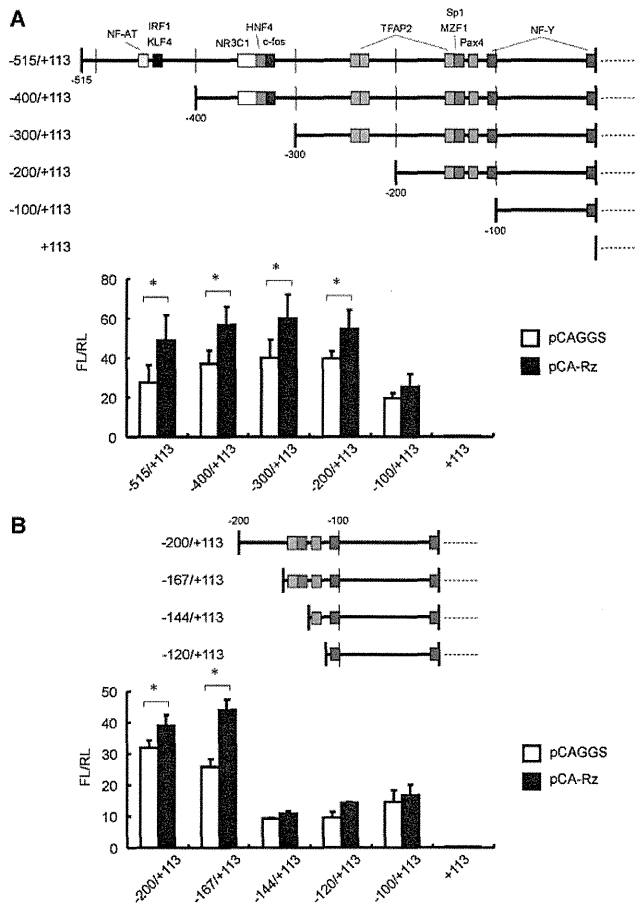

Fig. 3. Responsiveness of the *DHCR24* promoter to the expression of HCV. **A:** A *DHCR24* promoter series with sequential 100-bp deletions was constructed and analyzed as described in the legend to Fig. 2B ($^*p < 0.05$). **B:** An additional deletion series (−167/+113, −144/+113, and −120/+113) was constructed and analyzed as described in (A).

A more detailed deletion series (−167/+113, −144/+113, and −120/+113) was constructed (Fig. 3B) to determine the minimum-binding motif that responds to HCV expression. The responsiveness to the expression of HCV was lost with the removal of the proximal portion (−167 to −145), which includes candidate-binding motifs for AP-2α, Sp1, and MZF-1. Thus, the identified HCV response element in the *DHCR24* promoter represents the minimum element of DNA sequence required for the promotion of the expression of DHCR24 induced by HCV.

HCV Expression Augments the Interaction Between the HCV Response Element and the Binding Molecule(s)

Transcription of *DHCR24* is upregulated significantly in RzM6-LC cells that show persistent expression of HCV [Nishimura et al., 2009]. Therefore, the effect of expression of HCV on the interaction between the HCV response element and its related transcription factor(s) was examined. Nuclear extracts were prepared from RzM6-LC cells, and an electrophoretic mobility shift assay (EMSA) using a DIG-labeled double-stranded oligonucleotide corresponding to the response element (−167/−140, 28 bp; Fig. 4A) was performed. The interaction between the response element and the nuclear factor was increased significantly in nuclear extracts from RzM6-LC cells compared with that in RzM6-0d cells (Fig. 4B). Thus, the binding affinity or quantity of the nuclear factor may be increased by the expression of HCV. The shifted band corresponding to the Sp1 consensus sequence also increased in RzM6-LC cells compared with that in control RzM6-0d cells, whereas no difference was

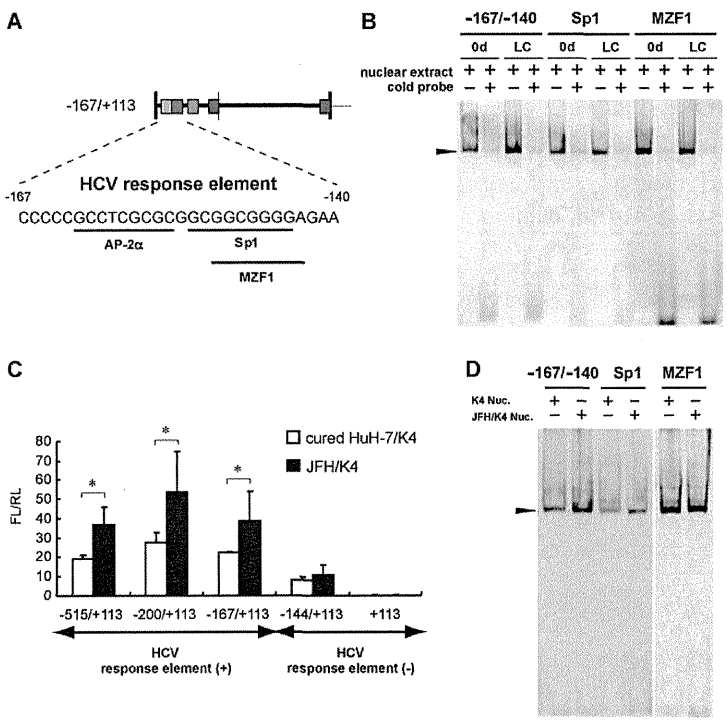

Fig. 4. The HCV response element mediates the overexpression of *DHCR24* induced by HCV. **A**: The HCV response element (−167/−140) in the 5′-flanking region of *DHCR24* includes sequences with similarity to the consensus-binding motifs for AP-2α, Sp1, and MZF-1. **B**: Nuclear extracts were prepared from RzM6-0d and RzM6-LC cells and subjected to an electrophoresis mobility shift assay (EMSA; 10 μg/sample) using the DIG-labeled HCV response element (28-bp), Sp1 (22-bp), or MZF-1 (21-bp) probes. Cold probe indicates unlabeled oligonucleotides. The arrowhead indicates the interaction between the binding factor(s) and each oligonucleotide. **C**: Cured HuH-7/K4 cells and JFH/K4 cells were co-transfected with each *DHCR24* promoter reporter plasmid (0.5 μg/well) and phRL-TK (0.05 μg/well) and analyzed as described in Fig. 2B ($^*P < 0.05$). (**D**) Nuclear extracts prepared from cured HuH-7/K4 cells or JFH/K4 cells were subjected to EMSA (25 μg/sample) using the DIG-labeled HCV response element, Sp1, or MZF-1 probes.

noted in the intensity of the shifted band for the MZF-1 sequence between the RzM6-LC and RzM6-0d cells (Fig. 4B). In contrast to Sp1, the ability of endogenous MZF-1 to bind to its target sequence (affinity and/or amount) in the RzM6-LC cells was approximately equivalent to that observed in the RzM6-0d cells. Thus, MZF-1 is not likely to be involved in the increase, mediated by HCV expression, in the shifted band corresponding to the response element.

HCV Infection Upregulates the Transcriptional Activity of the DHCR24 Promoter Through HCV Response Element

An in vitro model of HCV infection that replicates the entire HCV life cycle [Wakita et al., 2005] was used to confirm that transcription of *DHCR24* was mediated through the HCV response element. JFH/K4 cells, which show persistent infection with the HCV JFH-1 strain [Wakita et al., 2005], and control cells (cured HuH-7/K4) were transfected with the *DHCR24* promoter reporter plasmids, and promoter activity was measured. While *DHCR24* promoter reporters that included the HCV response element (−515/+113, −200/+113, and −167/+113) displayed significantly higher activity in JFH/K4 cells that in control cells, no difference was seen between the JFH/K4 cells and control cells transfected with the reporter lacking the HCV response element (−144/+113; Fig. 4C). These results suggest that the transcriptional activity of the *DHCR24* promoter was upregulated by HCV infection in a manner dependent on the response elements. Furthermore, augmentation of complex formation with the response element and the Sp1 probe was confirmed by EMSA using nuclear extracts from JFH/K4 and cured HuH-7/K4 cells (Fig. 4D).

Sp1 Binds to the HCV Response Element

The HCV response element (−167/−140) includes candidate-binding motifs for Sp1, MZF-1, and AP-2α (Fig. 4A). However, expression of AP-2 is repressed in the HepG2 cell line from which RzM6-LC cells are derived [Williams et al., 1988]. Thus, binding of AP-2α to the response element was investigated by a supershift assay using anti-Myc and nuclear extract from HepG2 cells transfected with a Myc-tagged AP-2α expression vector (Fig. 5A). The mobility of the DNA-AP-2α complex was supershifted by the addition of anti-Myc (lane 6) but not control IgG (lane 5), whereas an additional shifted band corresponding to the response element was not observed after addition of anti-Myc (lane 3). Therefore, although exogenous AP-2α protein expressed in HepG2 cells binds to the AP-2α consensus sequence, it does not bind to the HCV response element.

The ability of Sp1 to form a DNA–protein complex with the HCV response element was investigated by performing EMSAs in the presence of mithramycin A (MMA)—a GC-specific DNA-binding antibiotic that binds to the GC-box in the promoter to block binding of Sp1 or other Sp family proteins [Blume et al., 1991]. As shown in Fig. 5B, MMA (2.5, 5.0, and 10 μM) inhibited complex formation in a dose-dependent manner. In contrast, the formation of DNA–protein complexes with the MZF-1 probe was not affected by the addition of MMA, suggesting that the inhibition mediated by MMA was specific for the GC box-Sp1, and that complex formation with the response element requires the Sp1 binding site. A supershift assay using nuclear extract from HepG2 cells transfected with a Myc-tagged Sp1 expression vector and anti-Myc was also performed (Supplementary Fig. 2). The mobility of the HCV response element and the Sp1 consensus sequence was supershifted partially by addition of anti-Myc (lanes 3 and 6). The effect of silencing the expression of Sp1 with small interfering RNA (siRNA) was analyzed by EMSA using nuclear extracts from Sp1-knockdown RzM6-0d and RzM6-LC cells (Fig. 5C). DNA–protein complexes with the response element or the Sp1 probe were not observed (lanes 2, 4, 6, and 8); however, formation of DNA–MZF-1 complexes was not influenced by siRNA treatment (lanes 9–12). Immunoblotting was used to confirm efficient silencing of the Sp1 protein in cells used to generate the nuclear extracts (Fig. 5D). A significant decrease in the expression of DHCR24 was observed in the cytosolic fraction from RzM6 cells transfected with siRNA specific for Sp1 (Fig. 5D). Thus, these results indicate that Sp1, but neither AP-2α nor MZF-1, bound to the HCV response element, and that Sp1 may play an important role in the transcriptional regulation of *DHCR24*.

Transcriptional Regulation of DHCR24 Through the HCV Response Element Is Mediated by Oxidative Stress

DHCR24 functions as a mediator of the cellular response to oxidative stress [Greeve et al., 2000; Benvenuti et al., 2005; Di Stasi et al., 2005; Luciani et al., 2005; Lu et al., 2008] and is a hydrogen peroxide scavenger [Lu et al., 2008]. Expression of the *DHCR24* gene is also induced in response to oxidative stress [Wu et al., 2004; Benvenuti et al., 2006; Kuehnle et al., 2008]. Expression of the HCV gene elevates the level of reactive oxygen species (ROS) via dysregulation of ER-mediated calcium homeostasis, which results in oxidative stress [Tardif et al., 2005]. Therefore, the role of oxidative stress induced by HCV in the regulatory mechanism of the expression of *DHCR24* was examined. HepG2 cells were treated with hydrogen peroxide (H_2O_2) and transfected with reporter plasmids containing the *DHCR24* promoter deletion mutants. Measurement of promoter activity revealed a significant increase in transcription in response to oxidative stress (H_2O_2) for *DHCR24* promoters containing the HCV response element (−4976/+113, −2982/+113, −515/+113, and −167/+113) but not for the promoter lacking the response element (−144/+113; Fig. 6A). Therefore, enhanced transcription in response to oxidative stress by reporter constructs

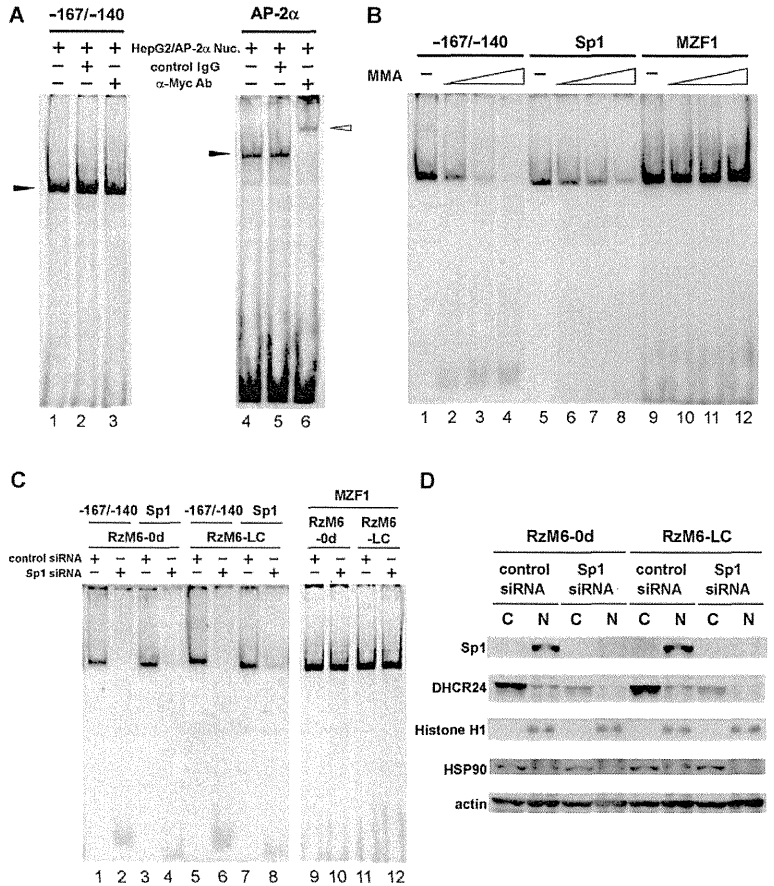

Fig. 5. Sp1 binds to the HCV response element. **A**: Nuclear extract was prepared from HepG2 cells transfected with pcDNA6-AP-2α-myc and subjected to EMSA (10 μg/sample) using DIG-labeled HCV response element or AP-2α probes (26-bp). For a supershift analysis of myc-tagged AP-2α, anti-Myc, or control IgG was added to the binding reaction. The closed arrowhead indicates the interaction between the binding factor(s) and each oligonucleotide, and an additional interaction with antibody is indicated by an open arrowhead. **B**: Nuclear extract from HepG2 cells was pre-incubated at 4°C for 1 h with different concentrations (2.5, 5, and 10 μM) of mithramycin A (MMA) and subjected to EMSA (10 μg/sample) using the DIG-labeled HCV response element, Sp1, or MZF-1 probes. **C**: Nuclear extracts were prepared from RzM6 cells transfected with Sp1 siRNA or control siRNA and subjected to EMSA (10 μg/sample) using the DIG-labeled HCV response element, Sp1, or MZF-1 probes. **D**: Expression of Sp1, DHCR24, and other proteins was detected in both the nuclear fraction (N), used for the EMSA shown in Fig. 4C, and in the cytosolic-membrane fraction (C).

containing the *DHCR24* promoter may be mediated through the HCV response element. The formation of complexes containing the response element or Sp1 probe was increased markedly in the nuclear extracts from the H_2O_2-treated HepG2 cells (Fig. 6B) or other hepatic cell lines (Supplementary Fig. 3), suggesting that oxidative stress enhances the binding affinity of Sp1 to the HCV response element.

Overexpression of DHCR24 in M6-LC Cells Is Blocked by an ROS Scavenger

The increase in the expression of DHCR24 induced by oxidative stress can be blocked by treatment with an ROS scavenger, *N*-acetylcysteine (NAC) [Wu et al., 2004], which is a precursor of the potent biological antioxidant glutathione. The H_2O_2-induced overexpression

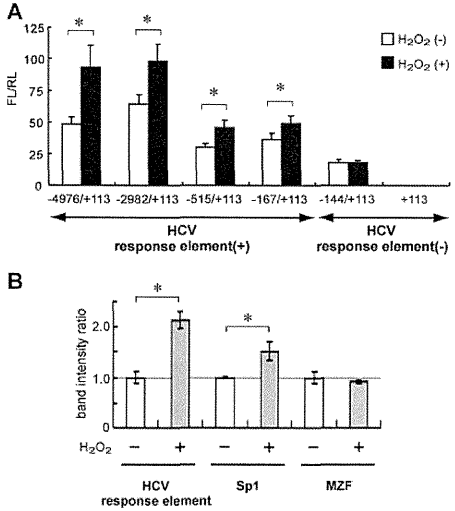

Fig. 6. Oxidative stress increases the transcription of *DHCR24* through the HCV response element and Sp1. **A**: HepG2 cells (1×10^4 cells/well in a 96-well plate) were co-transfected with individual *DHCR24* promoter reporter plasmids (0.5 μg/well) and phRL-TK (0.05 μg/well). Forty-four hours post-transfection, cells were treated with or without 1 mM H_2O_2 for 4 h and analyzed as described in Fig. 2B (*$P < 0.05$). **B**: Nuclear extracts prepared from H_2O_2-treated (1 mM, 4 h) or untreated HepG2 cells were subjected to EMSA (10 μg/sample) using the DIG-labeled HCV response element, Sp1, or MZF-1 probes. Densitometric analysis of shifted bands was performed using the Image Quant software. Data are shown as the mean + SD from triplicate quantifications of two representative experiments (*$P < 0.05$).

of DHCR24 was inhibited by pre-treatment with NAC and blocked partially by NAC treatment after the induction of oxidative stress (~50% suppression; Fig. 7A). The enhanced expression of DHCR24 in RzM6-LC cells decreased after 12 or 24 h of treatment with NAC without influencing the level of expression of HCV, suggesting that overexpression of DHCR24 in cells expressing HCV is mediated through oxidative stress.

Overexpression and Enhanced Phosphorylation of Sp1 in the Cells Expressing HCV

Sp1 is a transcription factor that is activated in response to a variety of cellular stressors, including oxidative stress [Schafer et al., 2003; Chu and Ferro, 2006; Dasari et al., 2006; Qin et al., 2009; Lin et al., 2011]. Thus, Sp1 may play an important role in linking oxidative stress and augmentation of *DHCR24* transcription in cells expressing HCV. Sp1 was overexpressed significantly in RzM6-LC cells treated with H_2O_2 compared with the control cells (Fig. 8A). Phosphorylation of Sp1 at Ser101 was also elevated under oxidative stress. Both the basal level and phosphorylation status of nuclear Sp1 were higher in the presence of HCV (RzM6-LC cells) than in the absence of HCV (RzM6-0d cells; Fig. 8B).

Phosphorylation of Sp1 at Ser101 is a target of the DNA damage signaling pathway mediated by ATM (ataxia telangiectasia mutated) and ATR (ATM and Rad3-related) kinases [Olofsson et al., 2007; Iwahori et al., 2008]. As shown in Fig. 8C, phosphorylation of Sp1 at Ser101 was no longer detectable following pretreatment with an ATM kinase inhibitor (KU55933) before exposure to H_2O_2. In contrast, phosphorylation was not affected by other kinase inhibitors (phosphatidylinositol-3 kinase inhibitor, LY294002 or MEK1 inhibitor, PD98059). Similarly, phosphorylation of Sp1 at Thr453, which is important for transcriptional activation of Sp1 [Milanini-Mongiat et al., 2002; D'Addario et al., 2006; Hsu et al., 2006; Lin et al., 2011], was not seen in response to oxidative stress following treatment with KU55933 (Fig. 8C). The induction of expression of DHCR24 after H_2O_2 exposure was suppressed significantly by treatment with KU55933 or NAC, which corresponds with inhibition of Sp1 phosphorylation. In the presence of MMA, the phosphorylation of Sp1 was not inhibited. However, since MMA blocks the binding of Sp1 [Blume et al., 1991], the induction of expression of DHCR24 by H_2O_2 was inhibited. Impairment of DHCR24 induction by H_2O_2 was also observed after treatment with siRNAs targeting ATM (Supplementary Fig. 4).

Studies on the relationship between HCV and ATM have reported that the interaction of NS3/4A with ATM results in delayed de-phosphorylation of both phosphorylated ATM and phosphorylated histone H2AX at Ser139 (γH2AX), which acts as a substrate for ATM in response to DNA damage [Lai et al., 2008]. In the present study, delayed de-phosphorylation of γH2AX was also observed in HCV replicon cells (Supplementary Fig. 5), which corresponded with increased phosphorylation of the H2AX Ser139 residue in cells expressing HCV (Fig. 8). Similarly, phosphorylation of ATM was sustained in HCV replicon cells (Supplementary Fig. 6). Therefore, DNA repair may be impaired in cells expressing or replicating HCV, resulting in sustained DNA damage. As a result, downstream substrates such as Sp1 Ser101 and Thr453 residues or the H2AX Ser139 residue may be phosphorylated to a greater extent in cells expressing HCV compared with control cells in the basal state or cells under oxidative stress (Fig. 8A and B).

Taken together, these results indicate that the oxidative stress induced by HCV may produce quantitative as well as qualitative activation of Sp1, thereby resulting in augmentation of *DHCR24* transcription.

DISCUSSION

HCV establishes chronic infection and induces persistent overexpression of DHCR24 in human hepatocytes [Nishimura et al., 2009]. HCV also confers

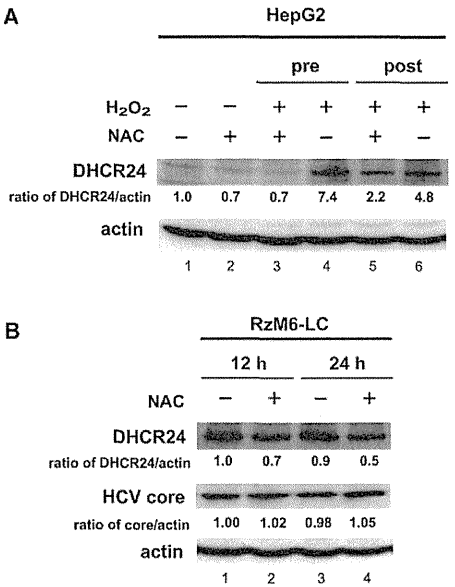

Fig. 7. Overexpression of DHCR24 in the cells expressing HCV is blocked by treatment with an oxidative stress scavenger. **A**: HepG2 cells were treated without (lanes 1, 4, and 6) or with (lanes 2 and 5) NAC (10 mM, 8 h). Cells treated with H_2O_2 (1 mM, 4 h) were also treated with 10 mM NAC for 8 h either before (pre; lanes 3 and 4) or after (post; lanes 5 and 6) H_2O_2 exposure. Whole-cell lysates (40 μg/lane) were analyzed by 10% SDS–PAGE and immunoblotting using a DHCR24/Seladin-1 mAb. Immunoblotting with an actin mAb served as the internal loading control. The ratio of DHCR24/actin was normalized to that of untreated cells (lane 1). **B**: RzM6-LC cells were treated with NAC (10 mM) for 12 h (lane 2) or 24 h (lane 4). Whole-cell lysates were analyzed as described in (A). The ratio of HCV core to actin protein was also calculated. Experiments were performed three times, and representative results are shown.

resistance to the apoptosis induced by oxidative stress and suppresses p53 activity by blocking nuclear p53 acetylation and increasing the interaction between p53 and HDM2 (p53-specific E3 ligase) in the cytoplasm, which may be mediated by inhibition of p53 degradation. Thus, the augmentation of DHCR24 by HCV reflects the tumorigenicity of hepatocytes. The present study identified the genomic region of *DHCR24* that is responsive to HCV, and showed that this response is mediated through the activation of Sp1 induced by oxidative stress. In general, expression of the HCV gene elevates the levels of ROS through dysregulation of ER-mediated calcium homeostasis [Tardif et al., 2005]. In healthy cells, ROS usually exist in equilibrium with antioxidants that scavenge ROS and prevent cellular injury. However, this critical balance may be disrupted in the cells infected with HCV, resulting in the accumulation of ROS and the development of constitutive oxidative stress.

Sp1 is a member of the Sp/KLF family of transcription factors that bind to GC elements of promoters [Black et al., 2001; Kaczynski et al., 2003; Chu and Ferro, 2005; Li and Davie, 2010]. Under a variety of endogenous and exogenous stimuli—including oxidative stress and DNA damage—activation of Sp1 may be mediated via induction of expression of Sp1 and post-translational modifications such as acetylation, sumoylation, O-linked glycosylation, and phosphorylation. Sp1 is phosphorylated by several kinases, including DNA-dependent protein kinase, casein kinase II, and cyclin A/cdk2, which exert both positive and negative effects on transcription [Jackson et al., 1990; Armstrong et al., 1997; Fojas de Borja et al., 2001; Ryu et al., 2003]. Sp1 is the only Sp/KLF family member to contain putative consensus SQ/TQ cluster domains within the transactivation domains, which suggests that Sp1 is a substrate of the PI3K-related kinases, for example, ATM, DNA-dependent protein kinase, and ATR. Indeed, Sp1 is a target of the ATM-dependent DNA damage response pathway [Iwahori et al., 2007, 2008; Olofsson et al., 2007]. ATM plays a central role in orchestrating molecular events involved in double-strand break signaling, which is mediated via the phosphorylation of a variety of substrate proteins—including p53 and BRCA1 transcription factors—involved in the DNA damage response. As a result, these phosphorylation events lead to cell cycle checkpoint activation, DNA repair, altered gene expression patterns, and/or apoptosis [Shiloh, 2006].

Given the role of Sp1 in oxidative stress [Schafer et al., 2003; Chu and Ferro, 2006; Dasari et al., 2006; Rojo et al., 2006; Qin et al., 2009; Lin et al., 2010], Sp1 may be regulated by the oxidative stress induced by HCV and the subsequent phosphorylation, which depends on ATM. However, little is known regarding the regulation of Sp1 in response to DNA damage. Although the precise role of phosphorylation of Sp1 at Ser101 in the DNA damage response is unclear, the similar kinetics of Sp1 and γH2AX phosphorylation [Olofsson et al., 2007] suggest that Sp1 is an early target of the DNA damage response pathway. Thus, Sp1 may be involved in modulating the cellular response to DNA damage to prevent cell death [Ryu et al., 2003]. Phosphorylation of Sp1 at Ser101 and histone H2AX, which occurs in parallel in response to oxidative stress, was enhanced in cells expressing HCV compared with that observed in control cells (Fig. 8A). Interestingly, augmentation of Sp1 phosphorylation in parallel with histone H2AX phosphorylation was also detected for cells expressing HCV in the basal state (Fig. 8A and B), which may be primarily due to the increase in endogenous Sp1 protein (Fig. 8A and B). In support of these results, enhanced phosphorylation of Ser101 on Sp1 occurs upon HSV-1 infection, and is mediated by ATM [Iwahori et al., 2007]. Thus, increased phosphorylation of Sp1 and γH2AX in cells expressing HCV is likely to reflect the higher activity

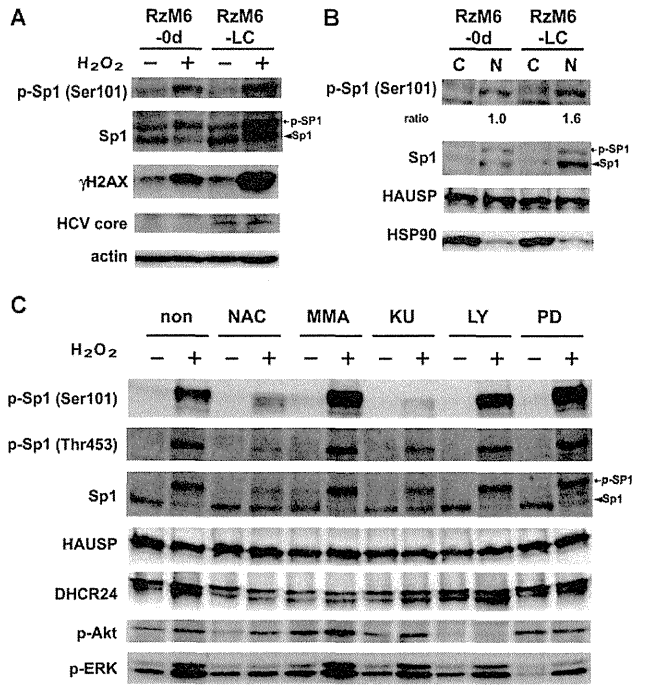

Fig. 8. Overexpression and elevated phosphorylation of Sp1 in the cells expressing HCV. **A**: RzM6-0d and RzM6-LC cells were treated with or without H_2O_2 (1 mM, 4 h). Whole-cell lysates (15 μg/lane) were analyzed by 15% SDS–PAGE and immunoblotting using phospho-H2AX (Ser139) (γH2AX) and HCV core mAbs. An actin mAb served as an internal loading control. Whole-cell lysates (25 μg/lane) were analyzed by 5% SDS–PAGE and immunoblotting using anti-Sp1 (phosphorylated Sp1 and native Sp1, as indicated) and anti-phospho-Sp1 (Ser101) was performed. **B**: RzM6-0d and RzM6-LC cells were fractionated to produce nuclear (N) and cytosolic-membrane fractions (C). Fractionated samples (15 μg/lane) were analyzed as described in (**A**). The ratio of phosphorylated Sp1 to Sp1 protein is indicated. Immunoblotting using anti-HAUSP served as a high-molecular-weight loading control. **C**: RzM6-0d cells were pre-treated for 8 h with NAC (10 mM), MMA (10 μM), KU55933 (KU; 10 μM), LY294002 (LY; 50 μM), or PD98059 (PD; 50 μM) and incubated for 4 h in the absence or presence of H_2O_2 (1 mM). Whole-cell lysates (40 μg/lane) were analyzed by 5% SDS–PAGE and immunoblotting using anti-phospho-Sp1 (Ser101), (Thr453), and polyclonal anti-Sp1 (white arrowhead, phosphorylated Sp1; black arrowhead, native Sp1). Detection of HAUSP was performed to confirm the quantity of loaded protein in each lane. Whole-cell lysates (25 μg/lane) were analyzed simultaneously by 10% SDS–PAGE and immunoblotting using anti-DHCR24/seladin-1 mAb, anti-phospho-Akt (Ser473), and anti-phospho-ERK antibodies.

of ATM, which may result from the accumulation and frequency of DNA damage caused by increased generation of endogenous ROS.

Oxidative stress is a common mechanism of liver injury [Loguercio and Federico, 2003] and is mediated by the direct effects of ROS on signal transduction pathways, including extracellular signal-regulated kinase 1/2 (ERK1/2), c-Jun N-terminal kinase (JNK), and p38 mitogen-activated protein kinases (MAPKs), which act as downstream kinases in the MAPK cascade to phosphorylate Sp1 Thr453/739 residues [Milanini-Mongiat et al., 2002; D'Addario et al., 2006; Hsu et al., 2006; Chuang et al., 2008; Lin et al., 2011]. These signal transduction pathways are also stimulated by oxidative stress in the hepatic cells expressing or replicating HCV, [Qadri et al., 2004; Burdette et al., 2010; Lin et al., 2010]. Therefore, oxidative stress in response to HCV may induce downstream signaling pathways, such as ERK1/2, JNK, and p38 MAPK as well as ATM/ATR, to activate Sp1 via post-translational modifications.

Sp1 is a host factor activated by several viral proteins, including HIV-1 Vpr, and HTLV-1 Tax [Peng et al., 2003; Amini et al., 2004; Chang et al., 2005; Zhang et al., 2009]. The HCV core and NS5A proteins also activate Sp1 [Lee et al., 2001; Xiang et al., 2010]. The HCV core upregulates the DNA-binding activity and phosphorylation of Sp1 [Lee et al., 2001], and NS5A may also exert a similar effect on Sp1 activity. However, a physical interaction between these

proteins and Sp1 has not yet been demonstrated. Both HCV core and NS5A proteins have a high potential for oxidative stress induction [García-Mediavilla et al., 2005; Dionisio et al., 2009], which may mediate activation of Sp1. On the other hand, individual viral proteins were insufficient to increase the expression of DHCR24 (Fig. 1A). Therefore, in addition to induction of oxidative stress by each viral protein, the persistence of the signaling pathways induced by oxidative stress, for example, ATM (Supplementary Fig. 6), may also be required for the Sp1-mediated increase in the expression of DHCR24.

The results of the present study revealed that knockdown of expression of Sp1 almost completely blocked the enhanced expression of DHCR24. Sp1 is expressed ubiquitously in various mammalian cells and is involved in regulating the transcriptional activity of genes implicated in many cellular processes [Black et al., 2001; Kaczynski et al., 2003; Chu and Ferro, 2005; Li and Davie, 2010]. Thus, Sp1 may represent an essential master regulator among the myriad of transcription factors involved in the direct regulation of *DHCR24* transcription.

In conclusion, HCV was shown to enhance the expression of DHCR24 via the activation of Sp1, which may shed light on the mechanism of tumorigenesis associated with HCV.

ACKNOWLEDGMENTS

The authors would like to thank Ms. Ryoko Takehara and Yuri Kasama for their technical support, Yuko Tokunaga for her comments, and Dr. Chieko Kai for her support.

REFERENCES

Amini S, Saunders M, Kelley K, Khalili K, Sawaya BE. 2004. Interplay between HIV-1 Vpr and Sp1 modulates p21(WAF1) gene expression in human astrocytes. J Biol Chem 279:46046–46056.

Armstrong SA, Barry DA, Leggett RW, Mueller CR. 1997. Casein kinase II-mediated phosphorylation of the C terminus of Sp1 decreases its DNA binding activity. J Biol Chem 272:13489–13495.

Benvenuti S, Luciani P, Vannelli GB, Gelmini S, Franceschi E, Serio M, Peri A. 2005. Estrogen and selective estrogen receptor modulators exert neuroprotective effects and stimulate the expression of selective Alzheimer's disease indicator-1, a recently discovered antiapoptotic gene, in human neuroblast long-term cell cultures. J Clin Endocrinol Metab 90:1775–1782.

Benvenuti S, Saccardi R, Luciani P, Urbani S, Deledda C, Cellai I, Francini F, Squecco R, Rosati F, Danza G, Gelmini S, Greeve I, Rossi M, Maggi R, Serio M, Peri A. 2006. Neuronal differentiation of human mesenchymal stem cells: Changes in the expression of the Alzheimer's disease-related gene seladin-1. Exp Cell Res 312:2592–2604.

Black AR, Black JD, Azizkhan-Clifford J. 2001. Sp1 and kruppel-like factor family of transcription factors in cell growth regulation and cancer. J Cell Physiol 188:143–160.

Blume SW, Snyder RC, Ray R, Thomas S, Koller CA, Miller DM. 1991. Mithramycin inhibits SP1 binding and selectively inhibits transcriptional activity of the dihydrofolate reductase gene in vitro and in vivo. J Clin Invest 88:1613–1621.

Bruchfeld A, Stahle L, Andersson J, Schvarcz R. 2001. Ribavirin treatment in dialysis patients with chronic hepatitis C virus infection—A pilot study. J Viral Hepat 8:287–292.

Burdette D, Olivarez M, Waris G. 2010. Activation of transcription factor Nrf2 by hepatitis C virus induces the cell-survival pathway. J Gen Virol 91:681–690.

Chang LK, Chung JY, Hong YR, Ichimura T, Nakao M, Liu ST. 2005. Activation of Sp1-mediated transcription by Rta of Epstein–Barr virus via an interaction with MCAF1. Nucleic Acids Res 33:6528–6539.

Chu S, Ferro TJ. 2005. Sp1: Regulation of gene expression by phosphorylation. Gene 348:1–11.

Chu S, Ferro TJ. 2006. Identification of a hydrogen peroxide-induced PP1-JNK1-Sp1 signaling pathway for gene regulation. Am J Physiol Lung Cell Mol Physiol 291:L983–992.

Chuang JY, Wang YT, Yeh SH, Liu YW, Chang WC, Hung JJ. 2008. Phosphorylation by c-Jun NH_2-terminal kinase 1 regulates the stability of transcription factor Sp1 during mitosis. Mol Biol Cell 19:1139–1151.

Crameri A, Biondi E, Kuehnle K, Lutjohann D, Thelen KM, Perga S, Dotti CG, Nitsch RM, Ledesma MD, Mohajeri MH. 2006. The role of seladin-1/DHCR24 in cholesterol biosynthesis, APP processing and Abeta generation in vivo. EMBO J 25:432–443.

D'Addario M, Arora PD, McCulloch CA. 2006. Role of p38 in stress activation of Sp1. Gene 379:51–61.

Dasari A, Bartholomew JN, Volonte D, Galbiati F. 2006. Oxidative stress induces premature senescence by stimulating caveolin-1 gene transcription through p38 mitogen-activated protein kinase/Sp1-mediated activation of two GC-rich promoter elements. Cancer Res 66:10805–10814.

Di Stasi D, Vallacchi V, Campi V, Ranzani T, Daniotti M, Chiodini E, Fiorentini S, Greeve I, Prinetti A, Rivoltini L, Pierotti MA, Rodolfo M. 2005. DHCR24 gene expression is upregulated in melanoma metastases and associated to resistance to oxidative stress-induced apoptosis. Int J Cancer 115:224–230.

Dignam JD, Lebovitz RM, Roeder RG. 1983. Accurate transcription initiation by RNA polymerase II in a soluble extract from isolated mammalian nuclei. Nucleic Acids Res 11:1475–1489.

Dionisio N, Garcia-Mediavilla MV, Sanchez-Campos S, Majano PL, Benedicto I, Rosado JA, Salido GM, Gonzalez-Gallego J. 2009. Hepatitis C virus NS5A and core proteins induce oxidative stress-mediated calcium signalling alterations in hepatocytes. J Hepatol 50:872–882.

Fojas de Borja P, Collins NK, Du P, Azizkhan-Clifford J, Mudryj M. 2001. Cyclin A-CDK phosphorylates Sp1 and enhances Sp1-mediated transcription. EMBO J 20:5737–5747.

García-Mediavilla MV, Sánchez-Campos S, González-Pérez P, Gómez-Gonzalo M, Majano PL, Lopez-Cabrera M, Clemente G, García-Monzon C, González-Gallego J. 2005. Differential contribution of hepatitis C virus NS5A and core proteins to the induction of oxidative and nitrosative stress in human hepatocyte-derived cells. J Hepatol 43:606–613.

Greeve I, Hermans-Borgmeyer I, Brellinger C, Kasper D, Gomez-Isla T, Behl C, Levkau B, Nitsch RM. 2000. The human DIMINUTO/DWARF1 homolog seladin-1 confers resistance to Alzheimer's disease-associated neurodegeneration and oxidative stress. J Neurosci 20:7345–7352.

Hsu MC, Chang HC, Hung WC. 2006. HER-2/neu represses the metastasis suppressor RECK via ERK and Sp transcription factors to promote cell invasion. J Biol Chem 281:4718–4725.

Iwahori S, Shirata N, Kawaguchi Y, Weller SK, Sato Y, Kudoh A, Nakayama S, Isomura H, Tsurumi T. 2007. Enhanced phosphorylation of transcription factor sp1 in response to herpes simplex virus type 1 infection is dependent on the ataxia telangiectasia-mutated protein. J Virol 81:9653–9664.

Iwahori S, Yasui Y, Kudoh A, Sato Y, Nakayama S, Murata T, Isomura H, Tsurumi T. 2008. Identification of phosphorylation sites on transcription factor Sp1 in response to DNA damage and its accumulation at damaged sites. Cell Signal 20:1795–1803.

Jackson SP, MacDonald JJ, Lees-Miller S, Tjian R. 1990. GC box binding induces phosphorylation of Sp1 by a DNA-dependent protein kinase. Cell 63:155–165.

Kaczynski J, Cook T, Urrutia R. 2003. Sp1- and Kruppel-like transcription factors. Genome Biol 4:206.

Kohara M, Tanaka T, Tsukiyama-Kohara K, Tanaka S, Mizokami M, Lau JY, Hattori N. 1995. Hepatitis C virus genotypes 1 and 2 respond to interferon-alpha with different virologic kinetics. J Infect Dis 172:934–938.

Koike K. 2007. Hepatitis C virus contributes to hepatocarcinogenesis by modulating metabolic and intracellular signaling pathways. J Gastroenterol Hepatol 22:S108–S111.

Kuehnle K, Crameri A, Kalin RE, Luciani P, Benvenuti S, Peri A, Ratti F, Rodolfo M, Kulic L, Heppner FL, Nitsch RM, Mohajeri MH. 2008. Prosurvival effect of DHCR24/Seladin-1 in acute and chronic responses to oxidative stress. Mol Cell Biol 28:539–550.

Lai CK, Jeng KS, Machida K, Cheng YS, Lai MM. 2008. Hepatitis C virus NS3/4A protein interacts with ATM, impairs DNA repair and enhances sensitivity to ionizing radiation. Virology 370:295–309.

Lavanchy D. 2009. The global burden of hepatitis C. Liver Int 29:74–81.

Lee S, Park U, Lee YI. 2001. Hepatitis C virus core protein transactivates insulin-like growth factor II gene transcription through acting concurrently on Egr1 and Sp1 sites. Virology 283:167–177.

Li L, Davie JR. 2010. The role of Sp1 and Sp3 in normal and cancer cell biology. Ann Anat 192:275–283.

Lin W, Tsai WL, Shao RX, Wu G, Peng LF, Barlow LL, Chung WJ, Zhang L, Zhao H, Jang JY, Chung RT. 2010. Hepatitis C virus regulates transforming growth factor beta1 production through the generation of reactive oxygen species in a nuclear factor kappaB-dependent manner. Gastroenterology 138:2509–2518.

Lin HH, Lai SC, Chau LY. 2011. Heme oxygenase-1/carbon monoxide induces vascular endothelial growth factor expression via p38 kinase-dependent activation of Sp1. J Biol Chem 286:3829–3838.

Loguercio C, Federico A. 2003. Oxidative stress in viral and alcoholic hepatitis. Free Radic Biol Med 34:1–10.

Lu X, Kambe F, Cao X, Kozaki Y, Kaji T, Ishii T, Seo H. 2008. 3Beta-hydroxysteroid-delta24 reductase is a hydrogen peroxide scavenger, protecting cells from oxidative stress-induced apoptosis. Endocrinology 149:3267–3273.

Luciani P, Gelmini S, Ferrante E, Lania A, Benvenuti S, Baglioni S, Mantovani G, Cellai I, Ammannati F, Spada A, Serio M, Peri A. 2005. Expression of the antiapoptotic gene seladin-1 and octreotide-induced apoptosis in growth hormone-secreting and nonfunctioning pituitary adenomas. J Clin Endocrinol Metab 90:6156–6161.

Milanini-Mongiat J, Pouyssegur J, Pages G. 2002. Identification of two Sp1 phosphorylation sites for p42/p44 mitogen-activated protein kinases: Their implication in vascular endothelial growth factor gene transcription. J Biol Chem 277:20631–20639.

Nakamura H, Ogawa H, Kuroda T, Yamamoto M, Enomoto H, Kishima Y, Yoshida K, Ito H, Matsuda M, Noguchi S. 2002. Interferon treatment for patients with chronic hepatitis C infected with high viral load of genotype 2 virus. Hepatogastroenterology 49:1373–1376.

Nishimura T, Kohara M, Izumi K, Kasama Y, Hirata Y, Huang Y, Shuda M, Mukaidani C, Takano T, Tokunaga Y, Nuriya H, Satoh M, Saito M, Kai C, Tsukiyama-Kohara K. 2009. Hepatitis C virus impairs p53 via persistent overexpression of 3beta-hydroxysterol Delta24-reductase. J Biol Chem 284:36442–36452.

Olofsson BA, Kelly CM, Kim J, Hornsby SM, Azizkhan-Clifford J. 2007. Phosphorylation of Sp1 in response to DNA damage by ataxia telangiectasia-mutated kinase. Mol Cancer Res 5:1319–1330.

Peng H, He H, Hay J, Ruyechan WT. 2003. Interaction between the varicella zoster virus IE62 major transactivator and cellular transcription factor Sp1. J Biol Chem 278:38068–38075.

Qadri I, Iwahashi M, Capasso JM, Hopken MW, Flores S, Schaack J, Simon FR. 2004. Induced oxidative stress and activated expression of manganese superoxide dismutase during hepatitis C virus replication: Role of JNK, p38 MAPK and AP-1. Biochem J 378:919–928.

Qin K, Zhao L, Ash RD, McDonough WF, Zhao RY. 2009. ATM-mediated transcriptional elevation of prion in response to copper-induced oxidative stress. J Biol Chem 284:4582–4593.

Rojo AI, Salina M, Salazar M, Takahashi S, Suske G, Calvo V, de Sagarra MR, Cuadrado A. 2006. Regulation of heme oxygenase-1 gene expression through the phosphatidylinositol 3-kinase/PKC-zeta pathway and Sp1. Free Radic Biol Med 41:247–261.

Ryu H, Lee J, Zaman K, Kubilis J, Ferrante RJ, Ross BD, Neve R, Ratan RR. 2003. Sp1 and Sp3 are oxidative stress-inducible, antideath transcription factors in cortical neurons. J Neurosci 23:3597–3606.

Schafer G, Cramer T, Suske G, Kemmner W, Wiedenmann B, Hocker M. 2003. Oxidative stress regulates vascular endothelial growth factor-A gene transcription through Sp1- and Sp3-dependent activation of two proximal GC-rich promoter elements. J Biol Chem 278:8190–8198.

Shiloh Y. 2006. The ATM-mediated DNA-damage response: Taking shape. Trends Biochem Sci 31:402–410.

Takano T, Kohara M, Kasama Y, Nishimura T, Saito M, Kai C, Tsukiyama-Kohara K. 2011a. Translocase of outer mitochondrial membrane 70 expression is induced by hepatitis C virus and is related to the apoptotic response. J Med Virol 83:801–809.

Takano T, Tsukiyama-Kohara K, Hayashi M, Hirata Y, Satoh M, Tokunaga Y, Tateno C, Hayashi Y, Hishima T, Funata N, Sudo M, Kohara M. 2011b. Augmentation of DHCR24 expression by hepatitis C virus infection facilitates viral replication in hepatocytes. J Hepatol 55:512–521.

Tardif KD, Waris G, Siddiqui A. 2005. Hepatitis C virus, ER stress, and oxidative stress. Trends Microbiol 13:159–163.

Tsukiyama-Kohara K, Tone S, Maruyama I, Inoue K, Katsume A, Nuriya H, Ohmori H, Ohkawa J, Taira K, Hoshikawa Y, Shibasaki F, Reth M, Minatogawa Y, Kohara M. 2004. Activation of the CKI-CDK-Rb-E2F pathway in full genome hepatitis C virus-expressing cells. J Biol Chem 279:14531–14541.

Wakita T, Pietschmann T, Kato T, Date T, Miyamoto M, Zhao Z, Murthy K, Habermann A, Krausslich HG, Mizokami M, Bartenschlager R, Liang TJ. 2005. Production of infectious hepatitis C virus in tissue culture from a cloned viral genome. Nat Med 11:791–796.

Waterham HR, Koster J, Romeijn GJ, Hennekam RC, Vreken P, Andersson HC, FitzPatrick DR, Kelley RI, Wanders RJ. 2001. Mutations in the 3beta-hydroxysterol Delta24-reductase gene cause desmosterolosis, an autosomal recessive disorder of cholesterol biosynthesis. Am J Hum Genet 69:685–694.

Williams T, Admon A, Luscher B, Tjian R. 1988. Cloning and expression of AP-2, a cell-type-specific transcription factor that activates inducible enhancer elements. Genes Dev 2:1557–1569.

Wu C, Miloslavskaya I, Demontis S, Maestro R, Galaktionov K. 2004. Regulation of cellular response to oncogenic and oxidative stress by Seladin-1. Nature 432:640–645.

Xiang Z, Qiao L, Zhou Y, Babiuk LA, Liu Q. 2010. Hepatitis C virus nonstructural protein-5A activates sterol regulatory element-binding protein-1c through transcription factor Sp1. Biochem Biophys Res Commun 402:549–553.

Zhang L, Zhi H, Liu M, Kuo YL, Giam CZ. 2009. Induction of p21(CIP1/WAF1) expression by human T-lymphotropic virus type 1 Tax requires transcriptional activation and mRNA stabilization. Retrovirology 6:35.

Contents lists available at SciVerse ScienceDirect

Virus Research

journal homepage: www.elsevier.com/locate/virusres

Short communication

Translocase of outer mitochondrial membrane 70 induces interferon response and is impaired by hepatitis C virus NS3

Yuri Kasama[a], Makoto Saito[a], Takashi Takano[b], Tomohiro Nishimura[c], Masaaki Satoh[a,d], Zhongzhi Wang[a], Salem Nagla Elwy Salem Ali[a,e], Shinji Harada[e], Michinori Kohara[f], Kyoko Tsukiyama-Kohara[a,*]

[a] Department of Experimental Phylaxiology, Faculty of Life Sciences, Kumamoto University, 1-1-1 Honjo Kumamoto City, Kumamoto 860-8556, Japan
[b] Division of Veterinary Public Health, Nippon Veterinary and Life Science University, 1-7-1 Kyonan, Musashino, Tokyo 180-8602, Japan
[c] KAKETSUKEN, Kyokushi, Kikuchi, Kumamoto 869-1298, Japan
[d] Department of Virology I, National Institute of Infectious Diseases, Tokyo 162-8640, Japan
[e] Department of Medical Virology, Faculty of Life Sciences, Kumamoto University, Japan
[f] Department of Microbiology and Cell Biology, Tokyo Metropolitan Institute of Medical Science, 2-1-6 Kamikitazawa, Setagaya-ku, Tokyo 156-8506, Japan

ARTICLE INFO

Article history:
Received 5 September 2011
Received in revised form 13 October 2011
Accepted 13 October 2011
Available online 20 October 2011

Keywords:
HCV
Tom70
MAVS
IFN
IRF-3
NS3

ABSTRACT

Hepatitis C virus (HCV) elevated expression of the translocase of outer mitochondrial membrane 70 (Tom70). Interestingly, overexpression of Tom70 induces interferon (IFN) synthesis in hepatocytes, and it was impaired by HCV. Here, we addressed the mechanism of this impairment. The HCV NS3/4A protein induced Tom70 expression. The HCV NS3 protein interacted in cells, and cleaved the adapter protein mitochondrial anti-viral signaling (MAVS). Ectopic overexpression of Tom70 could not inhibit this cleavage. As a result, IRF-3 phosphorylation was impaired and IFN-β induction was suppressed. These results indicate that MAVS works upstream of Tom70 and the cleavage of MAVS by HCV NS3 protease suppresses signaling of IFN induction.

Type I interferon (IFN) induction is the front line of host defense against viral infection. Intracellular double-stranded RNA is a viral replication intermediate and contains pathogen-associated molecular patterns (PAMPS) (Saito et al., 2008) that are recognized by pathogen-recognition receptors (PRRs) to induce IFN. One PRR family includes the Toll-like receptors (TLRs), which are predominantly expressed in the endosome (Heil et al., 2004). Another route of IFN induction takes place in the cytosol through activation of specific RNA helicases, such as retinoic acid-inducible (RIG)-I and melanoma differentiation associated gene 5 (MDA5). The ligand for RIG-I is an uncapped 5′ triphosphate RNA, which is found in viral RNAs of the *Flaviviridae* family, including hepatitis C virus (HCV), paramyxovirus, and rhabdoviruses (Kato et al., 2006). MDA5 recognizes viruses with protected 5′ RNA ends, for example, picornaviruses (Hornung et al., 2006). The adapter protein that links the RNA helicase to the downstream MAPK, NF-κB, and IRF-3 signaling pathways is referred to as the mitochondrial anti-viral signaling (MAVS) protein (Seth et al., 2005); alternative names include IPS-1, interferon-promoter stimulator 1; VISA, virus-induced signaling adaptor; and CARDIF, CARD adapter inducing IFN. HCV nonstructural protein 3 (NS3) possesses a serine protease domain at the N terminus (amino acids (aa) 1–180) and has been found to cleave adaptor proteins, MAVS at aa 508 (Meylan et al., 2005) and Toll/IL-1R domain-containing adapter inducing IFN-β-deficient (TRIF at aa 372; Ferreon et al., 2005). These cleavages provoke abrogation of the induction of the IFN pathway.

The translocase of the outer membrane (TOM) is responsible for initial recognition of mitochondrial preproteins in the cytosol (Baker et al., 2007; Neupert and Herrmann, 2007). The TOM machinery consists of 2 import receptors, Tom20 and Tom70, and, along with several other subunits, comprises the general import pore (Abe et al., 2000). Recently, Tom70 was found to interact with MAVS (Liu et al., 2010). Ectopic expression or silencing of Tom70, respectively, enhanced or impaired IRF3-mediated gene expression and IFN-β production. Sendai virus infection accelerated the Tom70-mediated IFN induction and the interaction of Tom70 with MAVS. These recent findings indicated that Tom70 might be a critical mediator during IFN induction (Liu et al., 2010).

We previously observed that HCV induces Tom70 and is related to the apoptotic response (Takano et al., 2011a). However, no synergistic effect was observed for IFN induction by Tom70 and HCV. Therefore, in the present study, we have investigated the mechanism of modification of the Tom70-induced IFN synthesis pathway by HCV and clarified a finely balanced system regulated by viral protein.

The expression of Tom70 protein was examined using western blotting and modification by HCV was characterized (Fig. 1A). The level of Tom70 protein was increased in RzM6-LC cells compared with that in RzM6-0d cells (Tsukiyama-Kohara et al., 2004). The full-length HCV-RNA expression was induced by 4-hydroxytamoxifen (100 nM) and passaged for more than 44 days in RzM6-LC cells, and HCV expression was not induced in RzM6-0d cells. Silencing of HCV expression by siRNA (R5; Thermo Scientific) abolished core protein expression, and decreased the level of Tom70 protein expression in RzM6-LC cells (Fig. 1A). Silencing of Tom70 by siRNA significantly decreased the level of HCV core protein expression in RzM6-LC cells (Fig. 1A). The siRNA against 3-beta-hydroxysterol-delta24 reductase (DHCR24) slightly decreased the level of Tom70 protein. In contrast, the

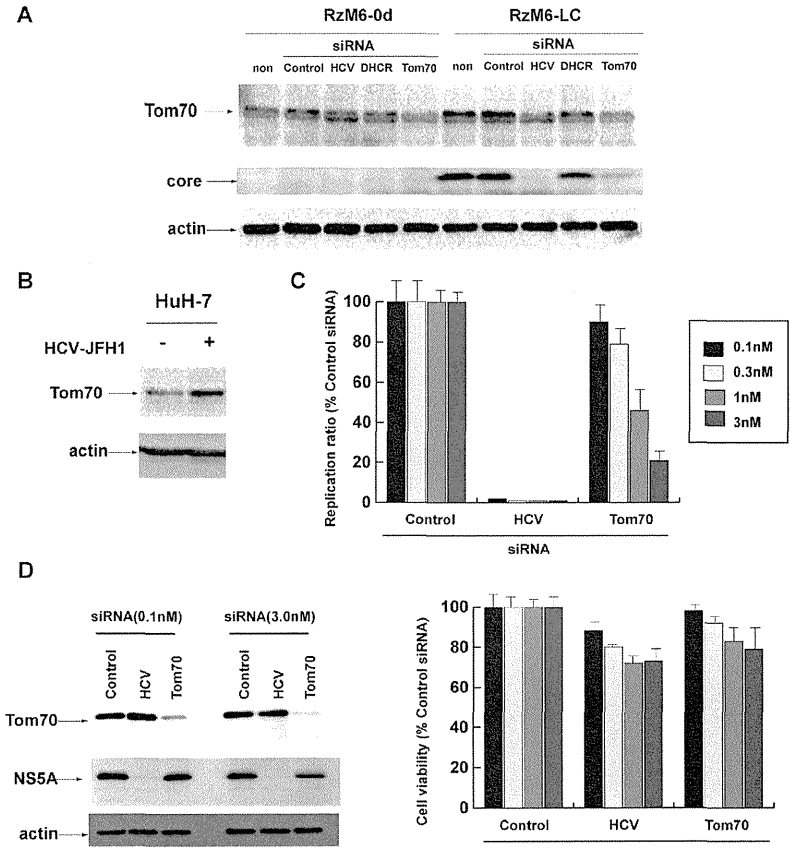

Fig. 1. HCV induces overexpression of Tom70 but impairs Tom70-induced IFN synthesis. (A) RzM6 cells (HCV-) and RzM6-LC cells (HCV+) were transfected with siRNAs of control (non-target siRNA#3: Thermo Fisher Scientific), HCV (R5: 5′-GUCUCGUAGACCGUGCAUCAuu-3′), DHCR24 (Nishimura et al., 2009), and Tom70 (Takano et al., 2011a). Control cells were mock-transfected. Tom70 protein was detected with MAb2-243a (Takano et al., 2011a) and actin protein was detected as an internal control (lower column). (B) HuH-7 cells were infected with HCV JFH-1 strain; Tom70 protein and actin protein were detected. (C) The HCV replicon cells (FLR3-1; Takano et al., 2011b) were transfected with siRNAs (control, HCV (R7: 5′-GUCUCGUAGACCGUGCACCAuu-3′), Tom70; 0.1, 0.3, 1, 3 nM) and HCV replication activity was measured with luciferase activity using the Bright-Glo luciferase assay kit (Promega). Cell viability was measured using WST-8 (Dojindo) reagent. Ratio with those of control siRNA treatment was calculated. Vertical bars were S.D. (D) HCV replicon cells (FLR3-1) were transfected with control, HCV (R7) and Tom70 siRNAs (0.1, 0.3 nM) and Tom70, NS5A and actin proteins were detected.

* Corresponding author. Present address: Transboundary Animal Diseases Center, Faculty of Agriculture, Kagoshima University, 1-21-24 Korimoto Kagoshima-shi, Kagoshima 890-0065, Japan. Tel.: +81 99 285 3589/96 373 5560; fax: +81 99 285 3589/96 373 5562.
E-mail address: kkohara@kumamoto-u.ac.jp (K. Tsukiyama-Kohara).

0168-1702/$ – see front matter © 2011 Elsevier B.V. All rights reserved.
doi:10.1016/j.virusres.2011.10.009

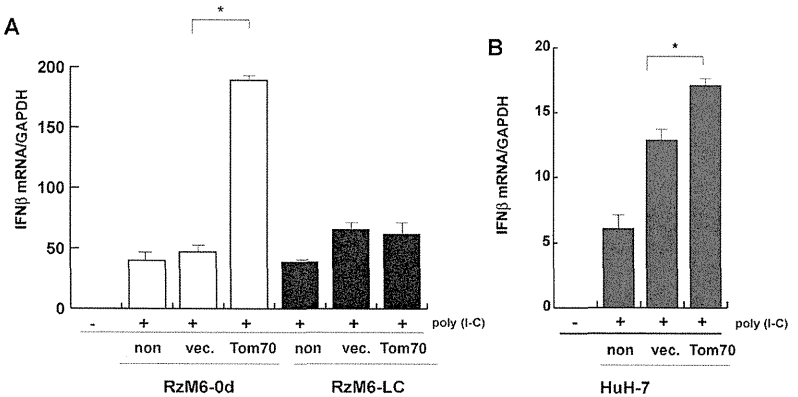

Fig. 2. Tom70-induced IFN synthesis was impaired by HCV. (A) RzM6-0d cells and LC cells were transfected with mock-vector, control pcDNA vector (vec.), or pcDNA-Tom70 expression vector, and the amount of IFN-β mRNA was measured by RTD-PCR and normalized to the amount of GAPDH mRNA using Gene expression assay kit (GE-Healthcare). Poly(I–C) (GE Healthcare) (5 μg) was transfected with RNAi Max reagent (Invitrogen) and IFN-βmRNA was measured after 6 h of poly(I–C) treatment. Vertical bars indicate S.D. $^*p < 0.05$. (B) HuH-7 cells were transfected with mock-vector, control vector, or Tom70 expression vector, and the amount of IFN-β mRNA was measured by RTD-PCR and normalized to the amount of GAPDH mRNA. Vertical bars indicate S.D. $^*p < 0.05$.

control siRNA did not have a significant effect on Tom70 protein expression.

We next examined the effects of HCV JFH-1 (Wakita et al., 2005) infection on Tom70 expression (Fig. 1B). Infection with HCV significantly increased the level of Tom70 protein expression. We also examine the role of Tom70 in HCV replication (Fig. 1C and D). Silencing of Tom70 by siRNA decreased the HCV replication in a dose dependent manner.

Thus, HCV induces Tom70 expression, and Tom70 is involved in viral replication.

It was recently shown that Tom70 recruits TBK1/IRF3 to mitochondria by binding to Hsp90 and inducing IFN-β synthesis (Liu et al., 2010). Therefore, we examined the effects of Tom70 overexpression on IFN synthesis and modification by HCV (Fig. 2). Level of IFN-β mRNA synthesis was quantitated by real-time detection (RTD) PCR. Overexpression of Tom70 by transfection of pcDNA6-Tom70 (Takano et al., 2011a) induced IFN-β mRNA synthesis in the absence of HCV after poly(I–C) treatment (RzM6-0d cells). However, the Tom70-mediated induction of IFN-β mRNA transcription was impaired in the presence of HCV (RzM6-LC cells) (Fig. 2A). Overexpression of Tom70 induced IFN-β mRNA synthesis in HuH-7 cells (Fig. 2B). Induction of IFN-β mRNA was lower in HuH-7 cells than HepG2 based RzM6 cells, which might be due to the defect in IFN induction system in HuH-7 cells (Preiss et al., 2008).

We have further addressed the mechanism of impairment of IFN-β mRNA transcription by HCV.

To identify the viral protein that was responsible for the induction of Tom70, we examined the Tom70 protein expression levels in HCV core, E1, E2, NS2, NS3/4A, NS4B, NS5A, and NS5B protein-expressing cells (data not shown), and Tom70 protein expression level was highest in the NS3/4A-expressing cells than was observed in cells expressing other proteins (Fig. 3A, data not shown), indicating an effect of HCV NS3/4A protein on Tom70 expression.

The expression vector of Myc- and His-tagged Tom70 was transfected into the empty control or NS3/4A-expressing cells and immunoprecipitated with anti-Myc antibody (Suppl. Fig. 1A). Results showed that Myc-Tom70 was precipitated in both cells (right panel) and NS3 protein was specifically precipitated by anti-Myc antibody in the NS3/4A-expressing cells (left panel). NS4A protein could not be detected (data not shown).

We next stained the NS3/4A-expressing cells with anti-NS3 and -Tom70 antibodies, and observed with confocal microscopy (Suppl. Fig. 1B). The signal of NS3 protein was clearly merged with that of Tom70, strongly supporting the possibility that the NS3 protein co-localizes with the Tom70 protein.

To clarify the effect of Tom70 on NS3, we transfected NS3/4A-expressing cells with the siRNA of Tom70 (Fig. 3A). Silencing of Tom70 decreased the level of NS3 protein in cells, but did not influence the levels of the MAVS and NF-κB proteins. These results suggest the possibility that Tom70 may increase the stability of NS3 protein in cells.

Tom70 reportedly interacts with MAVS during viral infection (Liu et al., 2010). Therefore, we examined the MAVS protein in cells expressing either the control empty or NS3/4A lenti-virus vector (Fig. 3B). Cleavage of MAVS (indicated as ΔMAVS) was observed in NS3/4A protein-expressing cells, as was reported previously (Meylan et al., 2005). Overexpression of Tom70 did not have a significant effect on the MAVS expression level and did not prevent MAVS cleavage by NS3. IRF-3 phosphorylation was suppressed in NS3/4A-expressing cells and was not influenced by Tom70 overexpression. The induction of IFN-β was impaired in NS3/4A-expressing cells, even in the presence of Tom70 overexpression (Fig. 3C). These data may indicate that MAVS exists upstream of Tom70 and that cleavage of MAVS by NS3/4A impaired the downstream signaling activation of IRF-3 phosphorylation (Suppl. Fig. 2).

Mitochondria provide a substantial platform for the regulation of IFN signaling. The MAVS adapter protein is a member of the family of RIG-I like receptors (RLRs), which links the mitochondria to the mammalian antiviral defense system (Seth et al., 2005). Proteomic studies have demonstrated that MAVS interacts with Tom70 (Liu et al., 2010). This interaction was accelerated by Sendai virus infection and synergized with ectopic expression of Tom70 to significantly increase the production of IFN-β (Liu et al., 2010). The results of the present study revealed that infection with HCV induced Tom70 expression, but the presence of HCV impaired IFN

Author's personal copy

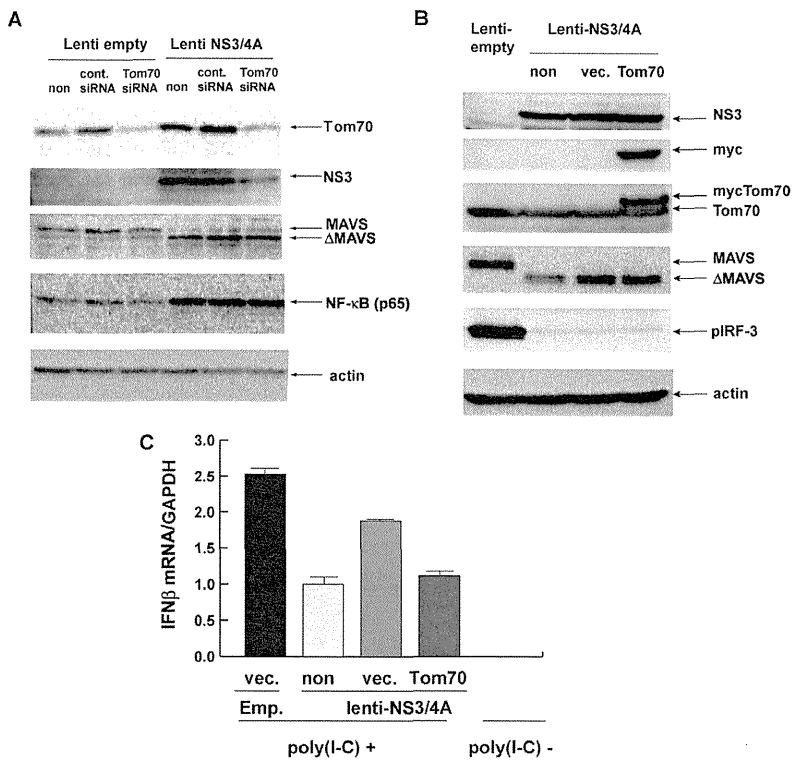

Fig. 3. Silencing of Tom70 decreased the level of NS3 and cleavage of MAVS by NS3/4A impaired IRF-3 phosphorylation even in the presence of Tom70. (A) Empty or NS3/4A-lenti virus vector expressing HepG2 cells were transfected with control siRNA and Tom70 siRNA or mock-transfected (non) as a control. MAVS, NS3, Tom70, and actin proteins were detected by western blot. (B) Empty or NS3/4A-expressing HepG2 cells were transfected with control pcDNA vector (vec.) and pcDNA6 (Invitrogen)-Tom70 or mock-transfected (non) as a control. NS3, Tom70, phosphorylated IRF-3, MAVS, and actin proteins were examined by western blot. (C) IFN-β mRNA was measured by RTD-PCR and normalized with GAPDH mRNA amount in empty or NS3/4A expressing cells with transfection of mock (non), pcDNA-vector (vec.) or pcDNA-Tom70 (Tom70). Poly(I–C) was treated, as described in the legend of Fig. 2.

induction. It has been reported that the C-terminal transmembrane domain (TM) of MAVS interacts with the N-terminal transmembrane domain of Tom70 (Liu et al., 2010). The HCV NS3 protein cleaves MAVS at residue 508 (Meylan et al., 2005), which should impair the interaction of MAVS and Tom70. This may attenuate the downstream signaling pathway (TBK-IRF3) and the induction of IFN synthesis (Suppl. Fig. 2). In our study, the level of NF-κB protein was not significantly influenced by Tom70 in the presence or absence of NS3. This may indicate that other pathways, such as TLR3 and downstream pathways, might compensate to maintain the NF-κB protein expression level in the absence of the MAVS-Tom70 signaling pathway.

Infection with HCV induced expression of Tom70, but the activation of the IFN signaling pathway was abrogated by the HCV NS3 protease. These findings indicate that recovery of the MAVS-Tom70 pathway may be a means to increase the efficacy of IFN therapy against HCV infection.

Recently, we observed that overexpression of Tom70 increased the resistance to the TNFα-induced apoptotic response (Takano et al., 2011a), indicating that Tom70 overexpression might contribute to the apoptotic resistance of HCV-infected cells and the establishment of persistent HCV infection. Thus, Tom70 might be a novel target for the regulation of HCV infection.

Acknowledgements

Authors thank Professor Yoshiharu Matsuura for providing the rabbit polyclonal NS5A antibody. This work was supported by grants from the Ministry of Health, Labor, and Welfare of Japan and the Ministry of Education, Culture, Sports, Science, and Technology of Japan.

Appendix A. Supplementary data

Supplementary data associated with this article can be found, in the online version, at doi:10.1016/j.virusres.2011.10.009.

References

Abe, Y., Shodai, T., Muto, T., Mihara, K., Torii, H., Nishikawa, S., Endo, T., Kohda, D., 2000. Structural basis of presequence recognition by the mitochondrial protein import receptor Tom20. Cell 100 (5), 551–560.

Baker, M.J., Frazier, A.E., Gulbis, J.M., Ryan, M.T., 2007. Mitochondrial protein-import machinery: correlating structure with function. Trends Cell Biol. 17 (9), 456–464.

Ferreon, J.C., Ferreon, A.C., Li, K., Lemon, S.M., 2005. Molecular determinants of TRIF proteolysis mediated by the hepatitis C virus NS3/4A protease. J. Biol. Chem. 280 (21), 20483–20492.

Heil, F., Hemmi, H., Hochrein, H., Ampenberger, F., Kirschning, C., Akira, S., Lipford, G., Wagner, H., Bauer, S., 2004. Species-specific recognition of single-stranded RNA via toll-like receptor 7 and 8. Science 303 (5663), 1526–1529.

Hornung, V., Ellegast, J., Kim, S., Brzozka, K., Jung, A., Kato, H., Poeck, H., Akira, S., Conzelmann, K.K., Schlee, M., Endres, S., Hartmann, G., 2006. 5′-Triphosphate RNA is the ligand for RIG-I. Science 314 (5801), 994–997.

Kato, H., Takeuchi, O., Sato, S., Yoneyama, M., Yamamoto, M., Matsui, K., Uematsu, S., Jung, A., Kawai, T., Ishii, K.J., Yamaguchi, O., Otsu, K., Tsujimura, T., Koh, C.S., Reis e Sousa, C., Matsuura, Y., Fujita, T., Akira, S., 2006. Differential roles of MDA5 and RIG-I helicases in the recognition of RNA viruses. Nature 441 (7089), 101–105.

Liu, X.Y., Wei, B., Shi, H.X., Shan, Y.F., Wang, C., 2010. Tom70 mediates activation of interferon regulatory factor 3 on mitochondria. Cell Res. 20 (9), 994–1011.

Meylan, E., Curran, J., Hofmann, K., Moradpour, D., Binder, M., Bartenschlager, R., Tschopp, J., 2005. Cardif is an adaptor protein in the RIG-I antiviral pathway and is targeted by hepatitis C virus. Nature 437 (7062), 1167–1172.

Neupert, W., Herrmann, J.M., 2007. Translocation of proteins into mitochondria. Annu. Rev. Biochem. 76, 723–749.

Nishimura, T., Kohara, M., Izumi, K., Kasama, Y., Hirata, Y., Huang, Y., Shuda, M., Mukaidani, C., Takano, T., Tokunaga, Y., Nuriya, H., Satoh, M., Saito, M., Kai, C., Tsukiyama-Kohara, K., 2009. Hepatitis C virus impairs p53 via persistent overexpression of 3beta-hydroxysterol Delta24-reductase. J. Biol. Chem. 284 (52), 36442–36452.

Preiss, S., Thompson, A., Chen, X., Rodgers, S., Markovska, V., Desmond, P., Visvanathan, K., Li, K., Locarnini, S., Revill, P., 2008. Characterization of the innate immune signalling pathways in hepatocyte cell lines. J. Viral Hepat. 15 (12), 888–900.

Saito, T., Owen, D.M., Jiang, F., Marcotrigiano, J., Gale Jr., M., 2008. Innate immunity induced by composition-dependent RIG-I recognition of hepatitis C virus RNA. Nature 454 (7203), 523–527.

Seth, R.B., Sun, L., Ea, C.K., Chen, Z.J., 2005. Identification and characterization of MAVS, a mitochondrial antiviral signaling protein that activates NF-kappaB and IRF 3. Cell 122 (5), 669–682.

Takano, T., Kohara, M., Kasama, Y., Nishimura, T., Saito, M., Kai, C., Tsukiyama-Kohara, K., 2011a. Translocase of outer mitochondrial membrane 70 expression is induced by hepatitis C virus and is related to the apoptotic response. J. Med. Virol. 83 (5), 801–809.

Takano, T., Tsukiyama-Kohara, K., Hayashi, M., Hirata, Y., Satoh, M., Tokunaga, Y., Tateno, C., Hayashi, Y., Hishima, T., Funata, N., Sudo, M., Kohara, M., 2011b. Augmentation of DHCR24 expression by hepatitis C virus infection facilitates viral replication in hepatocytes. J. Hepatol. 55 (3), 512–521.

Tsukiyama-Kohara, K., Tone, S., Maruyama, I., Inoue, K., Katsume, A., Nuriya, H., Ohmori, H., Ohkawa, J., Taira, K., Hoshikawa, Y., Shibasaki, F., Reth, M., Minatogawa, Y., Kohara, M., 2004. Activation of the CKI-CDK-Rb-E2F pathway in full genome hepatitis C virus-expressing cells. J. Biol. Chem. 279 (15), 14531–14541.

Wakita, T., Pietschmann, T., Kato, T., Date, T., Miyamoto, M., Zhao, Z., Murthy, K., Habermann, A., Krausslich, H.G., Mizokami, M., Bartenschlager, R., Liang, T.J., 2005. Production of infectious hepatitis C virus in tissue culture from a cloned viral genome. Nat. Med. 11 (7), 791–796.

J Gastroenterol (2012) 47:444–451
DOI 10.1007/s00535-011-0505-8

ORIGINAL ARTICLE—LIVER, PANCREAS, AND BILIARY TRACT

Decrease in alpha-fetoprotein levels predicts reduced incidence of hepatocellular carcinoma in patients with hepatitis C virus infection receiving interferon therapy: a single center study

Yukio Osaki · Yoshihide Ueda · Hiroyuki Marusawa · Jun Nakajima · Toru Kimura · Ryuichi Kita · Hiroki Nishikawa · Sumio Saito · Shinichiro Henmi · Azusa Sakamoto · Yuji Eso · Tsutomu Chiba

Received: 28 July 2011 / Accepted: 24 October 2011 / Published online: 23 November 2011

Abstract

Background Increasing evidence suggests the efficacy of interferon therapy for hepatitis C in reducing the risk of hepatocellular carcinoma (HCC). The aim of this study was to identify predictive markers for the risk of HCC incidence in chronic hepatitis C patients receiving interferon therapy.

Methods A total of 382 patients were treated with standard interferon or pegylated interferon in combination with ribavirin for chronic hepatitis C in a single center and evaluated for variables predictive of HCC incidence.

Results Incidence rates of HCC after interferon therapy were 6.6% at 5 years and 13.4% at 8 years. Non-sustained virological response (non-SVR) to antiviral therapy was an independent predictor for incidence of HCC in the total study population. Among 197 non-SVR patients, independent predictive factors were an average alpha-fetoprotein (AFP) integration value $\geq$10 ng/mL and male gender. Even in patients whose AFP levels before interferon therapy were $\geq$10 ng/mL, reduction of average AFP integration value to <10 ng/mL by treatment was strongly associated with a reduced incidence of HCC. This was significant compared to patients with average AFP integration values of $\geq$10 ng/mL ($P = 0.009$).

Conclusions Achieving sustained virological response (SVR) by interferon therapy reduces the incidence of HCC in hepatitis C patients treated with interferon. Among non-SVR patients, a decrease in the AFP integration value by interferon therapy closely correlates with reduced risk of HCC incidence after treatment.

Keywords Alpha-fetoprotein · Hepatocellular carcinoma · Hepatitis C · Interferon

Y. Osaki · J. Nakajima · T. Kimura · R. Kita · H. Nishikawa · S. Saito · S. Henmi · A. Sakamoto · Y. Eso
Department of Gastroenterology and Hepatology, Osaka Red Cross Hospital, 5-53 Fudegasaki-cho, Tennoji-ku, Osaka 543-8555, Japan

Y. Ueda (✉) · H. Marusawa · Y. Eso · T. Chiba
Department of Gastroenterology and Hepatology, Graduate School of Medicine, Kyoto University, 54 Kawahara-cho, Shogoin, Sakyo-ku, Kyoto 606-8507, Japan
e-mail: yueda@kuhp.kyoto-u.ac.jp

Introduction

Hepatitis C virus (HCV) infection is a predominant cause of liver cirrhosis and hepatocellular carcinoma (HCC) in many countries, including Japan, the United States, and countries of Western Europe [1–5]. The annual incidence of HCC in patients with HCV-related cirrhosis ranged from 1 to 8% [6–9]. Even in the absence of liver cirrhosis, patients with chronic hepatitis caused by HCV infection are at a high risk of developing HCC. Indeed, a large-scale Japanese cohort study showed that the annual incidence of HCC is 0.5% among patients with stage F0 or F1 fibrosis and 2.0, 5.3, and 7.9% among those with F2, F3, and F4 fibrosis, respectively [9]. Periodic surveillance is recommended to detect HCC as early as possible in patients with HCV-related chronic liver disease; however, this may not be cost-effective. For patients with chronic hepatitis C, more effective detection and prevention of HCC is being sought by two important routes: (1) the attempt to discover noninvasive predictive markers and (2) development of treatment strategies to reduce the risk of HCC. There have been several attempts to discover non-invasive markers capable of predicting the risk of HCC incidence in patients with chronic hepatitis C [6, 10]. For example, a cohort

derived from the Hepatitis C Antiviral Long-term Treatment Against Cirrhosis (HALT-C) Trial identified older age, African American race, lower platelet count, higher alkaline phosphatase, and esophageal varices as risk factors for HCC [11].

There have also been a number of studies to evaluate the effect of anti-viral treatment of chronic hepatitis C on the incidence of HCC [12–19]. The results were summarized in a meta-analysis, which concluded that the effect of interferon on risk of HCC is mainly apparent in patients achieving a sustained virological response (SVR) to interferon therapy [13]. In addition, a number of studies have suggested the incidence of HCC is reduced in treated patients compared to historical controls [12, 15, 16, 19]. However, the recent HALT-C randomized control trial revealed that long-term pegylated interferon therapy does not reduce the incidence of HCC among patients with advanced hepatitis C who do not achieve SVRs. Reduction in the risk of HCC by maintenance therapy was shown only in patients with cirrhosis [14, 17]. These controversial results suggest that interferon therapy reduces the risk of HCC only in a group of patients with HCV-related chronic liver disease. Thus, it is important to evaluate the risk of HCC development in hepatitis C patients receiving interferon therapy and it will be clinically useful to discover markers distinguishing high- and low-risk groups.

Serum alpha-fetoprotein (AFP) has been widely used as a diagnostic marker of HCC [20–22]. However, elevation of serum AFP levels is often found in non-neoplastic liver diseases without evidence of HCC, including acute liver injury and chronic viral hepatitis [23–27], especially among patients with advanced chronic hepatitis C [28]. An increase of AFP after liver damage is interpreted as a sign of dedifferentiated hepatic regeneration [27]. There have been some reports that AFP is a significant predictor of HCC in patients with chronic hepatitis C [4, 5, 29]. In addition, it has recently been shown that AFP levels decrease in response to interferon administration in patients with chronic hepatitis C [30, 31], and that long-term interferon therapy for aged patients with chronic HCV infection is effective in decreasing serum AFP levels and preventing hepatocarcinogenesis [32, 33]. However, little is known about the relationship between changes in serum AFP level over time during interferon therapy and the development of HCC.

The aim of this large single center study was to identify predictive markers for the risk of HCC development in patients receiving interferon therapy for chronic hepatitis C. For this purpose, patients treated with standard or pegylated interferon, in combination with ribavirin, for chronic hepatitis C were enrolled and subjected to scheduled periodic surveillance for HCC and a number of potential predictive markers, including AFP and alanine aminotransferase (ALT) integration values, at a single center.

Materials and methods

Patients

Between January 2002 and April 2010, 528 patients with chronic hepatitis C received combination therapy with standard interferon and ribavirin ($n = 84$) or pegylated interferon and ribavirin ($n = 444$) at Osaka Red Cross Hospital. Eligibility criteria for treatment were positivity for serum HCV RNA and histological evidence of chronic hepatitis C ($n = 427/444$; 80.9%), or positivity for serum HCV RNA, liver enzyme levels greater than the normal upper limit, and an ultrasound image demonstrating chronic liver damage ($n = 101/444$; 19.1%). Exclusion criteria for treatment were as follows: neutrophil count <750 cells/μL, platelet count <50,000 cells/μL, hemoglobin level ≤9.0 g/dL, and renal insufficiency (serum creatinine levels >2 mg/dL).

Of 528 patients who received interferon therapy for chronic hepatitis C, 146 were excluded from this study for the following reasons: follow-up <24 weeks after the termination of the interferon therapy ($n = 122$), previously treated for HCC ($n = 22$), or occurrence of HCC during or within 24 weeks after treatment ($n = 2$). Therefore, 382 patients were enrolled for the study and were retrospectively analyzed.

To detect early-stage HCC, ultrasonography, dynamic contrast enhanced computed tomography (CT), dynamic contrast enhanced magnetic resonance imaging (MRI), and/or measurement of tumor markers (including AFP) were performed for all patients at least every 6 months. HCC was diagnosed radiologically as liver tumors displaying arterial hypervascularity and venous or delayed phase washout by dynamic contrast enhanced CT or MRI.

The study protocol was approved by the Ethics Committee at Osaka Red Cross Hospital and performed in compliance with the Helsinki Declaration.

Treatment protocol and definition of responses to treatment

The basic treatment protocol for patients with chronic hepatitis C consisted of 6 mega units of interferon-α-2b 3 times a week or 1.5 μg/kg of pegylated interferon α-2b once a week, combined with ribavirin at an oral dosage of 600–1000 mg/day. Duration of the treatment was 48–72 weeks for those with HCV genotype 1 and serum HCV RNA titer of >5 log IU/mL, and 24 weeks for all other patients.

Patients who were negative for serum HCV RNA for >6 months after completion of interferon therapy were defined as showing an SVR. Patients whose serum ALT levels decreased to the normal range and remained normal for >6 months after the termination of interferon therapy were defined as showing a sustained biochemical response (SBR).

Patients who did not achieve SVR received ursodeoxycholic acid and/or glycyrrhizin containing preparation (Stronger Neo-Minophagen C), when serum ALT levels were higher than the upper limit of normal.

Virological assays

HCV genotype was determined by polymerase chain reaction (PCR) amplification of the core region of the HCV genome using genotype-specific PCR primers [34]. Serum HCV RNA load was evaluated once a month during and 24 weeks after treatment using a PCR assay (Cobas Amplicor HCV Monitor, Roche Molecular Systems, Pleasanton, CA, USA).

Measurement of AFP and calculation of average integration value

AFP was measured in serum samples obtained from each patient at intervals of 1–3 months. The median number of examinations was 15 (range 1–70) in each patient. Serum AFP levels were determined by enzyme-linked immunosorbent assay, which was performed using a commercially available kit (ELISA-AFP, International Reagents, Kobe, Japan). Integration values of AFP and ALT were calculated as described in previous reports [35]. For example, the integration value of AFP was calculated as follows, $(y_0 + y_1) \times x_1/2 + (y_1 + y_2) \times x_2/2 + (y_2 + y_3) \times x_3/2 + (y_3 + y_4) \times x_4/2 + (y_4 + y_5) \times x_5/2 + (y_5 + y_6) \times x_6/2$, i.e., the area of each trapezoid representing an AFP value was measured the sum of the resulting values used to calculate the integration value (Fig. 1). The average integration value was obtained by dividing the integration value by the observation period from initiation of the treatment.

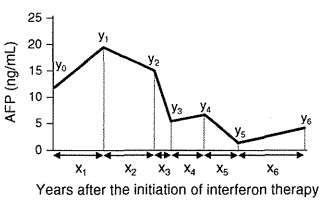

Fig. 1 Example plot of data used for calculation of average integration value of alpha-fetoprotein (AFP)

Statistical analysis

The Kaplan–Meier method was used to estimate the rates of development of HCC in patients after interferon therapy. Log-rank tests were used to evaluate the effects of predictive factors on incidence of HCC. Significance was defined as $P < 0.05$. Multivariate Cox regression analysis using the stepwise method was used to evaluate the association between HCC incidence and patient characteristics, and to estimate hazard ratio (HR) with a 95% confidence interval (CI). A P value of 0.1 was used for variable selection and was regarded as statistically significant. SAS version 9.2 (SAS Institute Inc., Cary, NC, USA) was used for statistical analysis.

Results

Characteristics of patients and incidence of HCC

This study included 382 patients treated for chronic hepatitis C with standard interferon or pegylated interferon in combination with ribavirin. Baseline clinical and virological characteristics of patients included in the study are summarized in Table 1. The median age of the patients at the outset of therapy was 59.0 years (range 18–81 years) and the median follow-up period was 4.1 years (range 0.1–8.4 years). The majority of patients were infected with HCV genotype 1b ($n = 229$; 60%), and median serum HCV RNA load was 6.1 log IU/mL (range 2.3–7.3 log IU/mL). Baseline (before interferon therapy) median serum AFP level was 6.9 ng/mL (range 1.6–478.3 ng/mL).

During follow-up, 23 patients (4.9%) developed HCC. The cumulative incidences of HCC, which was estimated using the Kaplan–Meier method, were 3.1, 6.6, and 13.4% at 3, 5, and 8 years, respectively (Fig. 2).

Predictive factors for incidence of HCC in all patients

Predictive factors for incidence of HCC in all 382 patients were analyzed using log-rank tests (Table 2). Univariate analysis showed that age ≥70 years ($P = 0.040$), non-SVR ($P < 0.0001$), non-SBR ($P = 0.027$), average ALT integration value ≥40 IU/L ($P = 0.001$), baseline AFP ≥10 ng/mL ($P = 0.005$), average AFP integration value ≥10 ng/mL ($P < 0.0001$), and baseline platelet count <150,000 platelets/μL ($P = 0.001$) were all significantly associated with the incidence of HCC. After multivariate analysis, the only variable remaining in the model was non-SVR (HR 8.413, 95% CI 1.068–66.300, $P = 0.043$).

Table 1 Characteristics of 382 patients with hepatitis C treated with interferon therapy in this study

Age (years)	59.0 (18–81)
[a]Males/females	192/190
Observation period (years)	4.1 (0.1–8.4)
[a]IFN + RBV/PEG-IFN + RBV	69/313
HCV genotype 1/2/unclassified	229/57/96
HCV RNA (log IU/mL)	6.1 (2.3–7.3)
White blood cell count (/μL)	4950 (2050–9970)
Hemoglobin (g/dL)	14.0 (10.3–18.8)
Platelet (10^4/μL)	15.0 (5.3–36.4)
AST (IU/L)	56 (17–244)
ALT (IU/L)	67 (16–416)
Bilirubin (mg/dL)	0.8 (0.3–2.4)
AFP (ng/mL)	6.9 (1.6–478.3)

Qualitative variables ([a]) are shown in number, and quantitative variables expressed as median (range)

IFN interferon, *RBV* ribavirin, *PEG-IFN* pegylated interferon, *AST* aspartate aminotransferase, *ALT* alanine aminotransferase, *AFP* alpha-fetoprotein

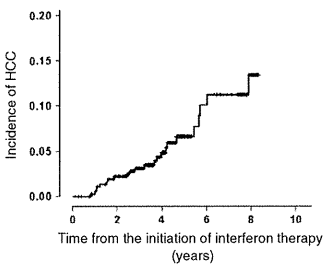

Fig. 2 Incidence of hepatocellular carcinoma (HCC) in 382 patients with hepatitis C who received interferon therapy, estimated using the Kaplan–Meier method

Further, although patients with average AFP integration values ≥10 ng/mL also appeared to have an increased risk of HCC, the difference did not reach statistical significance in the multivariate analysis ($P = 0.050$) (Table 3).

Predictive factors for incidence of HCC in non-SVR patients

Because non-SVR was the only predictive factor across the entire study cohort, to clarify predictive factors for incidence of HCC within this group, the same variables were further analyzed in non-SVR patients alone. By univariate analysis, average AFP integration value ≥10 ng/mL ($P = 0.019$) and baseline platelet count <150,000 ($P = 0.0022$) (Table 2) were again identified as significant predictive factors for incidence of HCC. In addition, male gender was significantly associated with incidence of HCC in non-SVR patients ($P = 0.022$). Multivariate analysis, however, indicated that only two variables were independently associated with incidence of HCC in non-SVR patients: average AFP integration value ≥10 ng/mL (HR 4.039, 95% CI 1.570–10.392, $P = 0.004$), and male gender

Table 2 Univariate analysis of predictive factors for incidence of hepatocellular carcinoma in all 382 and 197 non-SVR patients

Factors	All ($n = 382$)			Non-SVR ($n = 197$)		
	No.	Incidence of HCC ($n = 23$)		No.	Incidence of HCC ($n = 22$)	
		No. (%)	*P* value[a]		No. (%)	*P* value[a]
Age (years)						
<70	359	19 (5)	0.040	182	18 (10)	0.089
≥70	23	4 (17)		15	4 (27)	
Sex						
Female	190	8 (4)	0.125	111	8 (7)	0.022
Male	192	15 (8)		86	14 (16)	
HCV genotype						
1	229	12 (5)	0.452	137	12 (9)	0.796
Non-1	57	1 (2)		10	1 (10)	
Virological response						
SVR	185	1 (1)	<0.0001			
Non-SVR	197	22 (11)				
Biochemical response						
SBR	282	12 (4)	0.027	102	11 (11)	0.857
Non-SBR	86	11 (13)		81	11 (14)	
ALT before IFN therapy						
<40	79	2 (3)	0.274	39	2 (5)	0.319
≥40	301	21 (7)		158	20 (13)	
ALT integration value						
<40	238	6 (3)	0.001	79	5 (6)	0.153
≥40	142	17 (12)		118	17 (14)	
AFP before IFN therapy						
<10	230	7 (3)	0.005	102	7 (7)	0.124
≥10	116	14 (12)		75	13 (17)	
AFP integration value						
<10	258	8 (3)	<0.0001	115	8 (6)	0.019
≥10	63	12 (19)		53	11 (21)	
Platelet before IFN therapy						
<150,000	187	20 (11)	0.001	121	19 (16)	0.022
≥150,000	194	3 (2)		76	3 (4)	

[a] Log-rank test

SVR sustained virological response, *SBR* sustained biochemical response, *ALT* alanine aminotransferase, *IFN* interferon, *AFP* alpha-fetoprotein

Table 3 Multivariate analysis of the predictive factors for incidence of hepatocellular carcinoma in all 382 patients

Factors	Hazard ratio	95% CI	*P* value
Virological response			
SVR	1		
Non-SVR	8.413	1.068–66.300	0.043
AFP integration value			
<10	1		
≥10	2.580	0.999–6.659	0.050

SVR sustained virological response, *IFN* interferon, *AFP* alpha-fetoprotein

Table 4 Multivariate analysis of predictive factors for incidence of hepatocellular carcinoma in 197 non-SVR patients

Factors	Hazard ratio	95% CI	*P* value
AFP integration value			
<10	1		
≥10	4.039	1.570–10.392	0.004
Sex			
Female	1		
Male	3.636	1.383–9.563	0.009

AFP alpha-fetoprotein

(HR 3.636, 95% CI 1.383–9.563, $P = 0.009$) (Table 4). There was no significant difference in other variables including those identified as predictive factors in the entire study population (i.e., age, non-SBR, ALT integration value, AFP before interferon therapy) (Table 2).

AFP integration value as a predictive factor for HCC

Further analysis focused on the AFP integration value as this was the strongest predictive factor for incidence of HCC in non-SVR patients. Of the 382 patients, both baseline and AFP integration values were available for 321. These were divided into four groups: (1) AFP "low–low," (2) AFP "low–high," (3) AFP "high–low," and (4) AFP "high–high," for baseline AFP-average AFP integration values, respectively, where "high" is ≥10 ng/mL and "low" is <10 ng/mL. As shown in Fig. 3a, of the 321 patients, 211 (65.7%) showed baseline AFP levels <10 ng/mL. Of these 211, 207 (98%), were in the AFP low–low group, and only four in the AFP low–high groups. Baseline characteristics, including age, gender, serum HCV-RNA, aspartate aminotransferase (AST), ALT, bilirubin, white blood cell, hemoglobin, platelet, observation periods, and number of times of AFP measurement, were not different between AFP high–low group and high–high group. However, AFP-low group, which is a combination of the low–high and low–low groups, showed significantly lower AST level ($P < 0.00001$), lower ALT level ($P < 0.00001$), higher platelet count ($P < 0.00001$), shorter observation period ($P = 0.01448$), and fewer number of times of AFP examination ($P = 0.00035$), compared to both AFP high–high and AFP high–low group. Six patients (2.8%) with baseline AFP levels <10 ng/mL developed HCC in the follow-up period and none of these patients were among the four low–high group patients. Even in patients with high baseline AFP levels, incidence of HCC was only 3.9% among the AFP high–low group (2 of 51 patients). In contrast, 20.3% of patients in the AFP high–high group developed HCC during the follow-up period.

The incidence rate of HCC in three patient groups, "AFP-low" (a combination of the "low–high" and "low–low" groups),"high–low," and "high–high", was estimated using the Kaplan–Meier method and compared using log-rank tests (Fig. 3b). The rate of HCC incidence was significantly higher in the AFP high–high group compared to both the AFP high–low group and patients with low baseline AFP levels ($P = 0.009$ and 0.001, respectively). There was no significant difference between patients with low baseline AFP levels and the AFP high–low group. The 7-year incidence rate of HCC was 32.3% in the AFP high–high group, compared to only 6.6% in the AFP high–low group, and 8.1% in all patients with low pre-treatment levels.

Discussion

It is well recognized that the most effective strategy for the prevention of HCC development in patients with chronic hepatitis C is likely to be the complete elimination of the HCV infection accompanied by the resultant normalization of liver function [7, 12, 13, 15, 16, 19]. Indeed, we confirmed here that non-SVR is the most significant predictive factor for incidence of HCC in patients receiving interferon therapy for chronic hepatitis C. However, it should be noted that the risk of HCC, even in non-SVR patients, differs between individuals. In the current study, we identified AFP integration value and male gender as independent risk factors for incidence of HCC in non-SVR patients. The incidence of HCC was significantly reduced in individuals with average AFP integration values < 10 ng/mL after interferon therapy, which suggests that the decrease of AFP by interferon therapy lowers the risk of developing HCC. Indeed, even where patients had high baseline AFP levels, incidence of HCC was reduced when the AFP integration value decreased after interferon therapy. Thus, our current findings identify AFP integration value as a useful predictive marker of HCC development in non-SVR patients.

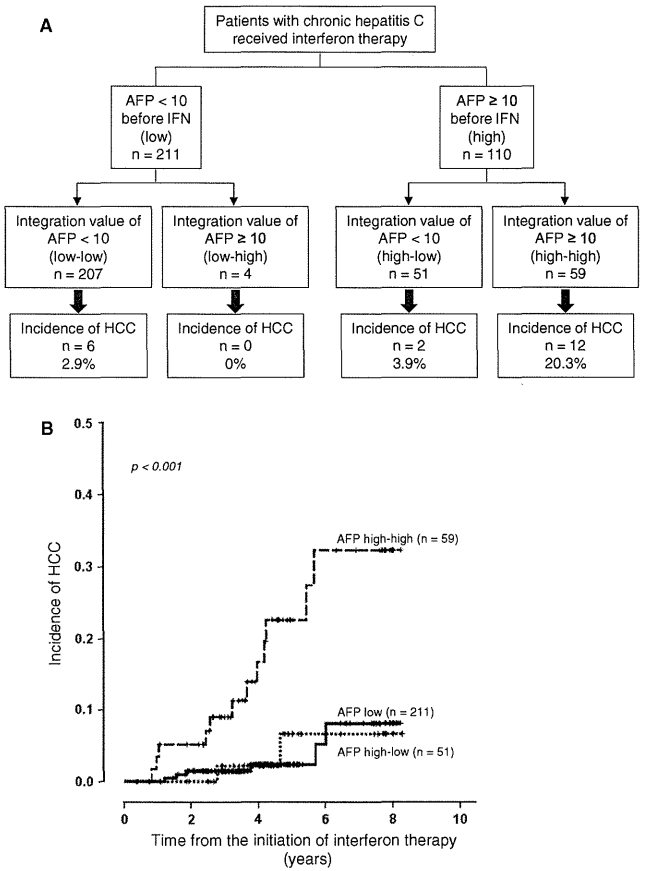

Fig. 3 AFP integration value as a predictive factor for HCC. **a** *Flow diagram* showing the number of patients (*n*) classified by baseline alpha-fetoprotein (AFP) levels before interferon (IFN) therapy and average AFP integration value, and the incidence of hepatocellular carcinoma (HCC) of each group. **b** Kaplan–Meier estimates of the incidence of HCC. *Solid line* AFP-low group (AFP levels before interferon therapy <10 ng/mL); *dotted line* AFP high–low group (baseline AFP levels ≥10 ng/mL, average AFP integration value <10 ng/mL); *dashed line* AFP high–high group (both baseline and average AFP integration values ≥10 ng/mL)

Data from several previous studies suggest that the continuous normalization of alanine aminotransferase (ALT) levels by interferon therapy can reduce the risk of HCC development [36–39]. In addition, one recent study suggested that the ALT integration value is a predictive factor for HCC [35]. In contrast to published data (22), our multivariate analysis did not identify the ALT integration value as a significant predictive factor for HCC incidence, although it was identified as significant by univariate analysis in all 382 patients. Since the previous study did not evaluate AFP levels as a factor for prediction of HCC [35], our results indicate that the AFP integration value is superior to that of ALT as a predictive factor for incidence of HCC. We do not know the reason for this result, but it is speculated that significance of AFP as a marker of hepatic regeneration resulted in the more accurate prediction of hepatocarcinogenesis by integration value of AFP than that of ALT.

As AFP is a diagnostic marker for the existence of HCC, high integration value of AFP in the present study might be a result of HCC development. However, we concluded that the high AFP integration values in patients who developed HCC were not caused by a result of existence of HCC, because of the following two reasons. First, the last AFP values before detection of HCC were not the highest level in the follow-up periods in 19 of 23 patients who developed

HCC, suggesting that the AFP was not produced by the developing HCC in these patients. Second, to exclude the influence of the remaining four patients whose last AFP levels were the highest in the follow-up periods, we analyzed the same statistical analysis by using average AFP integration values excluded the last two examinations of AFP before the detection of HCC. The results of the analysis also showed average integration value of AFP as a significant predictive factor for incidence of HCC.

Male gender was also identified as an independent risk factor for HCC in non-SVR patients in this study. Several reports have shown that men are at a higher risk of developing HCC than women [6, 10, 33, 40, 41]. The male gender also appears to be a risk factor for more severe disease and a greater risk of developing cirrhosis in chronic hepatitis C [42]. Although the association of male gender with the risk of HCC is as yet unexplained, hormonal or genetic factors may lead to increased risk for HCC and cirrhosis in men as previously discussed [10].

In conclusion, a decrease in the AFP integration value predicts reduced incidence of HCC in patients with hepatitis C receiving interferon therapy. Further prospective studies with a larger number of patients are required to validate the significance of these findings.

Acknowledgments This work was supported by Grants-in-aid for Scientific Research from the Ministry of Education, Culture, Sports, Science and Technology, and the Ministry of Health, Labor and Welfare of Japan.

Conflict of interest The authors declare that they have no conflict of interest.

References

1. Bruix J, Barrera JM, Calvet X, Ercilla G, Costa J, Sanchez-Tapias JM, Ventura M, Vall M, Bruguera M, Bru C, et al. Prevalence of antibodies to hepatitis C virus in Spanish patients with hepatocellular carcinoma and hepatic cirrhosis. Lancet. 1989;2:1004–6.
2. Colombo M, Kuo G, Choo QL, Donato MF, Del Ninno E, Tommasini MA, Dioguardi N, Houghton M. Prevalence of antibodies to hepatitis C virus in Italian patients with hepatocellular carcinoma. Lancet. 1989;2:1006–8.
3. Hasan F, Jeffers LJ, De Medina M, Reddy KR, Parker T, Schiff ER, Houghton M, Choo QL, Kuo G. Hepatitis C-associated hepatocellular carcinoma. Hepatology. 1990;12:589–91.
4. Ikeda K, Saitoh S, Koida I, Arase Y, Tsubota A, Chayama K, Kumada H, Kawanishi M. A multivariate analysis of risk factors for hepatocellular carcinogenesis: a prospective observation of 795 patients with viral and alcoholic cirrhosis. Hepatology. 1993;18:47–53.
5. Tsukuma H, Hiyama T, Tanaka S, Nakao M, Yabuuchi T, Kitamura T, Nakanishi K, Fujimoto I, Inoue A, Yamazaki H, et al. Risk factors for hepatocellular carcinoma among patients with chronic liver disease. N Engl J Med. 1993;328:1797–801.
6. Fattovich G, Stroffolini T, Zagni I, Donato F. Hepatocellular carcinoma in cirrhosis: incidence and risk factors. Gastroenterology. 2004;127:S35–50.
7. Ikeda K, Marusawa H, Osaki Y, Nakamura T, Kitajima N, Yamashita Y, Kudo M, Sato T, Chiba T. Antibody to hepatitis B core antigen and risk for hepatitis C-related hepatocellular carcinoma: a prospective study. Ann Intern Med. 2007;146:649–56.
8. Liang TJ, Heller T. Pathogenesis of hepatitis C-associated hepatocellular carcinoma. Gastroenterology. 2004;127:S62–71.
9. Yoshida H, Shiratori Y, Moriyama M, Arakawa Y, Ide T, Sata M, Inoue O, Yano M, Tanaka M, Fujiyama S, Nishiguchi S, Kuroki T, Imazeki F, Yokosuka O, Kinoyama S, Yamada G, Omata M. Interferon therapy reduces the risk for hepatocellular carcinoma: national surveillance program of cirrhotic and noncirrhotic patients with chronic hepatitis C in Japan. IHIT Study Group. Inhibition of hepatocarcinogenesis by interferon therapy. Ann Intern Med. 1999;131:174–81.
10. Heathcote EJ. Prevention of hepatitis C virus-related hepatocellular carcinoma. Gastroenterology. 2004;127:S294–302.
11. Lok AS, Seeff LB, Morgan TR, di Bisceglie AM, Sterling RK, Curto TM, Everson GT, Lindsay KL, Lee WM, Bonkovsky HL, Dienstag JL, Ghany MG, Morishima C, Goodman ZD. Incidence of hepatocellular carcinoma and associated risk factors in hepatitis C-related advanced liver disease. Gastroenterology. 2009;136:138–48.
12. Effect of interferon-alpha on progression of cirrhosis to hepatocellular carcinoma: a retrospective cohort study. International Interferon-alpha Hepatocellular Carcinoma Study Group. Lancet. 1998;351:1535–9.
13. Camma C, Giunta M, Andreone P, Craxi A. Interferon and prevention of hepatocellular carcinoma in viral cirrhosis: an evidence-based approach. J Hepatol. 2001;34:593–602.
14. Di Bisceglie AM, Shiffman ML, Everson GT, Lindsay KL, Everhart JE, Wright EC, Lee WM, Lok AS, Bonkovsky HL, Morgan TR, Ghany MG, Morishima C, Snow KK, Dienstag JL. Prolonged therapy of advanced chronic hepatitis C with low-dose peginterferon. N Engl J Med. 2008;359:2429–41.
15. Fattovich G, Giustina G, Degos F, Diodati G, Tremolada F, Nevens F, Almasio P, Solinas A, Brouwer JT, Thomas H, Realdi G, Corrocher R, Schalm SW. Effectiveness of interferon alfa on incidence of hepatocellular carcinoma, decompensation in cirrhosis type C. European Concerted Action on Viral Hepatitis (EUROHEP). J Hepatol. 1997;27:201–5.
16. Hayashi K, Kumada T, Nakano S, Takeda I, Kiriyama S, Sone Y, Toyoda H, Shimizu H, Honda T. Incidence of hepatocellular carcinoma in chronic hepatitis C after interferon therapy. Hepatogastroenterology. 2002;49:508–12.
17. Lok AS, Everhart JE, Wright EC, Di Bisceglie AM, Kim HY, Sterling RK, Everson GT, Lindsay KL, Lee WM, Bonkovsky HL, Dienstag JL, Ghany MG, Morishima C, Morgan TR. Maintenance peginterferon therapy and other factors associated with hepatocellular carcinoma in patients with advanced hepatitis C. Gastroenterology. 2011;140:840–9.
18. Nishiguchi S, Kuroki T, Nakatani S, Morimoto H, Takeda T, Nakajima S, Shiomi S, Seki S, Kobayashi K, Otani S. Randomised trial of effects of interferon-alpha on incidence of hepatocellular carcinoma in chronic active hepatitis C with cirrhosis. Lancet. 1995;346:1051–5.
19. Okanoue T, Itoh Y, Minami M, Sakamoto S, Yasui K, Sakamoto M, Nishioji K, Murakami Y, Kashima K. Interferon therapy lowers the rate of progression to hepatocellular carcinoma in chronic hepatitis C but not significantly in an advanced stage: a retrospective study in 1148 patients. Viral Hepatitis Therapy Study Group. J Hepatol. 1999;30:653–9.
20. Izuno K, Fujiyama S, Yamasaki K, Sato M, Sato T. Early detection of hepatocellular carcinoma associated with cirrhosis by combined assay of des-gamma-carboxy prothrombin and alpha-fetoprotein: a prospective study. Hepatogastroenterology. 1995;42:387–93.

21. Trevisani F, D'Intino PE, Morselli-Labate AM, Mazzella G, Accogli E, Caraceni P, Domenicali M, De Notariis S, Roda E, Bernardi M. Serum alpha-fetoprotein for diagnosis of hepatocellular carcinoma in patients with chronic liver disease: influence of HBsAg and anti-HCV status. J Hepatol. 2001;34:570–5.
22. Zoli M, Magalotti D, Bianchi G, Gueli C, Marchesini G, Pisi E. Efficacy of a surveillance program for early detection of hepatocellular carcinoma. Cancer. 1996;78:977–85.
23. Alpert E, Feller ER. Alpha-fetoprotein (AFP) in benign liver disease. Evidence that normal liver regeneration does not induce AFP synthesis. Gastroenterology. 1978;74:856–8.
24. Bloomer JR, Waldmann TA, McIntire KR, Klatskin G. Alpha-fetoprotein in nonneoplastic hepatic disorders. JAMA. 1975;233:38–41.
25. Ruoslahti E, Seppala M. Normal and increased alpha-fetoprotein in neoplastic and non-neoplastic liver disease. Lancet. 1972;2:278–9.
26. Sakurai T, Marusawa H, Satomura S, Nabeshima M, Uemoto S, Tanaka K, Chiba T. *Lens culinaris* agglutinin-A-reactive alpha-fetoprotein as a marker for liver atrophy in fulminant hepatic failure. Hepatol Res. 2003;26:98–105.
27. Taketa K. Alpha-fetoprotein: reevaluation in hepatology. Hepatology. 1990;12:1420–32.
28. Di Bisceglie AM, Sterling RK, Chung RT, Everhart JE, Dienstag JL, Bonkovsky HL, Wright EC, Everson GT, Lindsay KL, Lok AS, Lee WM, Morgan TR, Ghany MG, Gretch DR. Serum alpha-fetoprotein levels in patients with advanced hepatitis C: results from the HALT-C Trial. J Hepatol. 2005;43:434–41.
29. Tateyama M, Yatsuhashi H, Taura N, Motoyoshi Y, Nagaoka S, Yanagi K, Abiru S, Yano K, Komori A, Migita K, Nakamura M, Nagahama H, Sasaki Y, Miyakawa Y, Ishibashi H. Alpha-fetoprotein above normal levels as a risk factor for the development of hepatocellular carcinoma in patients infected with hepatitis C virus. J Gastroenterol. 2011;46:92–100.
30. Murashima S, Tanaka M, Haramaki M, Yutani S, Nakashima Y, Harada K, Ide T, Kumashiro R, Sata M. A decrease in AFP level related to administration of interferon in patients with chronic hepatitis C and a high level of AFP. Dig Dis Sci. 2006;51:808–12.
31. Tamura Y, Yamagiwa S, Aoki Y, Kurita S, Suda T, Ohkoshi S, Nomoto M, Aoyagi Y. Serum alpha-fetoprotein levels during and after interferon therapy and the development of hepatocellular carcinoma in patients with chronic hepatitis C. Dig Dis Sci. 2009;54:2530–7.
32. Arase Y, Ikeda K, Suzuki F, Suzuki Y, Kobayashi M, Akuta N, Hosaka T, Sezaki H, Yatsuji H, Kawamura Y, Kumada H. Prolonged-interferon therapy reduces hepatocarcinogenesis in aged-patients with chronic hepatitis C. J Med Virol. 2007;79:1095–102.
33. Asahina Y, Tsuchiya K, Tamaki N, Hirayama I, Tanaka T, Sato M, Yasui Y, Hosokawa T, Ueda K, Kuzuya T, Nakanishi H, Itakura J, Takahashi Y, Kurosaki M, Enomoto N, Izumi N. Effect of aging on risk for hepatocellular carcinoma in chronic hepatitis C virus infection. Hepatology. 2010;52:518–27.
34. Ohno O, Mizokami M, Wu RR, Saleh MG, Ohba K, Orito E, Mukaide M, Williams R, Lau JY. New hepatitis C virus (HCV) genotyping system that allows for identification of HCV genotypes 1a, 1b, 2a, 2b, 3a, 3b, 4, 5a, and 6a. J Clin Microbiol. 1997;35:201–7.
35. Kumada T, Toyoda H, Kiriyama S, Sone Y, Tanikawa M, Hisanaga Y, Kanamori A, Atsumi H, Takagi M, Nakano S, Arakawa T, Fujimori M. Incidence of hepatocellular carcinoma in hepatitis C carriers with normal alanine aminotransferase levels. J Hepatol. 2009;50:729–35.
36. Arase Y, Ikeda K, Suzuki F, Suzuki Y, Kobayashi M, Akuta N, Hosaka T, Sezaki H, Yatsuji H, Kawamura Y, Kumada H. Interferon-induced prolonged biochemical response reduces hepatocarcinogenesis in hepatitis C virus infection. J Med Virol. 2007;79:1485–90.
37. Kasahara A, Hayashi N, Mochizuki K, Takayanagi M, Yoshioka K, Kakumu S, Iijima A, Urushihara A, Kiyosawa K, Okuda M, Hino K, Okita K. Risk factors for hepatocellular carcinoma, its incidence after interferon treatment in patients with chronic hepatitis C. Osaka Liver Disease Study Group. Hepatology. 1998;27:1394–402.
38. Kurokawa M, Hiramatsu N, Oze T, Mochizuki K, Yakushijin T, Kurashige N, Inoue Y, Igura T, Imanaka K, Yamada A, Oshita M, Hagiwara H, Mita E, Ito T, Inui Y, Hijioka T, Yoshihara H, Inoue A, Imai Y, Kato M, Kiso S, Kanto T, Takehara T, Kasahara A, Hayashi N. Effect of interferon alpha-2b plus ribavirin therapy on incidence of hepatocellular carcinoma in patients with chronic hepatitis. Hepatol Res. 2009;39:432–8.
39. Suzuki K, Ohkoshi S, Yano M, Ichida T, Takimoto M, Naitoh A, Mori S, Hata K, Igarashi K, Hara H, Ohta H, Soga K, Watanabe T, Kamimura T, Aoyagi Y. Sustained biochemical remission after interferon treatment may closely be related to the end of treatment biochemical response and associated with a lower incidence of hepatocarcinogenesis. Liver Int. 2003;23:143–7.
40. Kurosaki M, Hosokawa T, Matsunaga K, Hirayama I, Tanaka T, Sato M, Yasui Y, Tamaki N, Ueda K, Tsuchiya K, Kuzuya T, Nakanishi H, Itakura J, Takahashi Y, Asahina Y, Enomoto N, Izumi N. Hepatic steatosis in chronic hepatitis C is a significant risk factor for developing hepatocellular carcinoma independent of age, sex, obesity, fibrosis stage and response to interferon therapy. Hepatol Res. 2010;40:870–7.
41. Takahashi H, Mizuta T, Eguchi Y, Kawaguchi Y, Kuwashiro T, Oeda S, Isoda H, Oza N, Iwane S, Izumi K, Anzai K, Ozaki I, Fujimoto K. Post-challenge hyperglycemia is a significant risk factor for the development of hepatocellular carcinoma in patients with chronic hepatitis C. J Gastroenterol. 2011;46:790–8.
42. Forns X, Ampurdanes S, Sanchez-Tapias JM, Guilera M, Sans M, Sanchez-Fueyo A, Quinto L, Joya P, Bruguera M, Rodes J. Long-term follow-up of chronic hepatitis C in patients diagnosed at a tertiary-care center. J Hepatol. 2001;35:265–71.

uicc
global cancer control

IJC
International Journal of Cancer

Cancer Cell Biology

Excessive activity of apolipoprotein B mRNA editing enzyme catalytic polypeptide 2 (APOBEC2) contributes to liver and lung tumorigenesis

Shunsuke Okuyama, Hiroyuki Marusawa, Tomonori Matsumoto, Yoshihide Ueda, Yuko Matsumoto, Yoko Endo, Atsushi Takai and Tsutomu Chiba

Department of Gastroenterology and Hepatology, Graduate School of Medicine, Kyoto University, Shogoin, Sakyo-Ku, Kyoto, Japan

Apolipoprotein B mRNA editing enzyme catalytic polypeptide 2 (APOBEC2) was originally identified as a member of the cytidine deaminase family with putative nucleotide editing activity. To clarify the physiologic and pathologic roles, and the target nucleotide of APOBEC2, we established an APOBEC2 transgenic mouse model and investigated whether APOBEC2 expression causes nucleotide alterations in host DNA or RNA sequences. Sequence analyses revealed that constitutive expression of APOBEC2 in the liver resulted in significantly high frequencies of nucleotide alterations in the transcripts of eukaryotic translation initiation factor 4 gamma 2 (*Eif4g2*) and phosphatase and tensin homolog (*PTEN*) genes. Hepatocellular carcinoma developed in 2 of 20 APOBEC2 transgenic mice at 72 weeks of age. In addition, constitutive APOBEC2 expression caused lung tumors in 7 of 20 transgenic mice analyzed. Together with the fact that the proinflammatory cytokine tumor necrosis factor-α induces ectopic expression of APOBEC2 in hepatocytes, our findings indicate that aberrant APOBEC2 expression causes nucleotide alterations in the transcripts of the specific target gene and could be involved in the development of human hepatocellular carcinoma through hepatic inflammation.

The number of coding sequences in the genome is limited, but the genomic information encoded in DNA or RNA sequences can be manipulated to produce a wide range of expression products in cells.[1] Apolipoprotein B mRNA editing enzyme catalytic polypeptide (APOBEC) family members are nucleotide-editing enzymes capable of inserting somatic mutations in DNA and/or RNA through their cytidine deaminating activity.[2] The APOBEC family comprises APOBEC1, -2, -3A, -3B, -3C, -3DE, -3F, -3G, -3H, -4, activation-induced cytidine deaminase (AID) in humans, and APOBEC1, -2, -3, and AID in mice, and contribute to producing various physiologic outcomes by modifying target gene sequences.[3–5] For example, APOBEC1 participates in lipid metabolism by deaminating a specific cytidine to uridine in Apolipoprotein (Apo-) B transcript sequences. The nucleotide change induced by APOBEC1 activity results in the formation of a termination codon in an Apo-B48 mRNA, leading to the production of molecules about half the size of a full-length genomically encoded Apo-B100.[6,7] APOBEC3G is a cytidine deaminase that induces hypermutation in viral DNA sequences and acts as a host defense factor against various viruses, including HIV-1 and hepatitis B viruses.[8–15] On the other hand, AID is expressed in germinal center B-cells and induces somatic hypermutation and class switch recombination of the immunoglobulin genes encoded in human DNA sequences, resulting in the amplification of immune diversity.[16,17] APOBEC1, APOBEC3G and AID thus create nucleotide changes in their preferential target DNA or RNA structures. In contrast to these APOBEC proteins, little is known about the function and editing activity of APOBEC2. Although previous reports indicate that murine APOBEC2 mRNA and protein are expressed exclusively in heart and skeletal muscle, the substrate and function of APOBEC2 and whether APOBEC2 has nucleotide editing activity remain unknown.[18,19]

Accumulating evidence suggests that excessive or aberrant activity of APOBEC family members leads to tumorigenesis through their nucleotide editing of tumor-related genes.

Key words: APOBEC2, hepatocellular carcinoma, lung cancer

Abbreviations: APOBEC: Apolipoprotein B mRNA editing enzyme catalytic polypeptide; EIF4G2: Eukaryotic translation initiation factor 4 gamma 2; AID: activation-induced cytidine deaminase; Apo-: Apolipoprotein; Tg: transgenic; NF-κB: nuclear factor-κB; HCC: hepatocellular carcinoma; TNF: tumor necrosis factor; cDNA: Complimentary DNA; RT-PCR: real-time reverse-transcription polymerase chain reaction; ER: estrogen receptor

Additional Supporting Information may be found in the online version of this article.

Grant sponsors: Japan Society for the Promotion of Science (JSPS), a Grant from the Ministry of Health, Labor, and Welfare, Japan, the Takeda Science Foundation

DOI: 10.1002/ijc.26114

History: *Received 8 Jan 2011; Accepted 25 Mar 2011; Online 5 Apr 2011*

Correspondence to: Hiroyuki Marusawa, MD, PhD, Department of Gastroenterology and Hepatology, Graduate School of Medicine, Kyoto University, 54 Kawahara-cho, Shogoin, Sakyo-ku, Kyoto 606-8507, Japan, Tel.: +81-75-751-4302, Fax: +81-75-751-4303, E-mail: maru@kuhp.kyoto-u.ac.jp

Transgene expression of APOBEC1 causes dysplasia and carcinoma in mouse and rabbit liver due to its aberrant editing of the eukaryotic translation initiation factor 4 gamma 2 (Eif4g2).[20,21] A more striking tumor phenotype is observed in mice with constitutive and ubiquitous AID expression. We previously demonstrated that AID transgenic (Tg) mice developed tumors in various organs, including liver, lung, stomach and lymphoid organs, accompanied by the accumulation of somatic mutations on several tumor-related genes such as *Tp53* and *Myc*.[22,23] Interestingly, we also found that proinflammatory cytokine stimulation induces a substantial upregulation of APOBEC2 transcription *via* the activation of the transcriptional factor nuclear factor-κB (NF-κB) in hepatoma-derived cells, whereas only trace amounts of endogenous APOBEC2 expression are detectable in normal hepatocytes.[24] On the basis of the fact that most human hepatocellular carcinoma (HCC) arises in the setting of chronic liver disease with the features of chronic hepatitis or liver cirrhosis, we hypothesized that APOBEC2 enzyme activity has a role in the accumulation of genetic alterations in tumor-related genes under conditions of hepatic inflammation, thereby contributing to the development of HCC. In this study, we investigated the putative nucleotide editing ability of APOBEC2 on the host genes in hepatocytes, and its relevance to carcinogenesis by establishing Tg mice that constitutively express APOBEC2.

Material and Methods

APOBEC2 Tg mice

Total RNA was extracted from murine liver using Sepasol-RNA 1 Super (Nacalai Tesque, Kyoto, Japan) according to the manufacturer's protocol. Complimentary DNA (cDNA) was synthesized from total RNA with random hexamer primers using a Transcriptor First Strand cDNA Synthesis Kit (Roche, Mannheim, Germany). After amplification of the murine APOBEC2 gene using high-fidelity Phusion Taq polymerase (Finnzymes, Espoo, Finland) with oligonucleotide primers, 5′-GCAGAATTCCACCATGGCTCAGAAGGAAG AGGC-3′(forward) and 5′-ACTCTCGAGCCTACTTCAGGA TGTCTGCC-3′ (reverse), murine APOBEC2 cDNA (1.2 kbp) was cloned downstream of the chicken β-actin (CAG) promoter. The purified fragment of the CAG promoter and APOBEC2 transgene was microinjected into fertilized eggs of the Slc:BDF1, the hybrid of C57BL/6CrSlc and DBA/2CrSlc (Japan SLC, Shizuoka, Japan), to generate APOBEC2 Tg mice. Tg mice were maintained in specific pathogen-free conditions at the Institute of Laboratory Animals of Kyoto University. Control mice were littermates carrying no transgene. Tissue samples from Tg mice were removed and fixed in 4% (w/v) formaldehyde, embedded in paraffin, stained with hematoxylin and eosin and examined for histologic abnormalities. Tissue samples were also frozen immediately in liquid nitrogen for nucleotide extraction. The mice received humane care according to the "Guide for the Care and Use of Laboratory Animals" prepared by the National Academy of Sciences and published by the National Institutes of Health, USA (NIH publication 86-23).

Quantitative real-time reverse transcription PCR

Quantitative real-time reverse-transcription polymerase chain reaction (RT-PCR) for murine *APOBEC1* and *APOBEC2* amplification was performed using a LightCycler® 480 instrument (Roche). cDNA was synthesized from 1 μg of total RNA isolated from the cells with random hexamer primers in a total volume of 20 μL using Transcriptor First Strand cDNA Synthesis Kit (Roche). Real-time PCRs were set up in 20 μL of FastStart Universal SYBR Green (Roche) with the RT product and the following oligonucleotide primers: APOBEC1, 5′-CGAAGCTTATTGGCCAAGGT-3′ (forward) and 5′-AAGGAGATGGGGTGGTATCC-3′ (reverse); APOBEC2, 5′-CCCTTCGAGATTGTCACTGG-3′ (forward) and 5′-TGTTCATCCTCCAGGTAGCC-3′ (reverse). Target cDNAs were normalized to the endogenous RNA levels of the housekeeping reference gene for *18S ribosomal RNA* (*18S rRNA*).[25] For simplicity, the expression levels of *APOBEC2* are represented as relative values compared with the control specimen in each experiment.

Immunoblotting

Homogenates of murine specimens were diluted in 2× sodium dodecyl sulfate sample buffer (62.5 mM Tris-HCl, pH 6.8; 2% SDS; 5% β-mercaptoethanol; 10% glycerol, and 0.002% bromophenol blue) and boiled for 5 min. Protein samples were separated by sodium dodecyl sulfate-polyacrylamide gel electrophoresis on 12% (w/v) polyacrylamide gels and subjected to immunoblotting analysis.[26] A polyclonal antibody against human and murine APOBEC2 was generated using purified recombinant APOBEC2 protein as an immunogen. A mouse monoclonal antibody against α-tubulin was purchased from Calbiochem (San Diego, CA).

Cell culture and transfection

Human hepatoma-derived cell lines HepG2 and Huh7 were maintained in Dulbecco's modified Eagle's medium (Gibco-BRL) containing 10% fetal bovine serum. Trans-IT 293 transfection reagent (Mirus Bio Corporation, Madison, WI) was used for plasmid transfection. To generate stable cell lines, pcDNA3-ERT2 was made by inserting the ERT2 fragment, which was cut out from pERT2[27] with *Bam*HI and *Eco*RI. pcDNA3-APO2-ERT2 was made by inserting the PCR-amplified coding sequence of human *APOBEC2*, which was synthesized by RT-PCR with the oligonucleotide primers 5′-ATAGG TACCATGGCCCAGAAGGAAGAGGC-3′ (forward) and 5′-ATAGGATCCAGCTTCAGGATGTCTGCCAAC-3′ (reverse), into the *KpnI-BamHI* site of pcDNA3-ERT2. HepG2 cells were transfected with a *Sca*I-linearized pcDNA3-APO2-ERT2 vector encoding the active form of APOBEC2 fused with the hormone-binding domain of the human estrogen receptor (ER), designated APOBEC2-ER, and cultured in medium containing G418 (Roche) until colonies of stably transfected clones arose.

Subcloning and sequencing of the target genes

The oligonucleotide primers for the amplification of the human *EIF4G2*, *PTEN*, and *TP53*, and murine *Eif4G2*, *Pten*, *Bcl6* and *Tp53*, genes are shown in Supporting Information Table S1. Amplification of the target sequences was performed using high-fidelity Phusion Taq polymerase (Finnzymes, Espoo, Finland), and the products were subcloned into a pcDNA3 vector (Invitrogen, Carlsbad, CA) using pGEM(R) -T Easy Vector System (Promega, Madison, WI) according to the manufacture's instruction. The resulting plasmids were subjected to sequence analysis as described.[28]

Results

Detection of endogenous APOBEC2 protein expression in hepatocytes

We previously reported that transcription of *APOBEC2* is induced by the proinflammatory cytokine tumor necrosis factor (TNF)-α through the activation of NF-κB. To confirm whether endogenous APOBEC2 protein is elevated in response to TNF-α stimulation in human hepatocytes, we generated a rabbit polyclonal antibody against a common amino-acid sequence to human and murine APOBEC2. Using this anti-APOBEC2 antibody, we first confirmed that plasmid-derived exogenous APOBEC2 protein was efficiently detected by immunoblotting analysis (Fig. 1*a*). We then examined whether endogenous APOBEC2 protein was upregulated by TNF-α stimulation in Huh-7 cells. Immunoblotting analysis using the APOBEC2 antibody revealed that endogenous APOBEC2 protein expression was strongly induced after TNF-α stimulation, suggesting that APOBEC2 protein has a role in hepatocyte function under inflammatory conditions (Fig. 1*b*).

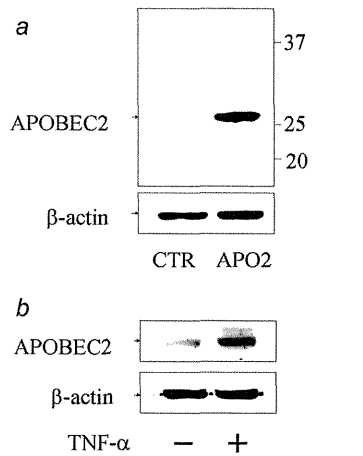

Figure 1. Detection of human APOBEC2 protein in hepatocytes by a specific anti-APOBEC2 antibody. (*a*) Huh7 cells were transfected with plasmid to induce the expression of human APOBEC2 (APO2) or control vector (CTR). After 48 hr, lysates of transfected cells were immunoblotted with anti-APOBEC2 antibody (upper panel) or anti-β-actin antibody (lower panel). (*b*) Huh7 cells were treated with tumor necrosis factor-α (100 ng/ml) for 48 hr followed by immunoblotting using anti-APOBEC2 antibody (upper panel) or anti-β-actin antibody (lower panel).

Establishment of a Tg mouse model constitutively expressing APOBEC2

To investigate the enzymatic activity of APOBEC2 *in vivo*, we generated a Tg mouse model with constitutive and ubiquitous expression of APOBEC2 under the control of CAG promoter. APOBEC2 Tg mice were born healthy and with a body weight similar to that of their wild-type littermates. The expression level of APOBEC2 in various organs of the Tg mice was examined by quantitative RT-PCR and compared with that in the wild-type mice. In wild-type mice, endogenous APOBEC2 transcript was expressed at high levels in heart and skeletal muscle, whereas little or no APOBEC2 expression was detected in the liver, gastrointestinal tracts, lung, spleen and kidney. In contrast, high expression of *APOBEC2* mRNA was ubiquitously detected in the Tg mice, but the expression levels of *APOBEC2* in the liver or lung of the Tg mice were relatively lower than those of the wild-type heart or skeletal muscle (Fig. 2*a*). Immunoblotting analysis using the specific antibodies against APOBEC2 also revealed widespread expression of APOBEC2 protein in various epithelial organs of the Tg mice, with relatively low expression in kidney and spleen (Fig. 2*b*).

Constitutive expression of APOBEC2 resulted in the accumulation of nucleotide alterations in RNA sequences of Eif4g2 and Pten genes in hepatocytes

To clarify whether APOBEC2 targets DNA or RNA, we first extracted total RNA from the nontumor liver tissues of 2 APOBEC2 Tg mice that developed HCC (described below) and their 3 APOBEC2 Tg littermates without any tumor phenotypes, and subjected them to sequence analyses. We chose 2 representative tumor-suppressor genes that are frequently mutated in human cancers, *Pten*, and *Tp53*. The *Bcl6* and *Eif4g2* genes were also included because they are the preferential targets for AID- and APOBEC1-mediated mutagenesis, respectively. We first confirmed that the transcription levels of the genes analyzed for RNA sequencing did not differ between the liver tissues of APOBEC2 Tg mice and wild-type littermates (Supporting Information Fig. S1). In addition, there was no difference in the quantitative levels of APOBEC1 expression between the APOBEC2-expressing liver and

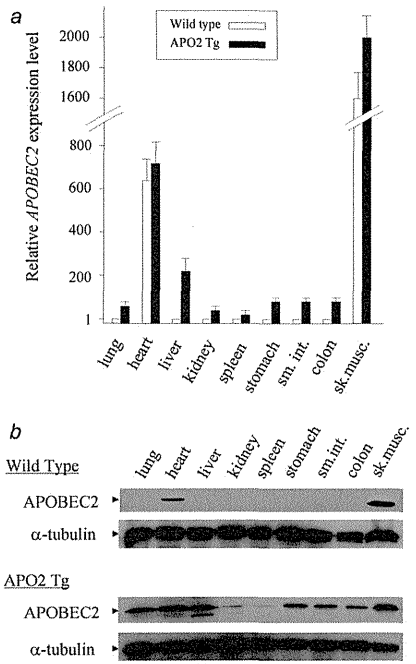

Figure 2. Expression analyses of APOBEC2 Tg mice. (*a*) Relative expression levels of *APOBEC2* transcripts calibrated by the amount of *18S rRNA* for indicated organs of adult APOBEC2 Tg mice (48-week-old) and their wild-type littermates. Data shown are mean results of quantitative real-time RT-PCR analyses for the indicated mouse groups ($n = 6$). Filled bar, APOBEC2 Tg mice; open bar, wild-type mice; sm.int, small intestine; sk.musc, skeletal muscle. (*b*) Results of immunoblot analysis using anti-APOBEC2 (upper panel) or anti-α-tubulin (lower panel) antibody for the lysates of the indicated organs of 48-week-old APOBEC2 Tg mice and their littermates.

normal liver of the wild-type mice (Supporting Information Fig. S2). Sequence analysis revealed a mean of 98,000 and 55,400 base reads per each gene transcript derived from the nontumor liver tissues of the APOBEC2 Tg and control mice, respectively. The total number of amplified clones and RNA sequence reads, and the frequency of nucleotide alterations detected in the nontumor liver tissues of 2 APOBEC2 Tg mice with HCC and the wild-type littermate of the same mouse line are shown in Table 1. The mutation frequencies were highest in the *Eif4g2* transcripts among the genes analyzed in APOBEC2-Tg mice, and were significantly greater compared with those in control tissues (mutation frequencies were 2.75 and 2.36 *vs.* 0.58 substitutions per 1×10^4 nucleotides; $p < 0.05$). Moreover, the nucleotide alteration frequency was significantly higher in the *Pten* gene transcripts from a APOBEC2-expressing liver (Tg-1) than in the control tissues (mutation frequencies were 2.43 *vs.* 0.44 substitutions per 1×10^4 nucleotides, respectively; $p < 0.01$). The *Pten* mRNA of a liver derived from another APOBEC2 Tg mouse (Tg-2; mutation frequency was 1.36 substitutions per 1×10^4 nucleotides) also had a higher nucleotide alteration frequency than that in the control mice, although the difference was not statistically significant ($p = 0.16$ *vs.* control). For the *Eif4g2* and *Pten* transcripts, nucleotide alterations were distributed over the sequences examined and all the alterations detected were different among clones (Fig. 3). Similar results were obtained from the analyses on the liver of 3 APOBEC2 Tg mice that lacked any tumor phenotypes. Indeed, several nucleotide changes had accumulated in both *Eif4g2* and *Pten* transcripts in the liver of all 3 APOBEC2 Tg mice examined (Supporting Information Table S2). In contrast, the mutation frequencies of *Tp53* and *Bcl6* genes of the liver of the APOBEC2 Tg mice were comparable with those of the wild-type mice.

APOBEC2 expression in the liver induced no nucleotide changes in DNA sequences

To clarify whether the nucleotide alterations that emerged in *Eif4g2* and *Pten* transcripts were due to DNA or RNA sequence changes, we determined the DNA sequences of both genes derived from the liver tissues of APOBEC2 Tg and control mice. DNA sequences with an average base length of 0.7 k containing exonic and intronic sequences were amplified, followed by sequence analyses. The total number of amplified clones and DNA sequences read, and the frequency of nucleotide alterations are shown in Supporting Information Table S3. In contrast to the analyses on the RNA sequences, there were no significant differences between the mutation frequency of APOBEC2 Tg mice and that of the wild-type mice of the DNA sequences of the *Eif4g2* and *Pten* genes in the liver. Indeed, no nucleotide alterations were observed in the DNA sequences of the *Eif4g2* gene in the liver of the APOBEC2 Tg mice. Similarly, no mutation was accumulated in the *Pten* DNA sequences of the APOBEC2-expressing liver, suggesting that constitutive expression of the APOBEC2 transgene had no effect on the DNA sequences of the examined regions in the *Eif4g2 and Pten* genes in hepatocytes.

APOBEC2 transgenic mice developed liver and lung tumors

Although most Tg mice were viable at 72 weeks, macroscopic liver and lung tumors developed in some of the APOBEC2 Tg mice. At 72 weeks of age, liver tumors were observed in 2 of 20 Tg male mice, and lung nodules were detected in 7 Tg mice. In contrast to the APOBEC2 Tg mice, none of the wild-type mice developed any tumors at the same age, except 1 with a very small adenoma in the lung. Histopathologic

Table 1. Summary of sequence analysis on the RNA extracted from the liver of the wild-type and APOBEC2 Tg mice

				Nucleotide alterations		
Gene	Mice	Clone	Sequence reads	Number	Frequency(/10^4)	APO2/Wt*
Eif4g2	Wt	82	50,949	3	0.58	
	Tg-1	83	50,835	14	2.75	4.7**
	Tg-2	90	54,986	13	2.36	4.1**
Pten	Wt	92	67,352	3	0.44	
	Tg-1	79	57,599	14	2.43	5.5***
	Tg-2	69	51,323	7	1.36	3.1
Bcl6	Wt	48	41,776	3	0.72	
	Tg-1	59	51,414	1	0.19	0.3
	Tg-2	48	42,413	4	0.94	1.3
Tp53	Wt	84	61,705	2	0.32	
	Tg-1	51	42,285	3	0.71	2.2
	Tg-2	50	40,880	3	0.73	2.3

*Frequency of nucleotide alteration in APOBEC2 Tg mice / in wild type mice. **$p < 0.05$, *vs.* Wt. ***$p < 0.01$, *vs.* Wt.
Abbreviations: Tg, APOBEC2 Tg mice; WT, wild type mice.

analysis of hepatic tumors developed in the APOBEC2 Tg mice revealed nodular aggregates of neoplastic hepatocytes and permeation of tumor cells into residual normal lobules (Fig. 4). Tumor cells had enlarged and hyperchromatic nuclei with chromatin clumping and occasional prominent nucleoli, which were similar to the morphologic characteristics of typical human HCC. On the other hand, lung tumors showed various degrees of cellular atypia, from adenoma to adenocarcinoma (Fig. 5*a*). In addition, monotonous atypical lymphocytes with cytologic features of lymphoblastic lymphoma, such as enlarged round nuclei, irregular nuclear contours, and frequent mitotic figures, massively invaded the spleens of 2 Tg mice (Fig. 5*b*). These findings suggest that constitutive expression of APOBEC2 causes the development of neoplasia in the epithelial organs, including the liver and the lung.

APOBEC2 induced the accumulation of nucleotide alterations of specific target RNA sequences in hepatocytes in vitro

To confirm whether APOBEC2 exerts genotoxic effects on RNA transcripts of the specific target genes, we investigated the alteration frequencies of RNA sequences in cells with constitutive APOBEC2 expression. For this purpose, we established a conditional expression system that allowed for APOBEC2 activation in the cells in response to an estrogen analogue, 4-hydroxytamoxifen (OHT). OHT treatment triggered a posttranslational conformational change and prompt activation of APOBEC2 in APOBEC2-ER expressing cells.[29] We analyzed 3 genes including *PTEN*, *TP53* and *EIF4G2* for the sequence analysis of APOBEC2-mediated mutagenesis *in vitro*. Total RNA was extracted from the APOBEC2-ER expressing HepG2 cells treated with OHT for 8 weeks and the coding RNA sequences of the selected genes were determined by sequence analyses. The total number of amplified clones and RNA sequence reads, and the frequency of nucleotide alterations are shown in Supporting Information Table S4. We found that the emergence of nucleotide alterations in the *PTEN* and *EIF4G2* transcripts was detected at higher frequencies in the cells with APOBEC2 activation compared with control cells treated with OHT, while these differences were not statistically significant ($p = 0.23$ *vs.* control, and $p = 0.39$ *vs.* control, respectively). In contrast, the frequency of nucleotide alterations in the transcripts of the *TP53* in the cells with APOBEC2 activation was comparable with that in the control cells. Similar to the findings obtained from the APOBEC2 Tg mice liver tissues, there were no significant differences between APOBEC2-expressing hepatocytes and control cells in the incidence of nucleotide alterations in the *PTEN* and *EIF4G2* genes (Supporting Information Table S5). These data further suggest that APOBEC2 exerts mutagenic activity in hepatocytes and preferentially achieves nucleotide substitutions in the coding sequences of the specific target genes.

Discussion

Among the APOBEC family members, APOBEC2 and AID homologs can be traced back to bony fish, whereas APOBEC1 and APOBEC3s are restricted to mammals.[30,31] The broad preservation of the APOBEC2 homolog among vertebrates suggests that APOBEC2 has a critical role in the physiology of many species. Little is currently known, however, about the biologic activity of APOBEC2 in any type of cells. Moreover, it is not known whether APOBEC2 possesses nucleotide editing activities like other APOBEC family member proteins. In the present study, we demonstrated for the first time that APOBEC2 expression triggered nucleotide alterations in RNA sequences of the specific genes in hepatocytes. In addition, our findings suggest that APOBEC2 could

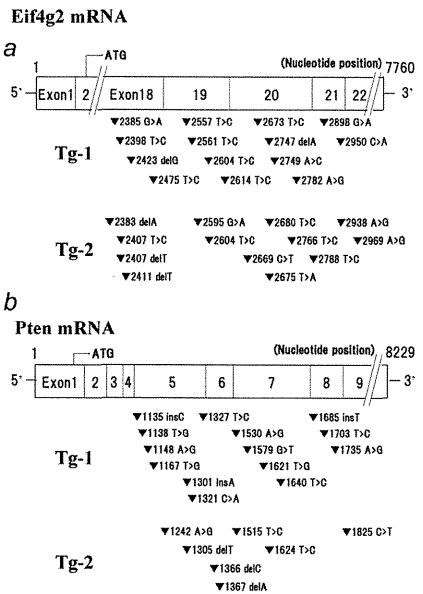

Figure 3. Distribution of nucleotide alterations in the Eif4g2 and Pten trascripts in the APOBEC2-expressing hepatocytes. The mRNA sequences between exon 18 and exon 21 of the Eif4g2 gene (*a*), and the mRNA sequences between exon 5 and exon 8 of the Pten gene (*b*) were determined in the nontumor liver tissues of 2 APOBEC2 Tg mice. The nucleotide positions of the mutations emerged in the Eif4g2 and Pten mRNA of APOBEC2-expressing liver are shown.

contribute to tumorigenesis via the nucleotide alterations of RNA sequences of the target genes.

On the basis of the close sequence homology of APOBEC2 with other APOBEC proteins, APOBEC2 is thought to exhibit deamination activity to achieve nucleotide editing. Indeed, crystal structure analysis indicates that APOBEC2 contains amino acid residues with 4 monomers in each asymmetric unit that form a tetramer with an atypical elongated shape, and this prominent feature of the APOBEC2 tetramer suggests that the active sites are accessible to large RNA or DNA substrates.[32] In the present study, in a mouse model with constitutive APOBEC2 expression, nucleotide alterations were induced in RNA sequences of the *Eif4g2* and possibly the *Pten* genes in hepatocytes. Similar to its effect *in vivo*, aberrant APOBEC2 expression in cultured hepatocyte-derived cells induced nucleotide alterations in the

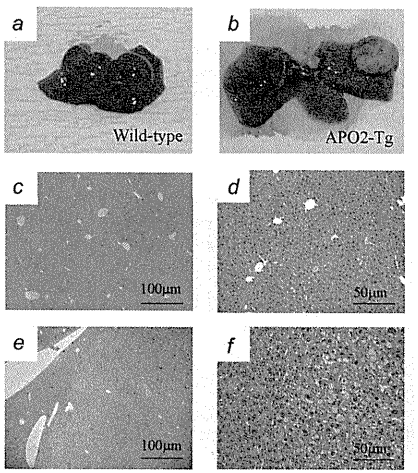

Figure 4. Tumors developed in the liver of APOBEC2 Tg mice. Macroscopic (*b*) and microscopic (haematoxylin and eosin) images (*e, f*) of the HCC that developed in a 72-week-old APOBEC2 Tg mouse and the non-cancerous liver of the same animal (*c,d*). Macroscopic image of the liver of a wild-type littermate is also shown (*a*). (Original magnifications: 3*c,e* ×40; 3*d,f* ×100).

EIF4G2 transcripts. Although our findings demonstrate potential mutator activity of the APOBEC2 protein, it is unclear why the *EIF4G2* transcripts were more sensitive to APOBEC2 activity than other genes in hepatocytes. APOBEC1 expression in hepatocytes also induced somatic mutations in the transcripts of the *EIF4G2* gene.[21] Thus, the sequences of the *EIF4G2* gene might be a common target for the nucleotide editing effects of both the APOBEC1 and APOBEC2 proteins. Further analysis is required to identify the specific target genes of APOBEC2-mediated nucleotide editing in hepatocytes.

An intriguing finding was that the mouse model with constitutive and ubiquitous APOBEC2 expression spontaneously developed epithelial neoplasia in the lung and liver tissues as well as lymphoma. Similar phenotypic findings are observed in mouse models expressing APOBEC1 or AID. Tg mice with RNA-editing enzyme APOBEC1 expression develop HCC at high frequencies with an accumulation of somatic mutations at multiple sites on *Eif4g2* mRNA.[20,21] We also demonstrated that AID Tg mice develop tumors in several organs, including the liver, lung, stomach, and the lymphoid tissues through the accumulation of genetic changes induced by the genotoxic effect of AID.[22,23,28] The molecular mechanisms underlying the contribution of constitutive APOBEC2

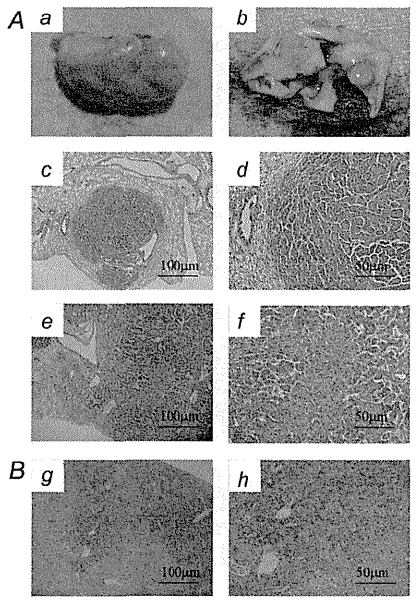

Figure 5. Lung tumors and lymphoma developed in APOBEC2 Tg mice. (*A*) Macroscopic view of a lung tumor that developed in a 72-week-old APOBEC2 Tg mouse (*b*). Microscopic view of a lung adenoma (*c,d*) and adenocarcinoma (*e,f*) that developed in a 72-week-old APOBEC2 Tg mouse. Macroscopic view of the lung of the wild-type littermate (*a*). (*B*) Histologic findings for lymphoma detected in the spleen of APOBEC2 Tg mice. (Original magnifications: 4*c,e,g* ×40; 4*d,f, h* ×100).

expression to tumorigenesis remain unknown. The number of mRNA mutations observed in the *Eif4g2 and Pten* genes in the liver of APOBEC2 Tg mice suggests that these genetic alterations by APOBEC2 have a role in the development of HCC. Indeed, the *EIF4G2* gene is a candidate molecule responsible for oncogenesis caused by the overexpression of APOBEC1,[21] and is frequently downregulated in human cancer tissues.[33] In addition, *PTEN* is one of the most frequently mutated tumor-suppressor genes in human cancers.[34] Thus, the tumorigenesis caused by constitutive APOBEC2 expression might be a consequence of promiscuous nucleotide editing.

Recent studies revealed that the expression of a subset of APOBEC family members is induced by cytokine stimulation in liver tissues. For example, we and other investigators demonstrated that APOBEC3G expression is triggered by interferon-α in hepatocytes, suggesting that APOBEC3G acts as a host defense in response to interferon signaling against viral infection.[35–37] In this study, we showed that TNF-α induced APOBEC2 protein expression in human hepatocytes. Considering the fact that chronic inflammation has important roles in human HCC development,[38,39] the finding that APOBEC2 is induced by proinflammatory cytokine stimulation and induces nucleotide alterations in tumor-related genes in hepatocytes provides a novel idea that aberrant expression of APOBEC2 in epithelial cells acts as a genotoxic factor linking inflammation and cancer development. The tumorigenic phenotype of the APOBEC2-Tg mice further suggests that APOBEC2 is involved in carcinogenesis of the liver tissue under conditions of chronic inflammation, the typical procancerous background of human HCC.

In conclusion, our findings provide the first direct evidence that APOBEC2 induces nucleotide changes preferentially in the *Eif4g2* and possibly the *Pten* genes, and the constitutive expression of APOBEC2 in epithelial tissues contributes to the development of various tumors including HCC and lung cancers. Understanding the pathologic role of APOBEC2 provides new insight into the mechanisms of cancer development in the liver underlying chronic inflammation. During our manuscript preparation, Sato *et al.* reported that they could not find the evidence of APOBEC2's affinity for RNA or high-stoichiometry association with a partner which usually associated with the known RNA editing enzymes.[40] Thus, further analyses would be required to clarify whether APOBEC2 dose possess an RNA-editing activity against specific target genes or overexpression of APOBEC2 causes nucleotide alterations in genome senquences in a promiscuous manner in hepatocytes.

References

1. Wedekind JE, Dance GS, Sowden MP, Smith HC. Messenger RNA editing in mammals: new members of the APOBEC family seeking roles in the family business. *Trends Genet* 2003;19:207–16.
2. Cascalho M. Advantages and disadvantages of cytidine deamination. *J Immunol* 2004; 172:6513–8.
3. Conticello SG, Thomas CJ, Petersen-Mahrt SK, Neuberger MS. Evolution of the AID/APOBEC family of polynucleotide (deoxy)cytidine deaminases. *Mol Biol Evol* 2005;22:367–77.
4. OhAinle M, Kerns JA, Malik HS, Emerman M. Adaptive evolution and antiviral activity of the conserved mammalian cytidine deaminase APOBEC3H. *J Virol* 2006;80:3853–62.
5. Pham P, Bransteitter R, Goodman MF. Reward versus risk: DNA cytidine deaminases triggering immunity and disease. *Biochemistry* 2005;44:2703–15.
6. Chen SH, Habib G, Yang CY, Gu ZW, Lee BR, Weng SA, Silberman SR, Cai SJ, Deslypere JP, Rosseneu M, *et al.* Apolipoprotein B-48 is the product of a messenger RNA with an organ-specific in-frame stop codon. *Science* 1987;238:363–6.
7. Powell LM, Wallis SC, Pease RJ, Edwards YH, Knott TJ, Scott J. A novel form of tissue-specific RNA processing produces apolipoprotein-B48 in intestine. *Cell* 1987; 50:831–40.

8. Mangeat B, Turelli P, Caron G, Friedli M, Perrin L, Trono D. Broad antiretroviral defence by human APOBEC3G through lethal editing of nascent reverse transcripts. *Nature* 2003;424:99–103.
9. Zhang H, Yang B, Pomerantz RJ, Zhang C, Arunachalam SC, Gao L. The cytidine deaminase CEM15 induces hypermutation in newly synthesized HIV-1 DNA. *Nature* 2003;424:94–8.
10. Harris RS, Bishop KN, Sheehy AM, Craig HM, Petersen-Mahrt SK, Watt IN, Neuberger MS, Malim MH. DNA deamination mediates innate immunity to retroviral infection. *Cell* 2003;113:803–9.
11. Shindo K, Takaori-Kondo A, Kobayashi M, Abudu A, Fukunaga K, Uchiyama T. The enzymatic activity of CEM15/Apobec-3G is essential for the regulation of the infectivity of HIV-1 virion but not a sole determinant of its antiviral activity. *J Biol Chem* 2003;278:44412–6.
12. Takaori-Kondo A. APOBEC family proteins: novel antiviral innate immunity. *Int J Hematol* 2006;83:213–6.
13. Noguchi C, Ishino H, Tsuge M, Fujimoto Y, Imamura M, Takahashi S, Chayama K. G to A hypermutation of hepatitis B virus. *Hepatology* 2005;41:626–33.
14. Suspene R, Guetard D, Henry M, Sommer P, Wain-Hobson S, Vartanian JP. Extensive editing of both hepatitis B virus DNA strands by APOBEC3 cytidine deaminases in vitro and in vivo. *Proc Natl Acad Sci USA* 2005;102:8321–6.
15. Noguchi C, Hiraga N, Mori N, Tsuge M, Imamura M, Takahashi S, Fujimoto Y, Ochi H, Abe H, Maekawa T, Yatsuji H, Shirakawa K, *et al.* Dual effect of APOBEC3G on Hepatitis B virus. *J Gen Virol* 2007;88:432–40.
16. Muramatsu M, Sankaranand VS, Anant S, Sugai M, Kinoshita K, Davidson NO, Honjo T. Specific expression of activation-induced cytidine deaminase (AID), a novel member of the RNA-editing deaminase family in germinal center B cells. *J Biol Chem* 1999;274:18470–6.
17. Muramatsu M, Kinoshita K, Fagarasan S, Yamada S, Shinkai Y, Honjo T. Class switch recombination and hypermutation require activation-induced cytidine deaminase (AID), a potential RNA editing enzyme. *Cell* 2000;102:553–63.
18. Liao W, Hong SH, Chan BH, Rudolph FB, Clark SC, Chan L. APOBEC-2, a cardiac- and skeletal muscle-specific member of the cytidine deaminase supergene family. *Biochem Biophys Res Commun* 1999;260:398–404.
19. Mikl MC, Watt IN, Lu M, Reik W, Davies SL, Neuberger MS, Rada C. Mice deficient in APOBEC2 and APOBEC3. *Mol Cell Biol* 2005;25:7270–7.
20. Yamanaka S, Balestra ME, Ferrell LD, Fan J, Arnold KS, Taylor S, Taylor JM, Innerarity TL. Apolipoprotein B mRNA-editing protein induces hepatocellular carcinoma and dysplasia in transgenic animals. *Proc Natl Acad Sci USA* 1995;92:8483–7.
21. Yamanaka S, Poksay KS, Arnold KS, Innerarity TL. A novel translational repressor mRNA is edited extensively in livers containing tumors caused by the transgene expression of the apoB mRNA-editing enzyme. *Genes Dev* 1997;11:321–33.
22. Morisawa T, Marusawa H, Ueda Y, Iwai A, Okazaki IM, Honjo T, Chiba T. Organ-specific profiles of genetic changes in cancers caused by activation-induced cytidine deaminase expression. *Int J Cancer* 2008;123:2735–40.
23. Okazaki IM, Hiai H, Kakazu N, Yamada S, Muramatsu M, Kinoshita K, Honjo T. Constitutive expression of AID leads to tumorigenesis. *J Exp Med* 2003;197:1173–81.
24. Matsumoto T, Marusawa H, Endo Y, Ueda Y, Matsumoto Y, Chiba T. Expression of APOBEC2 is transcriptionally regulated by NF-kappaB in human hepatocytes. *FEBS Lett* 2006;580:731–5.
25. Kou T, Marusawa H, Kinoshita K, Endo Y, Okazaki IM, Ueda Y, Kodama Y, Haga H, Ikai I, Chiba T. Expression of activation-induced cytidine deaminase in human hepatocytes during hepatocarcinogenesis. *Int J Cancer* 2007;120:469–76.
26. Iwai A, Marusawa H, Matsuzawa S, Fukushima T, Hijikata M, Reed JC, Shimotohno K, Chiba T. Siah-1L, a novel transcript variant belonging to the human Siah family of proteins, regulates beta-catenin activity in a p53-dependent manner. *Oncogene* 2004;23:7593–600.
27. Schroeder T, Just U. Notch signalling via RBP-J promotes myeloid differentiation. *Embo J* 2000;19:2558–68.
28. Endo Y, Marusawa H, Kinoshita K, Morisawa T, Sakurai T, Okazaki IM, Watashi K, Shimotohno K, Honjo T, Chiba T. Expression of activation-induced cytidine deaminase in human hepatocytes via NF-kappaB signaling. *Oncogene* 2007;26:5587–95.
29. Doi T, Kinoshita K, Ikegawa M, Muramatsu M, Honjo T. De novo protein synthesis is required for the activation-induced cytidine deaminase function in class-switch recombination. *Proc Natl Acad Sci USA* 2003;100:2634–8.
30. Zhao Y, Pan-Hammarstrom Q, Zhao Z, Hammarstrom L. Identification of the activation-induced cytidine deaminase gene from zebrafish: an evolutionary analysis. *Dev Comp Immunol* 2005;29:61–71.
31. Saunders HL, Magor BG. Cloning and expression of the AID gene in the channel catfish. *Dev Comp Immunol* 2004;28:657–63.
32. Prochnow C, Bransteitter R, Klein MG, Goodman MF, Chen XS. The APOBEC-2 crystal structure and functional implications for the deaminase AID. *Nature* 2007;445:447–51.
33. Buim ME, Soares FA, Sarkis AS, Nagai MA. The transcripts of SFRP1,CEP63 and EIF4G2 genes are frequently downregulated in transitional cell carcinomas of the bladder. *Oncology* 2005;69:445–54.
34. Salmena L, Carracedo A, Pandolfi PP. Tenets of PTEN tumor suppression. *Cell* 2008;133:403–14.
35. Tanaka Y, Marusawa H, Seno H, Matsumoto Y, Ueda Y, Kodama Y, Endo Y, Yamauchi J, Matsumoto T, Takaori-Kondo A, Ikai I, Chiba T. Anti-viral protein APOBEC3G is induced by interferon-alpha stimulation in human hepatocytes. *Biochem Biophys Res Commun* 2006;341:314–9.
36. Bonvin M, Achermann F, Greeve I, Stroka D, Keogh A, Inderbitzin D, Candinas D, Sommer P, Wain-Hobson S, Vartanian JP, Greeve J. Interferon-inducible expression of APOBEC3 editing enzymes in human hepatocytes and inhibition of hepatitis B virus replication. *Hepatology* 2006;43:1364–74.
37. Komohara Y, Yano H, Shichijo S, Shimotohno K, Itoh K, Yamada A. High expression of APOBEC3G in patients infected with hepatitis C virus. *J Mol Histol* 2006;37:327–32.
38. Thorgeirsson SS, Grisham JW. Molecular pathogenesis of human hepatocellular carcinoma. *Nat Genet* 2002;31:339–46.
39. Llovet JM, Burroughs A, Bruix J. Hepatocellular carcinoma. *Lancet* 2003;362:1907–17.
40. Sato Y, Probst HC, Tatsumi R, Ikeuchi Y, Neuberger MS, Rada C. Deficiency in APOBEC2 leads to a shift in muscle fiber-type, diminished body mass and myopathy. *J Biol Chem* 2009;285:7111–18.

Cancer Cell Biology

OPEN ACCESS Freely available online PLoS one

Dynamics of Hepatitis B Virus Quasispecies in Association with Nucleos(t)ide Analogue Treatment Determined by Ultra-Deep Sequencing

Norihiro Nishijima[1], Hiroyuki Marusawa[1]*, Yoshihide Ueda[1], Ken Takahashi[1], Akihiro Nasu[1], Yukio Osaki[2], Tadayuki Kou[3], Shujiro Yazumi[3], Takeshi Fujiwara[4], Soken Tsuchiya[4], Kazuharu Shimizu[4], Shinji Uemoto[5], Tsutomu Chiba[1]

1 Department of Gastroenterology and Hepatology, Graduate School of Medicine, Kyoto University, Kyoto, Japan, **2** Department of Gastroenterology and Hepatology, Osaka Red Cross Hospital, Osaka, Japan, **3** Department of Gastroenterology and Hepatology, Tazuke Kofukai Medical Research Institute, Kitano Hospital, Osaka, Japan, **4** Department of Nanobio Drug Discovery, Graduate School of Pharmaceutical Sciences, Kyoto University, Kyoto, Japan, **5** Department of Surgery, Graduate School of Medicine, Kyoto University, Kyoto, Japan

Abstract

Background and Aims: Although the advent of ultra-deep sequencing technology allows for the analysis of heretofore-undetectable minor viral mutants, a limited amount of information is currently available regarding the clinical implications of hepatitis B virus (HBV) genomic heterogeneity.

Methods: To characterize the HBV genetic heterogeneity in association with anti-viral therapy, we performed ultra-deep sequencing of full-genome HBV in the liver and serum of 19 patients with chronic viral infection, including 14 therapy-naïve and 5 nucleos(t)ide analogue(NA)-treated cases.

Results: Most genomic changes observed in viral variants were single base substitutions and were widely distributed throughout the HBV genome. Four of eight (50%) chronic therapy-naïve HBeAg-negative patients showed a relatively low prevalence of the G1896A pre-core (pre-C) mutant in the liver tissues, suggesting that other mutations were involved in their HBeAg seroconversion. Interestingly, liver tissues in 4 of 5 (80%) of the chronic NA-treated anti-HBe-positive cases had extremely low levels of the G1896A pre-C mutant (0.0%, 0.0%, 0.1%, and 1.1%), suggesting the high sensitivity of the G1896A pre-C mutant to NA. Moreover, various abundances of clones resistant to NA were common in both the liver and serum of treatment-naïve patients, and the proportion of M204VI mutants resistant to lamivudine and entecavir expanded in response to entecavir treatment in the serum of 35.7% (5/14) of patients, suggesting the putative risk of developing drug resistance to NA.

Conclusion: Our findings illustrate the strong advantage of deep sequencing on viral genome as a tool for dissecting the pathophysiology of HBV infection.

Citation: Nishijima N, Marusawa H, Ueda Y, Takahashi K, Nasu A, et al. (2012) Dynamics of Hepatitis B Virus Quasispecies in Association with Nucleos(t)ide Analogue Treatment Determined by Ultra-Deep Sequencing. PLoS ONE 7(4): e35052. doi:10.1371/journal.pone.0035052

Editor: Antonio Bertoletti, Singapore Institute for Clinical Sciences, Singapore

Received November 17, 2011; **Accepted** March 8, 2012; **Published** April 16, 2012

Funding: This work was supported by JSPS Grant-in-aid for Scientific Research 21229009, 23390196, and Health and Labor Science Research Grants (H22-08) and Research on Hepatitis from the Ministry of Health, Labor and Welfare, Japan. (http://mhlw-grants.niph.go.jp/). The funders had no role in study design, data collection and analysis, decision to publish, or preparation of the manuscript.

Competing Interests: The authors have declared that no competing interests exist.

* E-mail: maru@kuhp.kyoto-u.ac.jp

Introduction

Hepatitis B virus (HBV) is a non-cytopathic DNA virus that infects approximately 350 million people worldwide and is a main cause of liver-related morbidity and mortality [1–3]. The absence of viral-encoded RNA-dependent DNA polymerase proofreading capacity coupled with the extremely high rate of HBV replication yields the potential to rapidly generate mutations at each nucleotide position within the entire genome [4]. Accordingly, a highly characteristic nature of HBV infection is the remarkable genetic heterogeneity at the inter- and intra- patient level. The latter case of variability as a population of closely-related but nonidentical genomes is referred to as viral quasispecies [5,6]. It is well recognized that such mutations may have important implications regarding the pathogenesis of viral disease. For example, in chronic infection, G to A point mutation at nucleotide (nt) 1896 in the pre-core (pre-C) region as well as A1762T and G1764A mutations in the core-promoter region are highly associated with HBeAg seroconversion that in general results in the low levels of viremia and consequent clinical cure [7–9]. In contrast, acute infection with the G1896A pre-C mutant represents a high risk for fulminant hepatic failure [10,11]. Although these facts clearly illustrate the clinical implications of certain viral mutation, increasing evidence strongly suggests that

the viral genetic heterogeneity is more complicated than previously thought [12,13].

The major goals of antiviral therapy in patients with HBV infection are to prevent the progression of liver disease and inhibit the development of hepatocellular carcinoma [14]. Oral nucleos(t)ide analogue (NA) have revolutionized the management of HBV infection, and five such antiviral drugs, including lamivudine, adefovir, entecavir, tenofovir, and telbivudine, are currently approved medications [15,16]. These agents are well-tolerated, very effective at suppressing viral replication, and safe, but one of the major problems of NA therapy is that long-term use of these drugs frequently causes the emergence of antiviral drug-resistant HBV due to substitutions at specific sites in the viral genome sequences, which often negates the benefits of therapy and is associated with hepatitis flares and death [16,17]. It is unclear whether viral clones with antiviral resistance emerge after the administration of antiviral therapy or widely preexist among treatment-naïve patients.

There has been a recent advance in DNA sequencing technology [18]. The ultra-deep sequencers allow for massively parallel amplification and detection of sequences of hundreds of thousands of individual molecules. We recently demonstrated the usefulness of ultra-deep sequencing technology to unveil the massive genetic heterogeneity of hepatitis C virus (HCV) in association with treatment response to antiviral therapy [19]. On the other hand, there are a few published studies in which this technology was used to characterize genetic HBV sequence variations [20–22]. Margeridon-Thermet et al reported that the 454 Life Science GS20 sequencing platform provided higher sensitivity for detecting drug-resistant HBV mutations in the serum of patients treated with nucleoside and nucleotide reverse-transcriptase inhibitors [20]. Solmone et al also reported the strong advantage conferred by the same platform to detect minor variants in the serum of patients with chronic HBV infection [21]. Although in these previous studies low-abundant drug-resistant variants were successfully detected, the analyses were focused on the reverse-transcriptase region of circulating HBV in the serum and thus the whole picture of HBV genetic heterogeneity as well as the *in vivo* dynamics of HBV drug resistant variants in response to anti-viral treatment remains to be clarified. Moreover, intrahepatic viral heterogeneity in patients that achieved the clearance of circulating HBV is largely unknown.

By taking the advantage of an abundance of genetic information obtained by utilizing the Illumina Genome Analyzer II (Illumina, San Diego, CA) as a platform of ultra-deep sequencing, we determined the whole HBV sequence in the liver and serum of patients with chronic HBV infection to evaluate viral quasispecies characteristics. Moreover, we investigated the prevalence of rare drug-resistant HBV variants as well as detailed dynamic changes in the viral genetic heterogeneity in association with NA administration. Based on the abundant genetic information obtained by ultra-deep sequencing, we clarified the precise prevalence of HBV clones with G1896A pre-C mutations in association with HBe serostatus in chronically infected patients with or without NA treatment. We also detected a variety of minor drug-resistant clones in treatment-naïve patients and their dynamic changes in response to entecavir administration, demonstrating the potential clinical significance of naturally-occurring drug-resistant mutations.

Materials and Methods

Ethics Statement

The Kyoto University ethics committee approved the study, and written informed consent for participation in this study was obtained from all patients. The study was conducted in accordance with the principles of the Declaration of Helsinki.

Patients

The liver tissues of 19 Japanese patients that underwent living-donor liver transplantation at Kyoto University due to HBV-related liver disease were available for viral genome analyses. These individuals included 13 men and 6 women, aged 41 to 69 years (median, 55.2 years) and all but one were infected with genotype C viruses. Participants comprised 19 patients with liver cirrhosis caused by chronic HBV infection, including 14 antiviral therapy-naïve cases (chronic-naïve cases) and 5 cases receiving NA treatment, with either lamivudine or entecavir (chronic-NA cases) (Table 1). Serum HBV DNA levels were significantly higher in chronic-naïve cases than in chronic NA cases (median serum HBV DNA levels were 5.6, and <2.6 log copies/ml, respectively, Table 1). Liver tissue samples were obtained at the time of transplantation, frozen immediately, and stored at −80°C until use. Serologic analyses of HBV markers, including hepatitis B surface antigen (HBsAg), antibodies to HBsAg, anti-HBc, HBeAg, and antibodies to HBeAg, were determined by enzyme immunoassay kits as described previously [23]. HBV DNA in the serum before transplantation was examined using a polymerase chain reaction (PCR) assay (Amplicor HBV Monitor, Roche, Branchburg, NJ). To examine the dynamics of viral quasispecies in response to anti-HBV therapy, paired serum samples of 14 treatment-naïve patients before and after administration of daily entecavir (0.5 mg/day) were subjected to further analyses on viral genome.

Direct population Sanger sequencing

DNA was extracted from the liver tissue and serum using a DNeasy Blood & Tissue Kit (Qiagen, Tokyo, Japan). To define the consensus reference sequences of HBV in each clinical specimen, all samples were first subjected to direct population Sanger sequencing using the Applied Biosystems 3500 Genetic Analyzer (Applied Biosystems, Foster City, CA). Oligonucleotide primers for the HBV genome were designed to specifically amplify whole viral sequences as two overlapping fragments using the sense primer 169_F and antisense primer 2847_R to yield a 2679-bp amplicon (amplicon 1), and the sense primer 685_F and antisense primer 443_R to yield a 2974-bp amplicon (amplicon 2; Table S1). HBV sequences were amplified using Phusion High-Fidelity DNA polymerase (FINZYMES, Espoo, Finland). All amplified PCR products were purified using the QIAquick Gel Extraction kit (Qiagen) after agarose gel electrophoresis and used for direct sequencing. The serum of a healthy HBV DNA-negative volunteer was used as a negative control.

Viral genome sequencing by massively-parallel sequencing

Massively-parallel sequencing with multiplexed tags was performed using the Illumina Genome Analyzer II as described [19]. The end-repair of DNA fragments, addition of adenine to the 3′ ends of DNA fragments, adaptor ligation, and PCR amplification by Illumina PCR primers were performed as described previously [24]. Briefly, the viral genome sequences were amplified by high-fidelity PCR using oligonucleotide primers as described above, sheared by nebulization using 32 psi N2 for 8 min, and then the sheared fragments were purified and concentrated using a QIAquick PCR purification Kit (Qiagen). Nucleotide overhangs resulting from fragmentation were then converted into blunt ends using T4 DNA polymerase and Klenow

Table 1. Characteristics of patients with chronic HBV infection analyzed in this study.

	Chronic-naïve (N = 14)	Chronic-NA (N = 5)
Age†	55.5 (41–69)	55.0 (49–68)
Sex (male/female)	9/5	4/1
Alanine aminotransaminase (IU/l)†	41 (10–74)	30 (15–65)
Total bilirubin (mg/dl)†	0.9 (0.5–31.1)	1.7 (0.6–4.5)
Platelet count ($\times 10^4$/mm^3)†	12.7 (3.3–27.6)	5.1 (3.6–11.3)
HBV genotype		
B	1	0
C	13	5
Viral load (log copies /ml)†	5.6 (<2.6–8.8)*	<2.6 (<2.6–5.3)*
HBe-serostatus (HBeAg+/HBeAb+)	8/6	0/5
Fibrosis		
F0–F2	6	0
F3–F4	8	5
Activity		
A0–A1	7	3
A2–A3	7	2

†Values are median (range).
*P = 0.042.
doi:10.1371/journal.pone.0035052.t001

enzymes, followed by the addition of terminal 3′ A-residues. An adaptor containing unique 6-bp tags, such as "ATCACG" and "CGATGT" (Multiplexing Sample Preparation Oligonucleotide Kit, Illumina), was then ligated to each fragment using DNA ligase. We then performed agarose gel electrophoresis of adaptor-ligated DNAs and excised bands from the gel to produce libraries with insert sizes ranging from 200 to 350 bp. These libraries were amplified independently using a minimal PCR amplification step of 18 cycles by Illumina PCR primers with Phusion High-Fidelity DNA polymerase. The DNA fragments were then purified with a MinElute PCR Purification Kit (Qiagen), followed by quantification using the NanoDrop 2000C (Thermo Fisher Scientific, Waltham, MA) to make a working concentration of 10 nM. Cluster generation and sequencing was performed for 64 cycles on the Illumina Genome Analyzer II according to the manufacturer's instructions. The obtained images were analyzed and base-called using GA pipeline software version 1.4 with the default settings provided by Illumina.

Genome Analyzer sequence data analysis

Using the high performance alignment software "NextGene" (SoftGenetics, State College, PA), the 64 base-pair reads obtained from the Genome Analyzer II were aligned with the reference sequences of 3215 bp that were determined by direct population Sanger sequencing of each clinical specimen. Reads with 90% or more bases matching a particular position of the reference sequences were aligned. Furthermore, two quality filters were used for sequencing reads: the reads with a median quality score of more than 30 and no more than 3 uncalled nucleotides were allowed anywhere in the 64 bases. Only sequences that passed the quality filters, rather than raw sequences, were analyzed and each position of the viral genome was assigned a coverage depth, representing the number of times the nucleotide position was sequenced.

Allele-specific quantitative real-time PCR and semiquantitative PCR to determine the relative proportion of G1896A pre-C mutant

To determine the relative proportion of the G1896A pre-C mutant, allele-specific quantitative real-time PCR was performed based on the previously described method [25,26]. Oligonucleotide primers were designed individually to amplify the pre-C region of wild-type and the G1896A pre-C mutant HBV. Three primers were used for this protocol, two allele-specific sense primers, 1896WT_F (for wild-type) and 1896MT_F (for the G1896A pre-C mutant), and one common antisense primer, 2037_R (Table S1). Quantification of wild-type and the G1896A pre-C mutant was individually performed by real-time PCR using a Light Cycler 480 and Fast Start Universal SYBR Master (Roche, Mannheim, Germany) [27]. The relative proportion of the G1896A pre-C mutant was determined to calculate the G1896A pre-C mutant/total HBV ratios. Performance of this assay was tested using mixtures of two previously described plasmids, pcDNA3-HBV-wt#1 and pcDNA3-HBV-G1896A pre-C mutant [28]. Semiquantitative PCR was performed using primers described above, then agarose gel electrophoresis was performed.

Statistical analysis

Results are expressed as mean or median, and range. Pretreatment values were compared using the Mann-Whitney U-test or the Kruskal Wallis H-test. P values less than 0.05 were considered statistically significant.

The viral quasispecies characteristics were evaluated by analyzing the genetic complexity based on the number of different sequences present in the population. Genetic complexity for each site was determined by calculating the Shannon entropy using the following formula:

$$Sn = -\frac{\sum_{i=1}^{n} fi(lnfi)}{N}$$